THERMAL STABILITY STUDIES OF AMMONIUM NITRATE

A Dissertation

by

ZHE HAN

Submitted to the Office of Graduate and Professional Studies of
Texas A&M University
in partial fulfillment of the requirements for the degree of

DOCTOR OF PHILOSOPHY

Chair of Committee,	M. Sam Mannan
Committee Members,	James Holste
	Mahmoud El-Halwagi
	Debjyoti Banerjee
Head of Department,	M. Nazmul Karim

May 2016

Major Subject: Chemical Engineering

ABSTRACT

Ammonium nitrate (AN) is widely used in the fertilizer industry and is one of the most concentrated forms of nitrogen fertilizer. However, AN is associated with various hazards including fire and explosion, which have occurred continuously in the past. AN is not considered a flammable or combustible material at ambient temperature and pressure; however, it is a strong oxidizing agent that can detonate under certain conditions.

The primary goals of this work are to advance the understanding of the root causes associated with AN explosions and find out ways to make AN storage inherently safer by studying its thermal stability. This research focuses on condition-dependent AN decomposition, including the effect of additives, confinement, heating rate, temperature, thermal history, and sample size. Pseudo-adiabatic and adiabatic calorimeters are used to study the characteristics of AN decomposition. Thermodynamic and kinetic parameters are evaluated; models are proposed to predict the temperature rise of AN mixtures with additives; decomposition pathways are analyzed; safer AN storage conditions are identified; and AN explosion phenomenology are reported. In addition, this work discusses the role of water as a chemical, interfering physically and chemically with AN-related fire scenarios possibly leading to explosions.

Thermal stability analysis showed that AN is stable up to approximately 200 °C. Sodium sulfate is a good inhibitor for AN in that its presence can mitigate AN decomposition, while potassium chloride is a promoter because it intensifies the

runaway reaction. AN should be separately stored from promoters, even when inhibitors are also present. Furthermore, exposure of AN to heat and storage in confined spaces should be avoided, and the size of AN piles should be limited. While water remains the choice for tackling AN-related fires, care should be taken in doing so. It must be understood that a significantly sufficient quantity of water should be used. Actually, evidence shows that insufficient quantities of water may exacerbate the fires and consequences.

This work demonstrates the complexity and the multiple studies required for making AN safer as a fertilizer, providing suggestions to the fertilizer industry. It can also serve as a model for studies on various reactive chemicals.

DEDICATION

To my mother Chunling Zhang and my father Huoan Han, for always giving me their love and unconditional support, and for being the main motivation to move forward and become a better person every day.

ACKNOWLEDGEMENTS

Many people have been part of my doctoral journal at Texas A&M University, who have helped me accomplish goals, meet challenges, overcome difficulties, or simply made graduate school happier and memorable, and for that I am very thankful to each one of them.

I would like to sincerely thank my committee chair, Dr. M. Sam Mannan, for his mentoring, which has gone beyond the academic level, and for his kindness and support. His vision and inspiration for students to make a contribution in the process safety field guided me through my research, helps me to focus on the big picture, and will continue to encourage me to see things in perspective both at work and in life. I also thank him for giving me multiple opportunities to learn about real world problems, contribute with solutions, and gain valuable experience to develop myself both professionally and personally. His understanding in the difficult times is highly appreciated. I admire Dr. Mannan as a leader, a researcher, and a person.

I would like to offer my thanks to Dr. James Holste, Dr. Mahmoud El-Halwagi, and Dr. Debjyoti Banerjee, for serving as my committee members, and for their guidance and support throughout the course of this doctoral research.

I am deeply grateful to Dr. Maria Papadaki (University of Patras, Greece), Dr. Hans Pasman, and Dr. Simon Waldram, whose advice and expertise allowed me to complete my research project successfully. I am indeed thankful to them for their

continuous encouragement and support both in research and in life. Their advice has made me a better researcher and a stronger person.

I would like to express my deep gratitude to Dr. Sonny Sachdeva, Dr. Xinrui Li, and Dr. Alba Pineda for their constant and unconditional support, encouragement and friendship throughout my graduate studies. I am also grateful for their technical advice and insightful discussions about my research, and their help and teachings in the laboratory.

I also want to express my thanks to Randy Marek for his help with the maintenance, repair, and troubleshooting of laboratory equipment.

I would also like to extend my thanks to the staff and members of the Mary Kay O'Connor Process Safety Center. Thanks to Dr. Chad Mashuga for helping me with my research. Thanks to Valerie Green for her care and encouragement, to Tricia Hasan and Alanna Scheinerman for their assistance in reviewing several manuscripts.

There are not enough words to thank my parents, Chunling Zhang and Huoan Han, for their unconditional love, understanding, and support during every step towards reaching my goals. I am deeply thankful to them for instilling in me the importance of education and perseverance, and for their contribution towards shaping the person I am today. I thank them for being my motivation and pillar of strength. Thanks also to my extended family members for their support.

I would like to express my very great appreciation to Yizhi Hong for his love, support, and help in research and in life. I also thank his family for their care and generosity, and for accepting me as one of their own.

Thanks also go to my colleagues and the department faculty and staff for making my time at Texas A&M University a great experience. Special appreciation goes to all my friends for their long-standing friendship, encouragement, and wholehearted support, for helping me overcome setbacks, and for the old and new memories.

Finally, I thank all who helped me for giving the strength and clarity needed to complete my studies, for the happy and difficult moments lived, and for making my experience at Texas A&M one I will cherish forever.

TABLE OF CONTENTS

Page

Page

Page

Page

LIST OF FIGURES

Page

Page

Page

Page

LIST OF TABLES

Page

Page

1. INTRODUCTION [*]

Runaway reactions present a potentially serious threat to the chemical process industry and local community. Catastrophic incidents are not uncommon where ammonium nitrate (AN) is used. AN is one such material that has been extensively used as a fertilizer since it is an excellent source of nitrogen. At the same time, it has also been widely used as an explosive material for detonation in mines. According to literature, AN is not considered as a dangerous material at atmospheric conditions [1, 2], but it is a strong oxidizing agent that can result in incidents [3, 4]. A number of incidents have occurred due to the detonability of AN, which has caused extensive loss of property and life. One recent incident is the explosion in West, Texas, that killed 15 people and injured more than 250 people. Despite considerable research performed on understanding the detonability of AN, incidents like West, Texas, are still happening, and this calls for gaining even deeper understanding of the underlying causes of its unpredictable behavior at times.

This research investigated the mechanisms that cause AN to run away. The effects of different contaminants and environmental conditions, such as temperature,

---

[*] Part of this section is reprinted with permission from "Ammonium nitrate thermal decomposition with additives" by Z. Han, S. Sachdeva, M. Papadaki and M. S. Mannan, 2015. *Journal of Loss Prevention in the Process Industries*, 35, 307-315, Copyright 2014 by Elsevier and from "Calorimetry studies of ammonium nitrate – Effect of inhibitors, confinement, and heating rate" by Z. Han, S. Sachdeva, M. Papadaki and M. S. Mannan, 2015. *Journal of Loss Prevention in the Process Industries*, 38, 234-242, Copyright 2015 by Elsevier and from "Effects of inhibitor and promoter mixtures on ammonium nitrate fertilizer explosion hazards" by Z. Han, S. Sachdeva, M. Papadaki and M. S. Mannan, 2015. *Thermochimica Acta*, 624, 69-75, Copyright 2015 by Elsevier.

confinement, and heating rate, were studied using different types of calorimeters to understand their role in its detonability. In addition, predictive models were developed to understand its interaction with these contaminants and environmental conditions at a fundamental level. Furthermore, the complexities of fighting AN-related fires with water were discussed. Specifically, this work aims to reduce the explosion risk associated with AN while maintaining its agricultural benefit.

In this section, the dissertation outline is introduced in Section 1.1, followed by the properties and uses of AN in Section 1.2, AN-related incidents in Section 1.3, the regulations that apply to AN in Section 1.4, the decomposition pathways of AN in Section 1.5, the conditions that affect AN decomposition in Section 1.6, and the use of calorimetry in reactive chemical studies in Section 1.7.

1.1 Dissertation Outline

The remainder of Section 1 describes the main properties and uses of AN, incidents related with AN, thermal decomposition pathways, conditions that affect AN decomposition, and how calorimeters can be used to study AN.

Section 2 defines the research problem and describes the objectives of this work. Section 3 explains the methodology, equipment, analysis models, and procedures used to fulfill the objectives.

Section 4 to 5 are dedicated to the discussion of results obtained from experiments performed and summarize the knowledge acquired through this research.

Section 4 presents the thermal stability of AN with sodium sulfate and potassium chloride, and Section 5 illustrates the experimental results of AN decomposition under various conditions. The two sections focus on the alternatives to make AN safer as a fertilizer by reducing its explosivity, by studying the effect of additives, confinement, heating rate, starting temperature of Heat-Wait-Search (HWS) mode, thermal history, sample size, and isothermal testing on AN thermal decomposition using the Reactive Systems Screening Tool (RSST) and the Automated Pressure Tracking Adiabatic Calorimeter (APTAC). In these sections, the thermodynamic and kinetic parameters are evaluated; models are proposed to predict the key parameters of AN mixtures with two additives; decomposition pathways are analyzed; and safer conditions for AN storage are identified.

Section 6 discusses the use of water fighting AN-related fires and its complications. Topics discussed are the use of sprinkler systems in general and AN explosion phenomenology including decomposition, deflagration, and detonation. Then the complexities of fighting AN storage area fires with water are reported.

Finally, Section 7 summarizes the main findings of the work presented in this dissertation and outlines the opportunities to continue this work.

1.2 Ammonium Nitrate – Properties and Uses

The structural formula of AN is shown in Figure 1. The molar mass of AN is 80.052 $g \cdot mol^{-1}$ and the density is 1.725 $g \cdot cm^{-3}$ at 20 °C [5].

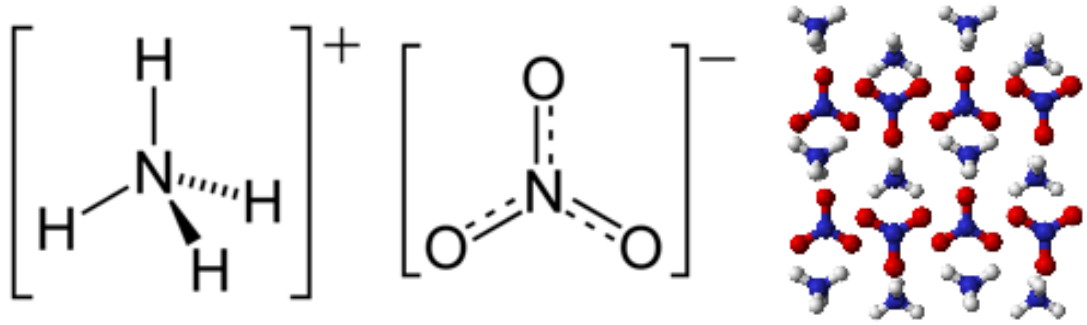

Figure 1. Structural formula of AN

AN is widely used both as a fertilizer and an explosive material [6]. AN has been used as a fertilizer for a long time. The annual consumption of AN in the US industry is millions of tons, among which around 20% is used as fertilizers and 80% is used as explosives or blasting agents [7]. The US consumption of AN in 2011 was 0.7 million tons [8]. Compared to AN-based explosives, AN fertilizer has a lower porosity and a higher density. To become an explosive, AN is mixed with fuel oil, called ammonium nitrate fuel-oil (ANFO) [2]. In the explosion of ANFO, the following oxygen-balanced, exothermic reaction Eq. (1) occurs, where a hydrocarbon is represented by CH_2 [9]. To compare with TNT, the heat of combustion of TNT is ΔH = - 4196 kJ·kg^{-1} [10].

Eq. (1) $3(NH_4NO_3) + CH_2 \rightarrow 3N_2 + 7\ H_2O + CO_2$ ΔH = - 4017 kJ·kg^{-1}

Plants can only absorb their required nutrients if they are present in easily dissolved and accessible chemical compounds. Most plants get their basic nutrients of carbon (C), hydrogen (H), and oxygen (O) from air and water. There are six macronutrients for plants [11, 12] which include nitrogen (N), phosphorus (P),

potassium (K), calcium (Ca), magnesium (Mg), and sulfur (S). Of these macronutrients, N, P, and K are the most important, hence accelerating the development of NPK blended fertilizers. The nine micronutrients [11, 12] needed by plants are boron (B), chlorine (Cl), copper (Cu), iron (Fe), manganese (Mn), molybdenum (Mo), zinc (Zn), nickel (Ni), and cobalt (Co).

Both organic and inorganic fertilizers provide the same needed chemical compounds. Compared with inorganic fertilizers, organic fertilizers are nearly always more difficult to absorb; harder to handle, transport, and distribute; have much lower concentrations of plant nutrients; are needed in larger volumes; and have the usual problems of uneconomical collection, containing undesired organisms, and higher prices [13, 14]. Therefore, inorganic fertilizers are more popular because of their low cost, high concentration of nutrients, and ease of handling.

Nearly all nitrogen that plants use is in the form of ammonia or nitrate compounds. As a fertilizer, AN is an excellent source of nitrogen for all crops, one of the most concentrated forms of nitrogen fertilizer (35% N), and referred to as AN-based fertilizer [1]. AN accounts for more than 15% of the world's nitrogen fertilizer market [15]. 40% of the world's food production is dependent on mineral fertilizer and this percentage is growing [16]. It is popular because it is very soluble in water, and hence in the soil and the nitrate can move deep into the root zone under wet conditions. In spring, the use of AN is especially good because it helps plants to grow faster. Furthermore, AN fertilizer and AN-based fertilizers are relatively inexpensive.

Some researchers argue that AN could be replaced by inherently safer alternatives. However, other nitrogen-rich fertilizers have their demerits that prevent them from substituting AN. For example, anhydrous ammonia [17, 18] is hard to handle, easy to volatilize, and more expensive than AN per ton. Urea [17] has the risk of nitrogen loss and volatilization concerns. In addition, urea could result in low plant yield. Ammonium sulfate's [17-19] nitrogen content (21% N) is low compared with AN, and its high acidity limits its use in some areas. Liquid nitrogen (half urea and half AN) [17, 20] is corrosive and will destroy brass, bronze, and zinc fittings. As of now, there is no good universal alternative or substitute for AN. The use of AN could be decreased to some extent, but not eliminated. If handled and stored properly in compliance with all the regulations, with inherently safer designs such as adding stabilizers, incidents involving AN can be prevented or mitigated.

AN is not considered a flammable chemical or combustible material at ambient temperatures [1, 2]. However, it is a strong oxidizing agent that can detonate [21] under certain conditions which include elevated temperature, presence of impurities [22], and confinement [3, 4]. AN is classified as a strong oxidizing agent in the Globally Harmonized System (GHS) [23], the world's classification system for hazardous materials. Based on United Nations (UN) recommendations on the transport of dangerous goods, AN is covered by Division 5.1 (oxidizers), Division 9 (AN-based fertilizer), and Division 1.1 (AN-based fertilizer). Section 38 of the United Nations Economic Commission for Europe (UNECE) classification [24] introduces the UN' scheme for the classification of AN fertilizers of Class 9. According to this

classification, to assess whether an AN fertilizer is capable of undergoing self-sustaining decomposition, there is a test procedure designed to find out if a decomposition initiated in a localized area will spread throughout the mass. AN has a National Fire Protection Association (NFPA) instability/reactivity rating of 3, indicating that AN is capable of detonation, and explosive decomposition or reaction may occur. The US Department of Transportation regulates AN with more than 0.2% combustible substances as an explosive material with specific storage requirements and restrictions in cargo vessels [7].

The hazard types [2] of AN are fire-related hazards (as an oxidizer), self-sustained decomposition (SSD) [25], and explosion hazards.

The root causes of an AN explosion include, but are not limited to, chemical contamination [22], elevated temperature, confinement [3, 4], and other storage conditions, such as humidity, heating rate, and gas atmosphere. It is evident from past AN incidents that the presence of impurities and environmental conditions have a huge effect on the detonation of AN during storage. Therefore, continuous research needs to be performed to gain deeper understanding on the effect of contamination and environmental conditions on the decomposition of AN. No research group has been able to cause AN to detonate on the small-scale in the laboratory so, as yet, there is no methodology for a scientific study of the factors that promote detonation of AN other than through AN incident reports or perhaps molecular modelling.

1.3 AN-Related Incidents

AN-related fires and explosions continue to occur time and again, despite the fact that AN has been extensively investigated. There have been more than 70 AN-related incidents during the last century, which reemphasize the dire need for further research on AN reactive hazards. Table 1 lists 79 AN-related incidents, out of which 42 occurred in the US.

One of the most recent AN explosions occurred in Tianjin, China, on August 12, 2015, and killed 165 people including 99 firefighters who responded to the fire and 11 police officers. Eight more people were missing and 798 were injured [26, 27]. Two explosions occurred 43 minutes after the first fire, and the second explosion was devastating [27]. From the evidence of a typical crater in the ground, AN, perhaps with other substances, is believed to have detonated in the explosion, leading to significant devastation [28]. The investigators said stocks of nitrocellulose at the Ruihai warehouses became too dry because of the loss of humidifying agents, and began to heat up in the hot summer weather. The material then started to burn and the flames then spread to illegal stores of the combustible fertilizer AN, initiating two massive explosions [29].

Table 1. AN-related incidents [22, 30-33]

Location	Year	Location	Year
Kensington, UK	1896	Typpi, Oy, Finland	1963
Faversham, Kent, UK	1916	Mt. Vernon, MO, US	1966
Oakdale, PA, US	1916	Peytona, WV, US	1966
Gibbstown, NJ, US	1916	Amboy, IL, US	1966
Morgan, NJ, US	1918	Potosi, WI, US	1967
Stolberg, Germany	1920	Taroom, Queensland, Australia	1972
Vergiati, Italy	1920	France	1972
Barksdale, WI, US	1920	Cheerokee, Prvor, OK, US	1973
Brooklyn, NY, US	1920	Bucharest, Romania	1974
Kriewald, Germany	1921	Tahawas, NY, US	1976
Oppau, Germany	1921	Delaware City, DE, US	1977
Knurów, Poland	1921	Rocky Mountain, NC, US	1978
Sinnnemahoning, PA, US	1922	Moreland, ID, US	1979
Cleveland, OH, US	1922	UK	1982
Nixon, NewBrunswick, NJ, US	1924	Kansas City, MO, US	1988
Muscle Shoals, AL, US	1925	Joplin, MO, US	1989
Emporium, PA, US	1925	Porgera Valley, Papua New Guinea	1994
Gibbstown, NJ, US	1932	Port Neal, IA, US	1994
Merano, Italy	1936	Brazil	1997
Gibbstown, NJ, US	1940	Xingping, Shanxi, China	1998
Rouen, France	1940	Kentucky, US	1998
Miramas, France	1940	FL, US	2000
Tessenderloo, Belgium	1942	Toulouse, France	2001
Milan, TN, US	1944	Cartagena, Murcia, Spain	2003
Benson, AZ, US	1944	Saint-Romain-en-Jarez, France	2003
Texas City, TX, US	1947	Keyshabur, Khorasan, Iran	2004
Presque Isle, ME, US	1947	Barracas, Spain	2004
Brest, France	1947	Mihăileşti, Buzău, Romania	2004
St. Stephens, Canada	1947	Ryongchŏn, North Korea	2004
Independence, KS, US	1949	Estaca de Bares, Spain	2007
Pinole, CA, US	1953	Monclova, Coahuila, Mexico	2007
Red Sea, Israel	1953	Bryan, TX, US	2009
Red Sea	1954	Zhaoxian, Hebei, China	2012
New Castle, PA, US	1956	West, TX, US	2013
Mt. Braddock, PA, US	1958	Athens, TX, US	2014
Roseburg, OR, US	1959	Wyandra, Queensland, Australia	2014
Traskwood, AR, US	1960	B.C., Canada	2014
Boron, CA, US	1960	Ti Tree, Australia	2014
Norton, VA, US	1961	Tianjin, China	2015
Traskwood, AR, US	1963		

Only in the last three months of 2014, there have been three serious incidents related with AN around the world. On September 5, 2014, an AN truck explosion occurred in south-west Queensland, Australia [34]. The truck carrying 56 tons [34] of AN rolled over a bridge and exploded, injuring eight persons including the driver, a police officer, and six firefighters [35]. On November 6, 2014, a truck which was carrying about 40,000 kg of AN caught fire near Kamloops, B.C., Canada. The police extended an evacuation order to a 1,600 m radius of the fire [36]. On November 18, 2014, a trailer of AN caught fire on the Stuart Highway at Ti Tree, Australia. The trailer exploded after a while, and the police evacuated residents within 1,000 m radius of the spot [37].

Another incident occurred at the West fertilizer plant, in Texas, US, on April 17, 2013. In this explosion, 270 tons [38] of AN was involved, out of which approximately 30 tons detonated [39], which killed 15 people and injured more than 250 people [40]. The resulting blast-wave completely destroyed the entire facility and caused various levels of damage to many buildings, businesses, and homes at significantly long distances from the plant. There were more than 50 homes, a 50-unit apartment building, a nursing home, and four schools located in the impact zone, which was within around 600 m of the plant.

An explosion occurred on September 21, 2001, in the AZF (Azote de France) fertilizer factory in Toulouse, France [41], involving 300 tons of AN, resulting in 30 deaths and 2,242 injuries. At the time the incident occurred, there was no pump or no heat source. AN contaminated with sodium dichloroisocyanurate (*i.e.*, DClCNa) was

determined to be the root cause of this incident [42]. The off-specification granular AN was stored flat in a warehouse between process parts, and was separated by partitions when the explosion occurred. The explosion created a crater of 10 meters in depth and 50 meters in width. The resulting blast wave affected windows up to 3 kilometers away from the factory. The material damage was believed to be 2.3 billion euros (*i.e.*, 3.17 billion US dollars) [43].

On December 13, 1994, an AN solution explosion occurred in an AN plant at Terra International, Inc., in Port Neal, Iowa, and killed four workers [44]. The explosion was in a neutralizer vessel during a manufacturing process, resulting in severe consequences, such as damage to the ammonia tanks and the formation of an ammonia cloud.

One of the deadliest industrial incidents in US history occurred on April 16, 1947, in Texas City, Texas, where an AN explosion involving 2,300 tons of AN caused 581 fatalities and thousands of injuries [1]. In that incident, a fire caused the initial explosion of AN on a ship, which resulted in subsequent chain reactions of fires and explosions in other ships and facilities nearby. The AN that exploded was coated with wax to prevent caking [45]. It needs to be emphasized that new technologies and safe practices introduced in the 1950s eliminated the use of wax coatings, and recent AN produced for fertilizer use should contain less than 0.2 percent combustible material [7].

Similarly, on September 21, 1921, in Oppau, Germany, an AN explosion involving 450 tons of AN-based fertilizer caused 561 fatalities, 1,952 injuries, and left 7,500 people homeless [46]. The fertilizer used in Oppau was a mixture of AN and

ammonium sulfate with a ratio of 50:50. The root cause of the incident was that people tried to disaggregate caked fertilizer mixture by using industrial explosives. The method of disaggregation had been used over 20,000 times without any incident until the drying technology was changed, which made the AN more prone to detonation. The explosion created a (90 m) x (125 m) crater with a 20 m depth. According to the witnesses, there were two successive explosions, the first one being weak and the second one devastating. According to what was reported in the New York Times (dated 29 January 1922), the material loss was approximately 321,000,000 marks (*i.e.*, 1.7 million US dollars in the year when the incident occurred).

The Oklahoma City [47] terrorist attack on April 19, 1995, killing 168 people, which involved AN-based explosives, also brought awareness to the dangers of AN.

1.4 AN-Related Regulations and Rules

In the US, the Occupational Safety and Health Administration (OSHA) has specific regulations that apply to the use of AN, such as the Explosives and Blasting Agents Standard (29 CFR 1910.109). Furthermore, general requirements of OSHA include the "General Duty Clause" of the Occupational Safety and Health Act (P.L. 91-596, as amended), the Hazard Communication Standard (29 CFR 1910.1200), and an Emergency Action Plan (EAP) according to OSHA Standard 1910.38. The Environmental Protection Agency (EPA) [4] also has a general duty clause and specific regulations that apply to facilities that handle AN, including the Emergency Planning

and Community Right to Know Act (EPCRA) and Section 112(r) of the Clean Air Act Amendments (CAAA). The Department of Homeland Security (DHS) regulations include the proposed rule regulating the control of the purchase and the sales of AN (Section 563) and the Chemical Facility Anti-Terrorism Standards (CFATS). The Bureau of Alcohol, Tobacco, Firearms and Explosives (ATF) regulates AN-based blasting agents with regulations on the necessary distance to be maintained between AN and other explosive materials.

In the UK, two of the most relevant regulations that control the manufacture, importation, storage, and transportation of AN fertilizer include the Ammonium Nitrate Materials (High Nitrogen Content) Safety Regulations 2003 (AN Safety Regulations) and the Control of Major Accident Hazards Regulations 1999, as amended (COMAH).

1.5 Thermal Decomposition of AN

Thermal decomposition of AN has been studied in the literature using various types of calorimetry, such as Differential Scanning Calorimetry (DSC) [22], Setaram C80 Heat Flux Calorimeter (C80) [48], Accelerating Rate Calorimetry (ARC) [42], Thermogravimetric Analysis (TGA) [49], and Adiabatic Dewar Calorimeter (ADC) [50]. Due to the variation in levels of accuracy in each apparatus, the detected “onset” temperature of decomposition highly depends on the sensor sensitivity and accuracy of the calorimeter. Different “onset” temperatures have been reported when determined by different calorimeters, indicating that there is no consistent “onset” temperature of AN

decomposition available. According to Arrhenius law, reaction rates have an exponential dependency on temperature, reaction rates at low temperatures are very slow [51], and our ability to "detect" when a reaction "starts" depends on the sensitivity of the employed experimental equipment. In fact, at a molecular level, the decomposition reaction occurs without being measured. The "onset" temperature is related not only with the reaction, but the detection capacity of the equipment. The so-called "onset" temperature only marks the temperature at which the thermal effects caused by the reaction become detectable by the employed equipment. Depending on the sensitivity of the equipment to trace heating rates (or temperature rise rates), different "onset" temperatures of AN decomposition have been reported. The melting point of AN is around 170 °C and it is reported to decompose above 210 °C [3, 52]. Previous studies [53, 54] have reported that even at 200 °C, slow decomposition can occur. Other adiabatic calorimetry tests indicate that AN may decompose as early as 190 °C [24, 50]. These reported "onset" temperatures are dependent on the sensitivity of the device being used to measure them, and the reactions can still occur before the "onset" is detected by equipment.

Different macroscopic AN decomposition paths have been proposed and reported in the literature, of which the most accepted reactions are summarized here [9, 22, 49, 54-58]. An endothermic reversible reaction can occur at relatively low temperatures (*i.e.*, around 170 °C). It is believed that the vaporization of molten AN leads to the formation of ammonia and nitric acid, which could initiate the decomposition of AN through reaction Eq. (2) [9, 22, 49, 54-56, 58, 59].

Eq. (2) $NH_4NO_3 \rightleftharpoons HNO_3 + NH_3 \quad \Delta H=176\ kJ\cdot mol^{-1}$

At higher temperatures (*i.e.*, between 170 °C and 280 °C) exothermic irreversible reactions occur, as shown in Eq. (3) to Eq. (5) [9, 17, 22, 49, 54-56, 58, 59].

Eq. (3) $NH_4NO_3 \rightarrow N_2O + 2H_2O \quad \Delta H= -59\ kJ\cdot mol^{-1}$

Eq. (4) $NH_4NO_3 \rightarrow 1/2N_2 + NO + 2H_2O \quad \Delta H= -257\ kJ\cdot mol^{-1}$

Eq. (5) $NH_4NO_3 \rightarrow 3/4N_2 + 1/2NO_2 + 2H_2O \quad \Delta H= -944\ kJ\cdot mol^{-1}$

If the material is suddenly heated up, there will be explosive decompositions as shown in Eq. (6) and Eq. (7) [56].

Eq. (6) $2NH_4NO_3 \rightarrow 2N_2 + O_2 + 4H_2O \quad \Delta H= -1057\ kJ\cdot mol^{-1}$

Eq. (7) $8NH_4NO_3 \rightarrow 5N_2 + 4NO + 2NO_2 + 16H_2O \quad \Delta H= -600\ kJ\cdot mol^{-1}$

The generally accepted mechanism of AN decomposition is that the dissociation of HNO_3 leads to the subsequent oxidation of NH_3 [57], *e.g.*, Rosser *et al.* [55] proposed reaction Eq. (8) as the dissociation reaction of HNO_3, which generates NO_2^+, acting as the oxidizing species for NH_3 as listed in reaction Eq. (9), and leads to the formation of N_2O and water. In that study, a flow system was used to measure the rate of production of the reaction. Eq. (10) shows a more realistic reaction path of HNO_3 decomposition [57].

Eq. (8) $2HNO_3 \rightleftharpoons NO_2^+ + NO_3^- + H_2O$

Eq. (9) $NH_3 + NO_2^+ = \text{products } (N_2O, H_2O)$

Eq. (10) $2HNO_3 \rightleftharpoons 2NO_2 + H_2O + \frac{1}{2}O_2$

To explain reaction Eq. (8) and Eq. (9) in more detail, in the presence of water, using “acid” to indicate NH_4^+, H_3O^+, or HNO_3, the following decomposition mechanism Eq. (11) - Eq. (13) have been proposed [24], where reaction Eq. (12) is considered the controlling step due to its slow reaction rate.

Eq. (11) $HNO_3 + \text{acid} \rightleftharpoons H_2ONO_2^+ \rightarrow NO_2^+ + H_2O$

Eq. (12) $NO_2^+ + NH_3 \rightarrow [NH_3NO_2^+]$ *

Eq. (13) $[NH_3NO_2^+] \rightarrow NO_2 + H_3O^+ \rightarrow NO_2 + H_2O$

Reaction Eq. (12) is also described in terms of elementary reactions in the literature [60] at the temperature range 342-387 °C, where NO_2^+ subsequently oxidizes NH_3, as listed in reactions Eq. (14) - Eq. (19). Reaction Eq. (20) is the overall stoichiometry according to this theory.

Eq. (14) $NH_3 + NO_2 \rightarrow NH_2 + HNO_2$

Eq. (15) $NH_2 + NO_2 \rightarrow NH + HNO_2$

Eq. (16) $NH + NO_2 \rightarrow HNO + NO$

Eq. (17) $NH_2 + NO \rightarrow N_2 + H_2O$

Eq. (18) $2HNO \rightarrow N_2O + H_2O$

Eq. (19) $2HNO_2 \rightarrow NO_2 + H_2O + NO$

Eq. (20) $4NH_3 + 5NO_2 \rightarrow N_2O + 2N_2 + 6H_2O + 3NO$

Slightly different from the previous mentioned mechanism, another approach [61] assumes that the formation of a nitramide intermediate out of AN results in the decomposition of AN, as listed in reactions Eq. (21) to Eq. (25).

Eq. (21) $NH_4^+ + NO_3^- = NH_3 + HONO_2$

Eq. (22) $HONO_2 \rightarrow HO + NO_2$

Eq. (23) $HO + NH_3 \rightarrow HOH + NH_2$

Eq. (24) $NH_2 + NO_2 \rightarrow NH_2NO_2$

Eq. (25) $NH_2NO_2 \rightarrow N_2O + H_2O$

Nitrous oxide (N_2O) is a gaseous oxidizer. It will decompose exothermally. As an energetic oxidizer, presumably an electric spark through oxygen infused plastic seats could have started fires of N_2O gas [62]. One large N_2O explosion occurred in July 2007 in Mojave, CA [62]. Small-scale explosions have been observed during supercritical N_2O extraction processes [63]. Medical use of N_2O has both explosive risk and fire hazard [62]. The heat release of N_2O decomposition is relatively high, 163 $kJ \cdot mol^{-1}$. When it reacts with other gases, such as CO and NO, the heat of reaction can be as high as 139 – 557 $kJ \cdot mol^{-1}$ [64]. In condensed form it is even used as a mono-propellant for rocket propulsion as it deflagrates under pressure. It is to be considered an explosive gas, certainly at higher temperatures and pressures, and even more so in the vicinity of a fuel. At sufficiently high temperature it auto-ignites. Ammonia can act here as fuel. NH_3 mixed with air is explosive although the lower flammable limit (ca. 14%) and minimum ignition energy are relatively high, while the explosive severity is low (K_G about 5 $bar \cdot m \cdot s^{-1}$). Gas phase deflagration of the fumes coming off a mass of decomposing AN in a fire can therefore not be excluded.

1.6 Condition Dependent Decomposition of AN during Storage

As mentioned in Section 1.2, the decomposition of AN is affected by several factors, such as the presence of additives, water, confinement, temperature and heating rate. This section discusses those conditions that affect AN thermal stability.

In terms of regulations, the storage of AN should follow OSHA regulations, including the Explosives and Blasting Agents Standard (29 CFR 1910.109) [65], which regulates the storage, use, and transportation of explosives and blasting agents. Mixtures of fuel and oxidizers that might contain AN, are regulated. Based on the OSHA regulation for "Storage of ammonium nitrate" (1910.109(i)), the specific requirements for the storage of AN should be complied with, but not limited to: "*storage buildings shall not be over one storey in height, with adequate ventilation or be of a construction that will be self-ventilating in the event of fire; warehouses shall have adequate ventilation or be capable of adequate ventilation in case of fire; due to the corrosive and reactive properties of AN, avoid contamination; buildings and structures shall be dry and free from water seepage through the roof, walls, and floors*". The requirements for building materials, containers, and separation distances are also discussed. The storage conditions [66], such as the presence of additives [67], water, and confined space, have been highlighted by OSHA standard 29 CFR 1910.109 [65], which could be studied in a more detailed manner.

1.6.1 Effects of Additives

The explosion hazards of AN have been widely studied and a number of efforts have been made to study the thermal effects of AN with additives [41, 68-71]. The additives are classified into two types – inhibitors and promoters. Some chemicals behave as inert materials that result in the dilution of AN, or other materials will change the chemical reaction conditions due to incorporation, reducing the probability of an AN explosion [22]. These chemicals are called inhibitors because they can help mitigate the AN explosion potentials. Oxley *et al.* [22] have shown that the sodium, potassium, ammonium and calcium salts of sulfate, phosphate, or carbonate as well as certain high-nitrogen organics (urea, oxalate, formate, guanidinum salts) are good inhibitors as they enhance AN thermal stability and can be used as fertilizers. Sodium salts of weak acids (carbonic, acetic, formic, oxalic, and hydrofluoric) are also proven to be good inhibitors.

On the contrary, some other chemicals called promoters, accelerate the AN explosion rate. Promoters, *i.e.*, contaminants, were believed to be one of the contributing factors to some incidents, such as those that occurred in West, Texas City, and Toulouse. Though the cause of the Toulouse disaster is still unclear, one potential reason is that AN contaminated with chloride (*i.e.*, sodium dichloroisocyanurate (DClCNa)) caused the explosion. Laboratory-scale experiment showed that AN-DClCNa mixture has higher decomposition rates than pure AN [42]. In another research [72], it is reported that moistened AN-DClCNa mixture could produce NCl_3, leading to the detonation of the mixture in the applied laboratory-scale.

Promoters include explosive substances [1], such as nitrocellulose and aromatic nitro compounds; non-explosive combustible substances [1], such as sulphur, charcoal, flour, sugar, or oil; incombustible substances [1], such as pyrite [49], zinc, cadmium, and copper; chloride salts [48], such as ammonium chloride, barium chloride, calcium chloride, sodium chloride, and potassium chloride; cations of chromium, iron, and aluminum [53]; carbonaceous materials; hydrocarbon waxes [73]; inorganic acids, like sulfuric acid and hydrochloric acid [24]; common organic contaminants [2], such as animal fats, baled cotton, baled rags, baled scrap paper, bleaching powder, burlap or cotton bags, caustic soda, coke, charcoal, coal, cork, camphor, excelsior, fibers of any sort, fish oil, fish meal, foam rubber, hay, lubricating oil, linseed oil or drying oils, naphthalene, oakum, oiled clothing, oiled paper, oiled textiles, paint, straw, sawdust, wood shavings, and vegetable oil. It needs to be pointed out that when AN is in contact with organic contaminants, acid materials, chloride salts, or the mixture of any of those, it can self-heat from low temperatures to explosion.

The promoting effect of the above mentioned materials can be a result of their chemical affinity with AN; or they can affect the mass and heat transfer when the reaction occurs; or due to a constant supply of high temperature, because of the heat generated by the flammable compounds.

As explained below, only compounds which could be used as fertilizers are considered in this work. Despite the large number of additives identified in the literature, there is not an agreement of the explanation on the mechanism that drives the behavior of AN decomposition with these additives. Additionally, experiments with very low

quantities of AN have been performed which may not represent the actual situation adequately. Therefore, this research reports the thermal stability of AN with various additives.

Apart from AN decomposition with a single additive, which has been widely studied in literature, this work also focuses on AN mixed with two additives simultaneously. In literature, binary mixtures with AN have been studied mainly as explosives. Oxley *et al.* [22] obtained a relative ranking of the explosivity of energetic materials using the small-scale explosivity device (SSED) and compared SSED results with pipe bomb fragmentation data. They mixed AN with more than one additive, such as the mixture of ammonium sulfate, calcium carbonate, and urea. They found that low thermal stability was indeed related to high explosivity, but high thermal stability was no guarantee of low explosivity. Levchenko *et al.* [74] identified the optimal (most easily controlled) explosive composition of a three-component additive containing potassium salts and $Mg(NO_3)_2$ as oxidizing agent. The effect of heating rate on thermal runaway was investigated by Boddington *et al.* [75], by mixing AN with ethylenediaminedinitrate and potassium nitrate to make explosive materials. AN was mixed with potassium nitrate and complexone salts to phase-stabilize AN as oxidant by Klyakin and Taranushich [76]. In other publications, AN mixture with binary additives has also been reported. Klimova *et al.* [77] elucidated the thermodynamic effect of AN decomposition when mixed with Ca and Mg carbonates with or without the presence of boron, manganese and copper compounds, such as AN mixture with $CaCO_3$ and $CuSO_4$; $CaCO_3$ and H_3BO_3; $CaCO_3$ and MnO_2. They found that equilibrium concentrations do not depend on the carbonate

origin of $CaCO_3$, $MgCO_3$ or $CaMg(CO_3)_2$. In other work [78], AN was mixed with additives, such as FeS and urea, FeS_2 and NaF. Their conclusion was that salts of weak acids and urea stabilized AN formulations, even in the presence of destabilizing species.

1.6.2 Water Effects

In AN incidents involving fire, which often lead to AN explosions, if water is used to mitigate the fire, care should be taken to use ample quantities of water to tackle the fire [3]. In a fire scenario, if there is a lack of the sufficient amount of water needed to mitigate the fire, the water will evaporate and combine with the oxygen supplied by the nitrate. The presence of insufficient water at elevated temperature increases the intensity of the AN fire and the explosion potentials [79]. Ettouney *et al.* [80] proved that, by varying catalysis and acidity, or increasing temperature, AN in solution can also explode. There needs to be a procedure to calculate the amount of water needed to put out fires involving AN. That is to say, the threshold should be identified to what amount of water could increase the AN hazards, and what amount would be sufficient to tackle the fire without increasing its explosion potentials. This is of critical importance to guide firefighters responding to fires involving AN. The complexities of tackling AN-related fires with water is discussed in Section 6.3.

1.6.3 Confined Space

Confinement plays an important role in AN explosion, and was believed to help trigger the explosion in the Port Neal ammonium nitrate plant incident [44, 81]. The European Fertilizer Manufacturers Association's **(**EFMA) guidance document states that AN has high resistance to detonation; however, heating under strong confinement can lead to explosive behavior [82]. According to NFPA 49, if AN is subjected to strong shocks or heated under confinement causing a pressure build-up, it may undergo detonation [83]. Accelerating Rate Calorimeter (ARC) has been used to study the runaway behavior of nitroguanidine to observe the effects of confinement [84] by comparing its decomposition in both confined and non-confined system. The results show that in the confined system, the "onset" temperature of nitroguanidine decomposition is lower than that of the non-confined system, the self-heating rate is faster, the time to maximum rate is shorter, and the rate of pressure increase is faster. Also, it is believed that in the non-confined system, the increase in temperature was so small that it was hard to analyze the data. As a conclusion, confinement significantly affects the behavior of nitroguanidine decomposition. However, the effect of confinement on AN has not been reported in literature. Therefore, experiments to study the effect of confinement on AN and to identify similarities or difference with the reactive behavior of other nitro-compounds would be useful. One of the targets of this work is to study the effect of confinement on AN decomposition using a similar strategy to the one used by Lee and Back [84], *i.e.*, by varying the initial pressures of N_2 gas. By

understanding the risks of confined space, this study could potentially help reduce the hazards in AN storage and transportation, where confinement does exist. More work needs to be done on determining to what extent confinement will affect AN decomposition. For example, if a certain amount of AN is stored in a warehouse, how much space must be left within the warehouse, or how high a pile of material can be to ensure the confinement will not result in catastrophic explosions.

1.6.4 Effect of Temperature and Heating Rate

Heating rate is another important factor, which affects AN thermal decomposition. As described in Section 1.5, when AN is heated to around 200 °C, it begins to decompose and give off heat [56]. Furthermore, if the temperature goes beyond 260 °C, the decomposition of AN becomes much faster. Most of the work reported in literature has been performed using low heating rates, which are used to simulate AN storage conditions; however, high heating rates simulate the effects of fire or combustion conditions, and therefore, it is important to study decomposition at higher heating rates as well. The importance of heating rate on AN decomposition was elucidated by Anderson *et al.* [85, 86]. Fast heating rate experiments of AN decomposition are reported in literature [87]. It has been shown that surface decomposition of AN occurs endothermically producing NH_3 and HNO_3 at higher heating rates, but slow heating rates lead to bulk decomposition exothermically producing N_2O and H_2O [56, 88]. However, the results of different heating rates reported in literature employ different experimental

conditions, such as sample size, equipment, and pad gas; therefore, it is not possible to systematically compare different heating rates, as AN decomposition is condition dependent with the sample size in particular having a pronounced effect. This work reports the effect of heating rates using the RSST and the APTAC with samples of the order of a few grams.

1.6.5 Effect of Thermal History – Pre-heat

The effect of thermal history of AN will influence its behavior. In storage areas, the temperatures may vary at different time periods in one day, thus affecting the material behavior. Adopted from a similar study for the effect of temperature [89], the AN sample could be first heated to a desired temperature much lower than the melting point and then held at that temperature for a specified period of time. The sample should then be cooled to room temperature and tested to determine if the pre-treatment would have any effect on the runaway behavior. Another approach is to keep the sample at a particular temperature for a defined period of time, and then run the test. This will simulate the real world storage conditions of AN where ambient temperatures could increase to a relatively higher value. The pre-treatment time could vary based on real situation. The pre-treatment temperature could be either high or low. For high temperatures, it should be lower than the "onset" temperature or the melting point of AN, which is 169 °C, and it should be higher than the ambient temperature, but still be attainable by storage areas, *e.g.*, between 50-70 °C. For studies under very low

temperatures, the AN sample could be stored in an ice bath. Also, after pre-treatment, analytical techniques like XRD could be applied to observe the structural changes of the samples.

1.6.6 Effect of Humidity

AN is very hygroscopic by nature, and it readily absorbs water vapor from the atmosphere and forms aggregates with high mechanical resistance. In some cases, water vapor causes partial dissolution of powder which can lead to caking [90], self-compression, and self-confinement. According to Health and Safety Executive (HSE) [3], AN should be kept away from water contamination to prevent caking, which can increase the AN detonation hazards. For this reason, AN loading under raining and snowing conditions is not recommended. The humidity level that can aggravate detonation of AN has not been identified in literature and needs to be studied further. Section 6.3 discusses the complexities of fighting AN-related fires with water.

1.6.7 Effect of Surrounding Gas Atmosphere

The study of the effects of different types of gas atmospheres is important from the point of view of the influence of gas atmosphere in terms of propagation and mitigation of explosion potentials of AN. Studies under oxygen-rich atmospheres will provide more information on worst-case scenarios. It has been reported in the literature

[56] that AN releases ammonia continuously at a very slow rate during its storage in bags. It would be important to study the influence of an ammonia atmosphere to imitate those conditions. Nitrogen is also one of the products of AN decomposition [56]. As an inert gas, argon could be interesting in terms of mitigating the explosion potentials associated with AN. As the smallest atom, helium might lead to different decomposition behavior of AN. Carbon dioxide can be used as a carbon-based gas atmosphere to create smoke contamination of AN. Therefore, it is important to study the effect of different gas atmospheres. In studying nitroguanidine [84], it has been shown that air and nitrogen as different intitial gas atmospheres provide different results. Until now, limited research has been conducted to study the effects of gas atmosphere on the decomposition of AN, and further work needs to be conducted to gain a better understanding.

1.7 Calorimetry as a Tool to Evaluate Thermal Risk of Chemical Processes

The determination of thermo-kinetic parameters, heat transfer, and safety data can be achieved by the use of different calorimetric techniques [91]. Different calorimetric techniques allow the study of different sample sizes.

In runaway reactions, the hazard does not vary linearly with the amount of reactant. The hazard-indicators (*i.e.*, the "onset" temperature, peak pressure, maximum pressure rate, and total heat of reaction) of condition-dependent runaway reactions vary exponentially with the mass of reactant; thus, it is of paramount importance to evaluate

AN hazards with various sample sizes and to determine if the reaction follows a trend upon scale-up.

The importance of the scale-up of laboratory data has been addressed by Maschio *et al.* [91], where an integrated calorimetric approach was used to represent an efficient methodology to analyze and develop complex chemical processes. According to the authors, Differential Scanning Calorimetry (DSC), as a micro-calorimeter, has been used for the determination of fundamental thermo-kinetic process parameters. However, DSC data are not comparable with large-scale reactors, because the heat exchange capacity decreases as the reactor volume increases and the DSC data are usually obtained under conditions far from what is employed in industrial processes. Generally speaking, industrial runaway reactions are nearly adiabatic [92]. Additionally, thermodynamic data from adiabatic calorimeters, like adiabatic temperature rise and maximum pressure, can help determine process design parameters [92]. As a result, other reaction calorimeters, such as adiabatic calorimetry with larger sample sizes, should be utilized to better study reactions, which can provide more realistic information than a DSC.

Studies on the thermal behavior of AN are available in the literature. However, most previous research on AN with additives used a DSC, which tests only a few milligrams of sample. This work presents results of thermal decomposition of the AN under various conditions obtained using much larger sample sizes. The experimental data are compared with those reported in literature.

This work reports AN experimental data obtained by the Reactive Systems Screening Tool (RSST), a pseudo-adiabatic calorimeter, and the Automated Pressure

Tracking Adiabatic Calorimeter (APTAC), an adiabatic calorimeter, with sample sizes three orders of magnitude larger than the DSC. The details about those two calorimeters are introduced in Section 3.2, and Section 3.3 and Section 3.4 discuss the data analysis and experimental procedures respectively.

2. PROBLEM STATEMENT AND OBJECTIVES

As discussed in Section 1, AN has caused many deadly incidents which have led to the loss of life and property. The literature review performed in Section 1 identified a number of important gaps in the various studies done thus far.

In view of the above discussion, the primary objective of the research is the advancement of understanding of the effect of different conditions on the decomposition of AN and furthering the use of this particular knowledge to lower the explosivity of AN, mitigate the risks, and make it inherently safer. The design of an inherently safer way of storing AN or the modification of AN storage conditions could be one approach. More specifically, this work systematically studied the safety issues associated with AN. In addition, this work sets the foundation for a long-term research program in the field of similar runaway reactions.

This research looks at reducing the explosion risks associated with AN, including identifying the root causes associated with AN explosion, specifically the conditions that affect AN decomposition. On the one hand, the safety issues associated with the storage of AN were considered. On the other hand, thermodynamic and kinetic parameters related to AN were developed. The RSST and the APTAC were used for reactivity evaluation to study the mechanisms that result in AN explosions. The runaway behaviors of AN were characterized by obtaining important parameters, like “onset” temperature, self-heating rate and pressure-rise rate of AN decomposition, heat of reaction, and

activation energy of the reactions. In addition, the complexities of tackling AN-related fires with water are discussed.

2.1 Objectives

The ultimate goal of this study is to make AN safer as a fertilizer. To achieve this goal, it is necessary to collect the data that will provide better understanding of the reaction and will serve as the foundation for such reactive chemical studies. The various sub-objectives of this work follow.

- To evaluate the thermal stability of pure AN using adiabatic calorimetry, and to determine the runaway behavior and parameters associated with its decomposition.
- To identify inhibitors and promoters for the study of additives through various experiments, including the study of single additive and binary additives.
- To calculate the thermodynamic and kinetic parameters of the AN decomposition both individually and with additives, and to identify the key parameters, such as the “onset” temperature and maximum self-heating rate. Further, this work targets mathematical models to predict the results of certain additives.
- To analyze the mechanisms of decomposition associated with AN for both pure AN and AN mixture with additives, to explain the decomposition from a fundamental point of view.

- To study the condition-dependent thermal decomposition of AN, including the effect of additives, confinement, heating rate, thermal history, temperature, sample size, and isothermal testing; to calculate the thermodynamic and kinetic parameters of the AN decompositions under those conditions; and to determine the safe conditions for AN storage and transportation.
- To include the thermal inertia factor in the data analysis, so that the experimental errors are reduced substantially, and more accurate results are obtained.
- To explain the AN explosion phenomenology and to discuss the complexities of fighting AN storage-area fires. This could contribute to a better understanding of how AN fires propagate to deflagration or detonation, and treat the issue of tackling AN fires with inadequate amount of water.

3. METHODOLOGY

As mentioned earlier in previous sections, this work looks at reducing the explosion risks associated with AN, including identifying the root causes associated with AN explosion, specifically the conditions that affect AN decomposition. This section explains the steps followed to further the understanding on AN decomposition and also provides details on the experimental techniques, equipment, methods, and procedures used to analyze the data necessary to address the issues with AN hazards.

3.1 Research Methodology

In this project, experimental analysis, theoretical methods, and systematic approaches for reactivity evaluation were used to study the mechanisms that result in runaway reactions related with AN. The pseudo-adiabatic calorimetry, RSST, and adiabatic calorimetry, APTAC, were employed to study the effects of different factors on the condition-dependent AN decomposition. Thermodynamic and kinetic parameters were estimated based on the test data. The test results as well as the calculated parameters were compared with literature data acquired through other calorimetry and models.

A schematic of the research methodology is described in Figure 2. The methodology can be divided into three main parts: the analysis of AN decomposition with additives, the evaluation of storage conditions for AN, and the assessment of the

complexities of fighting AN-related fires with water. The first two parts were mainly based on the use of pseudo-adiabatic calorimetry and adiabatic calorimetry to characterize the AN decomposition with various conditions and to understand the safe storage conditions for AN. In addition, the AN decomposition phenomenology and complexities of fighting AN fires with water were discussed.

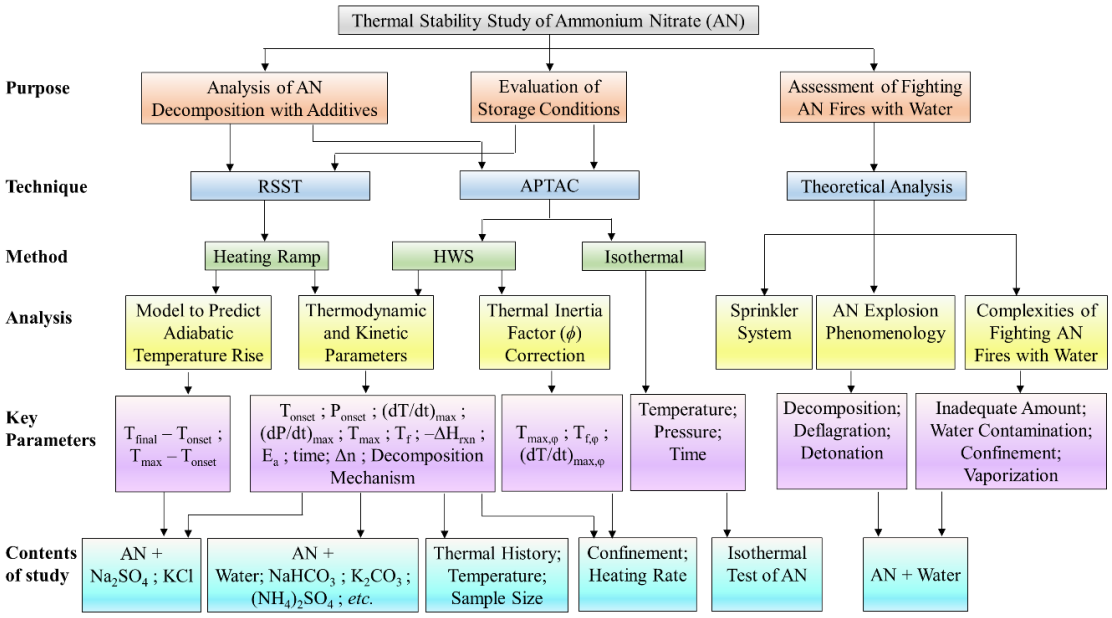

Figure 2. Research methodology for the current study

In terms of the analysis of AN decomposition with additives, there are two types of additives, *i.e.*, promoters that intensify an AN explosion and inhibitors that tend to stabilize AN. Despite exhaustive research in this area, the understanding for the underlying causes of the detonation of AN is limited. In view of this, this study presents research initiatives and strategies that need to be undertaken to better understand the

explosivity of AN. Both experimental and theoretical work was employed to understand the root causes that lead to the decomposition and further detonation of AN. To start with, the mixture of sodium sulfate and potassium chloride with AN in various concentrations were tested in the RSST and the APTAC. The thermodynamic and kinetic parameters were analyzed, and models to predict the temperatures were proposed. Some other chemicals were also mixed with AN and tested in various concentrations as well, which are explained in detail in the later sections.

AN decomposition is affected by other conditions, such as confinement, heating rate, thermal history, temperature, and sample size. Those conditions were also studied using the heating ramp mode in the RSST and the HWS mode in the APTAC. The thermodynamic and kinetic parameters were analyzed, and the data were corrected based on the thermal inertia factor to provide more accurate results. In addition, isothermal mode was used to study the decomposition of pure AN. Thus, the safe storage conditions for AN were identified.

For the issues of fighting AN-related fires with water, theoretical analysis was performed. The explosion phenomenology of AN was introduced, including thermal decomposition, deflagration, and detonation. Later on, the use of water to tackle AN-related fires was discussed in detail. Water is the only agent that should be used to fight a fire in an AN store, but too small amounts may exacerbate the conditions for a catastrophic explosion instead of attenuation. This work focused on the use of inadequate amount of water, water contamination, the use of water to AN in a confined

space, the vaporization of water when heated, and the use of water in AN fires with contamination.

3.2 Equipment – Calorimetry

Calorimetry is a widely used tool in assessing reactive chemical hazards, which helps to assess the thermal risks of runaway reactions. A thorough understanding of the results from calorimetry helps to understand the behavior of the chemical, which further helps to prevent reactive incidents.

In the research, calorimetric measurements using RSST and APTAC were used to complement previous studies on AN using other calorimetric techniques, such as DSC, in order to study the performance of AN with additives. Data from calorimetric measurements in this study, and from previous studies, also provide different parameters necessary for identifying AN hazards.

Previously other researchers have conducted experiments for the AN mixture with additives and developed kinetic models [56], but those models are limited and there is much need for additional work. Data obtained from calorimetric measurements can provide an estimation of the kinetic coefficients of the previously proposed models in a wider range as well.

To analyze the reaction mechanism of AN decomposition [24], this work identifies the key parameters, such as reaction order, activation energy, heat of reaction,

and “onset” temperature from calorimetric measurements. Section 3.3 provides a detailed method to analyze the thermodynamic and kinetic parameters.

3.2.1 Reactive System Screening Tool (RSST)

The Reactive System Screening Tool (RSST) is a calorimeter manufactured by Fauske and Associates. It can screen reactive chemical systems for temperatures up to 500 °C and pressures up to 3,549 kPa (490 psi). The RSST is capable of handling larger quantities of sample (approximately 3 g – 6 g) as compared to the DSC which can only test several milligrams of a sample. RSST is a pseudo-adiabatic calorimeter, which can compensate heat losses by providing additional energy generated from an electric heater. The RSST can be programmed to increase the temperature of the sample in a heating ramp mode; in this mode the sample is usually heated at a constant rate, which could vary from 0.25 $°C \cdot min^{-1}$ to 2 $°C \cdot min^{-1}$, until an exothermic reaction provoking a rapid temperature and pressure rise occurs. A typical temperature *vs*. time profile of the data from the RSST experiment is shown in Figure 3. This process is controlled by the feedback from type-K metal thermocouples, which have a sensitivity of about 41 $\mu V \cdot °C^{-1}$. The self-heating rate of exothermic systems can be found as a function of sample temperature, which has been adjusted for the heater input [93]. An open glass sample cell with a volume of 10 mL (10 cm^3) is placed inside a pressure containment vessel with a volume of 350 mL. To properly mix the contents of the cell when the testing is carried out in a liquid medium, a polymer coated magnetic stirrer bar could be used [94]. The

thermal inertia factor, namely the φ-Factor (see Section 3.3 for definition), can be as low as 1.04 [95, 96]. Because the test cell is open to the surrounding atmosphere, vapor losses from the sample may occur. To reduce these, a "pad" pressure of an inert gas (usually nitrogen) can be applied to the containment vessel before conducting tests. The RSST is recommended by the American Institute of Chemical Engineers (AIChE)'s Design Institute for Emergency Relief Systems [93]. A more detailed description of the RSST can be found in the references [93, 97]. The schematic diagram of the RSST is shown in Figure 4. The RSST is sometimes used as a screening tool, and it is often used with other instruments, like adiabatic calorimeters, to obtain more quantitative and precise results.

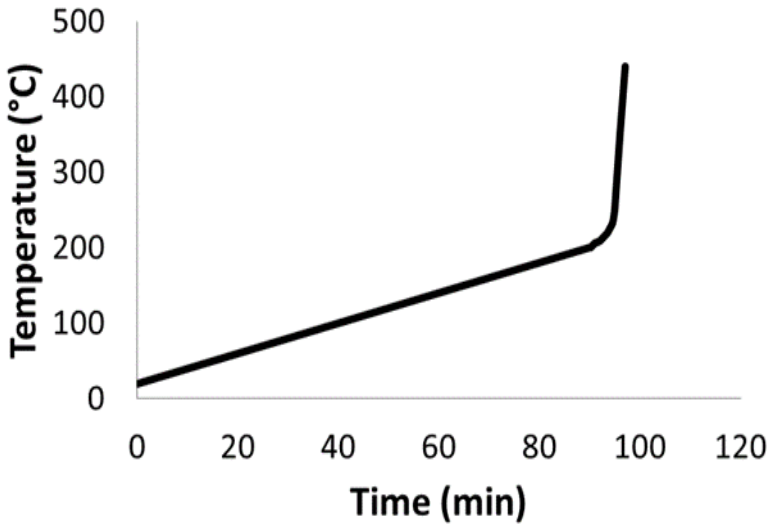

Figure 3. General temperature profile in the RSST

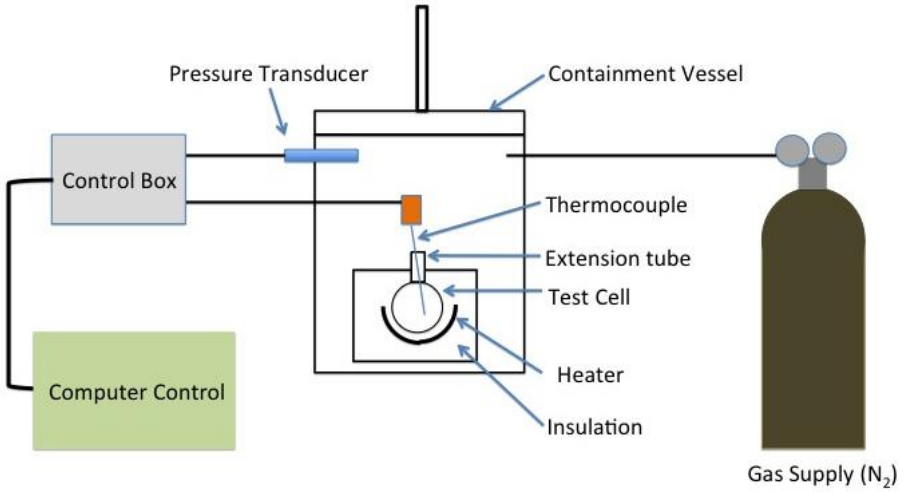

Figure 4. The schematic diagram of the RSST

Because of its relatively stable thermal behavior, cooking oil (from Daily Chef-Extra Virgin Olive Oil) tests were conducted four times to check the repeatability of the RSST with the initial pad pressure being 187 psig (1.4 MPa). The heating rate of 2.00 °C·min^{-1} was used for temperatures up to 100 °C; 1.00 °C·min^{-1} was used for temperatures from 100 °C to 150 °C; 0.50 °C·min^{-1} was used for temperatures from 150 °C to 180 °C; and 0.25 °C·min^{-1} was used for temperatures from 180 °C to 195 °C. The results are shown in Figure 5, and it is concluded that the RSST gives good repeatability of temperature and pressure trajectories for this sample.

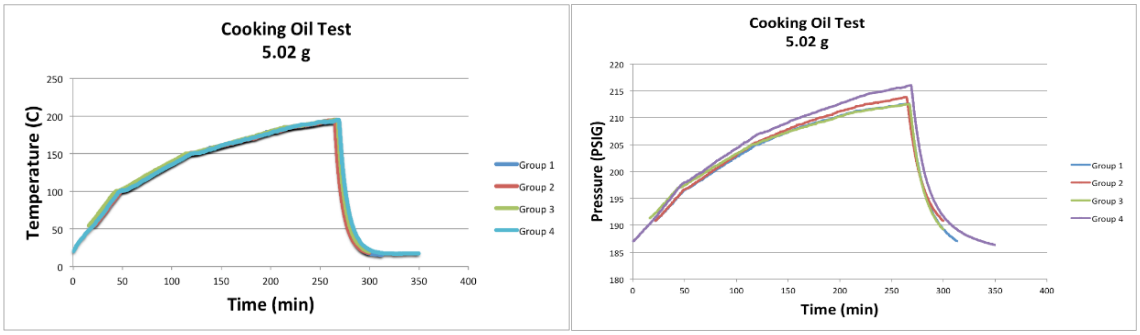

Figure 5. Cooking oil tests in the RSST

The key parameters are obtained from each experiment, such as "onset" temperature, "onset" pressure, maximum self-heating rate, maximum pressure-rise rate, maximum temperature, temperature at maximum self-heating rate, and final temperature. Based on the results, the plots are drawn including temperature *vs*. time, pressure *vs*. time, pressure *vs*. temperature, log plot of self-heating rate *vs*. temperature, and log plot of pressure rate *vs*. temperature.

3.2.2 Automatic Pressure Tracking Adiabatic Calorimeter (APTAC)

The runaway behavior of AN was also evaluated in the Automatic Pressure Tracking Adiabatic Calorimeter (APTAC), developed by Arthur D. Little and currently commercialized by Netzsch. It is fully automated, operated by an easy-to-use control program. The APTAC can be operated at temperatures up to 500 °C and pressures up to 2,000 psi (13.9 MPa) in a batch process. During the experiment, the sample is loaded to a reaction vessel and then it is placed inside a 500 mL pressure vessel. The reaction

vessel is a spherical flask, which can be constructed of various materials including glass, titanium, and stainless steel. The reaction cell is attached to the top heater and placed inside a containment vessel. The volume of the flask varies from 10 mL, 25 mL, 50 mL to 100 mL, and in most cases the volume of 100 mL is used. At the bottom of the vessel, a magnetic stirrer bar is used to stir the liquid reactants. The test cell is closed in the containment vessel, and the containment vessel is sealed with two safety clamps.

Heat losses are minimized by keeping the temperature of the surroundings as close as possible to the temperature of the sample. There are four main heaters, bottom, top, side, and tube heaters, insulated and placed in the pressure vessel. There are seven type-N (Nicrosil – Nisil) thermocouples, which have a sensitivity of about 39 $\mu V \cdot °C^{-1}$, measuring the temperatures of the sample, reaction vessel wall, and nitrogen gas within the pressure vessel, in order to monitor the temperatures, minimize heat losses, and keep the temperature surrounding the sample as close as possible to that of the sample, and maintaining adiabatic conditions. To prevent the reaction vessel from bursting from internal pressure generation, the pressure differential across the wall of the reaction vessel is maintained at less than 10 psi (69 kPa), by injecting nitrogen into the pressure vessel at a rate of up to 20,000 $psi \cdot min^{-1}$ (138 $MPa \cdot min^{-1}$).

The APTAC has different operating modes including: (1) Heat-Wait-Search (HWS) for precise detection of exotherms, (2) Heat-Ramp-Search for screening, (3) constant temperature difference ramp for fire exposure simulation, and (4) isothermal. In this work, only the HWS and isothermal modes were used.

In HWS mode, the sample is gradually heated up in several successive steps and the equipment searches for an exotherm at each step. After each temperature rise to a selected point (heat), the system temperature stabilizes and stays constant for a while (wait), and then it seeks for an exotherm (search). An exotherm means that the self-heating rate of the sample is greater than the pre-determined threshold (0.04 °C·min^{-1} or 0.05 °C·min^{-1}). When an exotherm is identified, the APTAC automatically shifts to adiabatic mode and the temperature, pressure, and other variables are tracked and recorded until the reaction finishes or the shutdown criteria is met. The "onset" temperature is defined as the temperature at which the exotherm is first detected. Figure 6 shows a simplified diagram of the APTAC [98], and Figure 7 shows a typical HWS tracks.

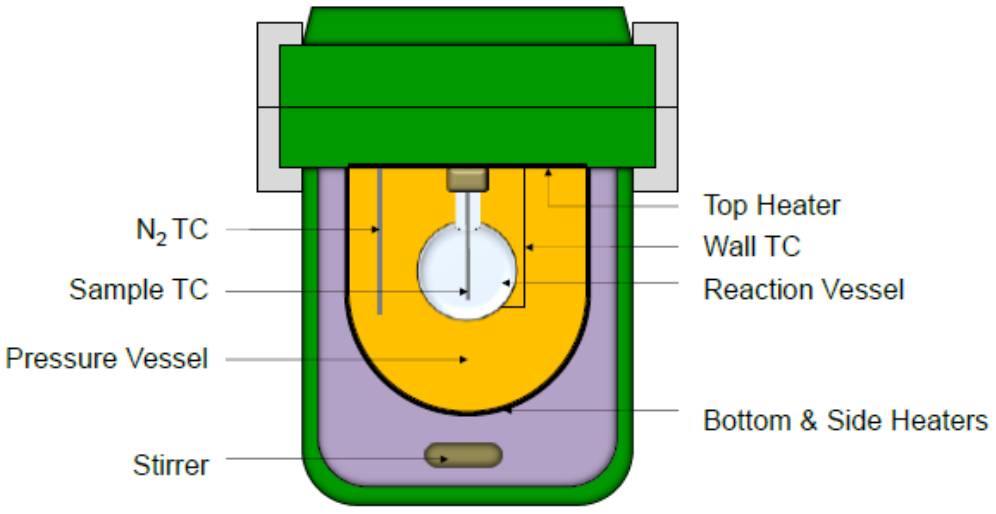

Figure 6. Simplified diagram of the APTAC [98]

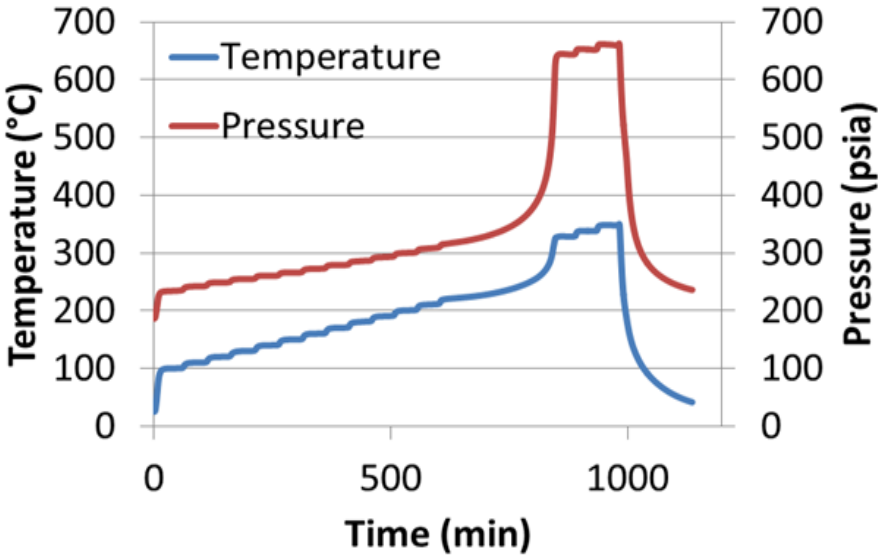

Figure 7. HWS mode of the APTAC

In the isothermal mode, the sample is heated to a desired temperature, and then kept constant at that temperature for a certain period. When the equipment detects an exotherm, it switches to adiabatic mode automatically. For the equipment to switch to adiabatic mode, two criteria must be met: the self-heating rate should be higher than 0.02 °C·min^{-1} and the sample temperature should be at least 1 °C greater than the pre-determined isothermal temperature. When the specified time limit is exceeded, the sample is cooled down.

During the experiment, several variables are recorded by the software, such as the temperatures of the sample, the nitrogen surrounding the test cell, the cell wall, and the pressure of the sample.

3.2.3 Parameters Obtained from Calorimetry Experiments

This section introduces the parameters associated with calorimetric studies, including the parameters that should be recorded before, during, and after conducting experiments; the parameters would be obtained from the experimental apparatus or the software from the interpretation of the raw experimental data; and the parameters that could be calculated based on the data obtained from the experimental apparatus.

3.2.3.1 Parameters Recorded Before and After Experiments

In the RSST, the parameters that need to be recorded are the heater resistance, weight of test cell, weight of the cell after experiment (to determine whether any mass was lost), initial pressure applied into the containment vessel before the experiments, rate of stirring of the stirrer (if applicable), rate of heating ramp, shut down criteria, weight of sample, and the pressure after cooling down (at ambient temperature after the experiment).

In the APTAC, the parameters that need to be recorded are the weight of the test cell, weight of the sample, weight of the test cell with sample, initial pressure applied to the test cell and containment vessel, the pressure after cooling down (at ambient temperature after the experiment), heating mode (if HWS mode is used, starting temperature of HWS, limit temperature of HWS, temperature increment, and heating

rate), exothem limit, shut down criteria, and the weight of the test cell after each experiment.

3.2.3.2 Parameters from Experimental Apparatus

In most cases, the parameters that could be obtained from checking the data of the experimental apparatus, the calorimeters, are summarized in Table 2. The meaning of each parameter are summarized after the table.

Table 2. The parameters from calorimetry experiments

Parameters	Units
T_o	°C
$(dT/dt)_{max}$	°C·s^{-1}
T_{max}	°C
T_f	°C
P_o	psig or Pa
$(dP/dt)_{max}$	psi·s^{-1} or Pa·s^{-1}
P_{max}	psig or Pa
P_f	psig or Pa
P_c	psig or Pa
$t_{runaway}$	min

– T_o : detected “onset” temperature (ºC), defined as the lowest temperature at which the calorimeter first detects the exothermic reaction (detailed description about

measuring T_o is given in Section 4.1.1). This parameter depends strongly on the sensitivity of the instrument.

– $(dT/dt)_{max}$: maximum self-heating rate ($^oC \cdot s^{-1}$) , the highest temperature rise rate during the entire reaction.

– T_{max} : temperature at the maximum self-heating rate (^oC), the temperature at which $(dT/dt)_{max}$ occurs.

– T_f : the final temperature of the reaction (^oC), the temperature when the reaction completes, which is also the maximum temperature detected during the entire reaction, representing the temperature when the self-heating rate equals to zero.

– P_o : "onset" pressure (psi or Pa), the pressure when the "onset" temperature occurs.

– $(dP/dt)_{max}$: maximum pressure-rise rate ($psi \cdot s^{-1}$ or $Pa \cdot s^{-1}$), the highest pressure-rise rate during the entire reaction.

– P_{max} : pressure at maximum pressure-rise rate (psi or Pa), the pressure at which $(dP/dt)_{max}$ occurs.

– P_f : the final pressure (psi or Pa), which is the maximum pressure achieved during the runaway under adiabatic conditions.

– P_c : the pressure after cooling down (psi or Pa), the pressure in the containment vessel when the temperature drops to ambient temperature, after the reaction completes and before venting.

– $t_{runaway}$: the time for the runaway reaction (min), which starts at the "onset" temperature and ends at the final temperature.

Based on the parameters, the results were plotted in terms of temperature *vs*. time, log plot of self-heating rate *vs*. temperature, log plot of pressure-rise rate *vs*. temperature, pressure *vs*. temperature, and log plot of pressure-rise rate *vs*. pressure.

3.2.3.3 Calculated Parameters Based on Experimental Data

The parameters that can be calculated based on experimental data are summarized in Table 3. The meaning of each parameter is shown after the table. The calculation methods are introduced in Section 3.3.

Table 3. The calculated parameters based on experimental data

Parameters	**Units**
φ	-
ΔT_{ad}	°C
n_1	mol
n_2	mol
Δn ($n_{generate}$)	mol
ΔH_{rxn}	$kJ \cdot mol^{-1}$
Ea	$kJ \cdot mol^{-1}$
A	-
n	-
$(dG/dt)_{max,\ \varphi>1}$	$mol \cdot s^{-1}$

– Thermal inertia factor : $\varphi = 1 + \frac{m_{cell} \cdot C_{P\ cell}}{m_{sample} \cdot C_{P\ sample}}$

– ΔT_{ad} : the adiabatic temperature rise $\Delta T_{ad} = T_f - T_o$

– Δn ($n_{generate}$) : moles of non-condensable gases formed during the runaway (mol). $\Delta n = n_2 - n_1$, where n_1 is the moles of gases before the experiment, and n_2 is the moles of gases after the experiment, in the cell.

– ΔH_{rxn} *:* heat of reaction

– *Ea* : activation energy

– *A* : pre-exponential factor

– *n* : order of reaction (calculated by fitting the adiabatic experimental data (time and temperature) to an n^{th} order type reaction kinetic model)

– $\left(\frac{dG}{dt}\right)_{max,\varphi>1}$: maximum gas production rate

3.3 Analysis of Thermodynamic and Kinetic Parameters

3.3.1 Model Analysis

For real calorimeters, the heating of the sample cell will use a certain fraction of heat generated by heaters, which is supposed to heat up the sample. Thus, the heat measured based on the temperatures of the sample is not able to represent the heat absorbed by the sample and the cell. Therefore a thermal inertia factor, φ, is introduced here to correct this deviation. The φ factor is defined by Eq. (26) as listed below.

Eq. (26) $\varphi = 1 + \frac{m_c \cdot C_{p,c}}{m_s \cdot C_{p,s}}$

where m is the mass, c_p is the heat capacity, and subscript s and c stand for the sample and the cell, respectively. $C_{p,c}$=0.2 cal·g^{-1}·°C^{-1}=0.84 J·g^{-1}·°C^{-1}.

From the calorimetric measurements, the heat of reaction, ΔH_{rxn}, which is the heat generated per mol reacted, can be estimated by Eq. (27) (provided that C_p can be assumed to be essentially independent of temperature) [99]:

Eq. (27) $-\Delta H_{rxn} = \frac{m \cdot C_p \cdot \Delta T_{ad}}{n_{rxn}}$

In this equation, ΔT_{ad} is the adiabatic temperature increase, and is corrected by considering φ according to equation $\Delta T_{ad} = \varphi \cdot \Delta T_{ad}^{mes}$, where ΔT_{ad}^{mes} is the adiabatic temperature rise measured by the calorimeter. $\Delta T_{ad}^{mes} = T_f - T_o$, where T_o is the temperature when the reaction starts (the "onset" temperature), and T_f is the temperature when the reaction completes (also when dT/dt equals to zero, at the highest temperature during the whole test process). Also, m means the sample mass, C_p is the heat capacity of the sample mass, and n_{rxn} is the moles of material reacted.

Kinetic modeling will be performed based on the test data to develop kinetic models, simulating the thermal decomposition of AN under various conditions. Two kinetic models are discussed here: n^{th} order reaction model [99] and autocatalytic reaction model [100].

3.3.1.1 n^{th} Order Reaction

For n^{th} order reaction with a single reactant [99], assuming the reaction occurs in a closed system with constant volume, negligible pressure change, and adiabatic environment, the reaction rate is expressed in the Eq. (28):

Eq. (28) $$\frac{dC}{dt} = r = -k \cdot C^n \quad \text{or} \quad C_0 \cdot \frac{d\alpha}{dt} = -r = k \cdot C_0^n \cdot (1-\alpha)^n$$

where C is the concentration of the reactant at time t, k is the reaction rate coefficient, n is the reaction order, α is the fractional conversion, and C_0 is the reactant initial concentration.

For exothermic reactions in an adiabatic environment, the heat generated by the exothermic reaction at T_o will increase temperature, accelerating the rate of the reaction. However, the reactant is dissipated and its concentration decreases. As a result, the reaction rate will decrease after reaching the maximum rate of temperature rise and diminish to zero when the reaction completes at T_f. If C_p is practically independent of temperature, the concentration of the reactant at any time can be related to temperature, *i.e.*, it is proportional to the temperature increase. The expression below, Eq. (29), describes the relationship.

Eq. (29) $$C = \frac{T_f - T}{T_f - T_0} \cdot C_0 = \frac{T_f - T}{\Delta T_{ad}} \cdot C_0 \quad \text{or} \quad \alpha = \frac{T - T_0}{T_f - T_0}$$

Differentiating Eq. (29) with respect to t and then substituting into Eq. (28), the following Eq. (30) is obtained.

Eq. (30) $$\frac{dT}{dt} = k \cdot \left(\frac{T_f - T}{\Delta T_{ad}}\right)^n \cdot \Delta T_{ad} \cdot C_0^{n-1}$$

where $\frac{dT}{dt}$ is the self-heating rate at any temperature.

Rearranging Eq. (30), the Eq. (31) is derived:

Eq. (31) $$k^* = k \cdot C_0^{n-1} = \frac{dT}{dt} \cdot \frac{(\Delta T_{ad})^{n-1}}{(T_f - T)^n}$$

where, k^* is a pseudo 0^{th} order rate constant at temperature T.

Based on the self-heating rate, T_f and ΔT_{ad}, k^* can be obtained from calorimetry tests.

On the other hand, usually the reaction rate coefficient follows Arrhenius equation, Eq. (32):

Eq. (32) $$k = A \cdot exp\left(\frac{-E_a}{RT}\right)$$

where A is the constant frequency factor, E_a is the activation energy, and R is the gas constant.

Substituting Eq. (32) into Eq. (31), the Eq. (33) is obtained.

Eq. (33) $$\ln(k^*) = \ln(A \cdot C_0^{n-1}) - \frac{E_a}{RT}$$

The plot of $\ln(k^*)$ versus $1/T$ yields a straight line, and the Arrhenius parameters A and E_a can be determined. The slope of the straight line is represented by E_a/R, and the intercept is determined by $\ln(AC_0^{n-1})$.

When the reaction is a first order reaction, $k^*=k$. The plot of k^* versus $-1/T$ yields a curve, which can be fitted into Eq. (32), thus, A and E_a can be obtained.

Alternatively, Eq. (34), Eq. (35), and Eq. (36) could be obtained.

Eq. (34) $$\alpha = \frac{T - T_o}{T_f - T_o}$$

Eq. (35) $\frac{d\alpha}{dt} = k \cdot (1-\alpha)^n$

Eq. (36) $ln\left(\frac{d\alpha}{dt}\right) = ln(A) - \frac{E_a}{RT} + n \cdot ln(1-\alpha)$

Using the experimental data obtained from each experiment, a linear regression could be performed to calculate n for each test. Then, the average values of the obtained n would be used to calculate the activation energies and pre-exponential factors.

When using the previously stated model, the following assumptions are made: single reaction, with n^{th} order kinetics; relation between the kinetic rate coefficient and the temperature follows the Arrhenius equation; sample heat capacity is constant; and conversion can be expressed in terms of the adiabatic temperature by the Townsend and Tou relation [99].

3.3.1.2 Autocatalytic Reaction

Autocatalytic reactions are reactions for which the reaction rate expression depends on the concentration of one or more products. In this study, the model used can be simplified as follows, where B is the product as well as the reactant.

$A \rightarrow B + \cdots$ initial stage

$A + B \rightleftharpoons 2\,B$ autocatalytic stage

For simple, single-stage reactions, the reaction model is selected as in Eq. (37) [100]:

Eq. (37) $\frac{d\alpha}{dt} = k \cdot (1-\alpha)^{n_a} \cdot (\alpha^{n_b} + z)$

where α is the fractional conversion, n_a and n_b are reaction orders, and z is a constant.

3.3.2 SADT and TMR

Self-Accelerating Decomposition Temperature (SADT) is the temperature at which the heat generation rate equals the heat loss rate, under adiabatic conditions. SADT is used to determine safe storage temperature for chemicals. When calculating SADT, it is assumed that in low temperature range (*i.e.*, low conversion), Eq. (38) applies.

Eq. (38) $$\frac{dT}{dt} = Aexp\left(-\frac{E_a}{RT}\right)$$

where A and E_a are calculated from the previous section.

Based on Semenov ignition theory for non-viscous liquids, Eq. (39) applies. Based on adiabatic model, Eq. (40), critical temperature for 7 days or 24 hr TMR (ADT24) can be determined [101].

Eq. (39) $$h \cdot S \cdot 60 \cdot \left(\frac{T_{SADT}^2}{B}\right) = V \cdot \rho \cdot c \cdot A \cdot e^{1-\frac{B}{T_{SADT}}}$$

Eq. (40) $$T = \frac{B}{ln\left(\frac{t_{mr} \cdot A \cdot B}{T^2}\right)}$$

where, A is the pre-exponential factor ($°C \cdot min^{-1}$), $B = -\frac{E_a}{R}$ is the activation temperature (K), t_{mr} is the time to maximum rate (min), V is the volume (m^3), ρ is the reactant density ($kg \cdot m^{-3}$), h is the effective heat transfer coefficient ($W \cdot m^{-1} \cdot K^{-1}$), S is the surface area (m^2), and c is the reactant specific heat ($J \cdot kg^{-1} \cdot K^{-1}$).

Time to Maximum Rate (TMR), t_{mr}, can be calculated based on Eq. (41).

Eq. (41) $$t_{mr} = \frac{T^2}{\frac{dT}{dt} \cdot B}$$

where, t is time in min, T is temperature in K, $\frac{dT}{dt}$ is the corresponding self-heat rate in K·min^{-1}, and $B = -\frac{E_a}{R}$ is the activation temperature (K).

3.3.3 Model Fitting

Non-linear optimization method [100] is a general approach to kinetic evaluation. By looking for the minimum difference between experimental and simulated results, this method will give the best fit. In most cases, nonlinear optimization algorithms are based on the Least Square Method (LSM), which uses the sum of squares of residuals as the measure to be minimized. In this study, the following objective function, Eq. (42), will be introduced.

Eq. (42) $$SS(\overline{P}) = \frac{1}{2}\sum_{(i)} \left(\frac{Y_{exp}(t_i) - Y_{sim}(\overline{P}, t_i)}{\varepsilon_i} \right)^2 \rightarrow min = SS(\overline{P_r})$$

where $SS(\bar{P})$ is the weighted sum of the squares of the residuals, $Y_{exp}(t_i)$ means the experimental data at time t_i, $Y_{sim}(\bar{P},t_i)$ represents the value of the simulated response, and $\mathcal{E}_i$ is the experimental error for the i^{th} observation.

3.3.4 Non-condensable Gas Generation

The non-condensable gas generated from the decomposition of AN may significantly contribute to the increased and accumulated pressure, resulting in

explosions. The gas generation rate is obtained from the measured calorimetry test data. During calculation, the vapor pressure of the decomposition product and its changes should be considered, which could be obtained from an Antoine equation [102]. However, in terms of the overall pressure of the system, other factors play a more dominant role than the vapor pressure, such as thermal expansion and gas production.

In the RSST open system test, the initial and final pressure at the same temperature can be compared to calculate the non-condensable gas generated, following Eq. (43).

Eq. (43) $$\Delta n = n_{final} - n_{initial} = \frac{P_c \cdot V}{R \cdot T_{ambient}} - \frac{P_{initial} \cdot V}{R \cdot T_{initial}} = \frac{(P_c - P_{initial}) \cdot V}{R \cdot T_{ambient}}$$

where Δn is the moles of non-condensable gases generated, n_{final} is the total moles of non-condensable gases (initial moles + non-condensable gas generated); n_{initial} is the moles of gas present in the cell at the beginning of the test (air moles); P_{initial} and T_{initial} are the initial (at the beginning of the experiment) pressure and temperature, respectively, and T_{initial} is the ambient temperature; P_c is the pressure after cooling down when the reaction completes, *i.e.*, the pressure at room temperature; V is the free head space volume in the cell, which was assumed to be constant; and R is the universal gas constant.

In this study, the non-condensable gas generation rate were estimated by Eq. (44), which removes the thermal expansion effect from the measured overall pressure rate of the whole system.

Eq. (44) $$\left(\frac{dn}{dt}\right) = \left(\frac{V}{RT}\right) \cdot \left[\left(\frac{dP}{dt}\right) - \left(\frac{P}{T}\right) \cdot \left(\frac{dT}{dt}\right)\right]$$

The maximum gas production rate for the closed cell experiments could be calculated from the maximum pressure-rise in the test cell using Eq. (45).

Eq. (45) $$\left(\frac{dG}{dt}\right)_{max,\varphi>1} = n_g \cdot \left\{\left(\frac{dP}{dt}\right)_{max} \cdot \frac{1}{P} - \left(\frac{dT}{dt}\right) \cdot \frac{1}{T}\right\}$$

where n_g is the number of moles of gases formed during the reaction, $(dP/dt)_{max}$ is the maximum pressure-rise rate in the test cell, and P, T, and dT/dt are the values taken at $(dP/dt)_{max}$.

3.3.5 Thermal Inertia Factor Correction

The importance of the thermal inertia factor, φ factor, was introduced in Section 3.3.1. In order to have a better understanding of the experimental data, the experimental values of T_o, (dT/dt), and $(dG/dt)_{max}$ should be corrected to φ=1. The correction method used in this work is described by Eq. (46) for the adiabatic "onset" temperature, Eq. (47) for the adiabatic temperature, Eq. (48) for the adiabatic temperature rise rate, and Eq. (49) for the adiabatic maximum gas production rate [103, 104].

Eq. (46) $$\frac{1}{(T_o)_{\varphi=1}} = \frac{1}{T_o} + \frac{R}{E_a} \cdot ln\varphi$$

Eq. (47) $$(T)_{\varphi=1} = (T_o)_{\varphi=1} + \varphi \cdot (T - T_o)$$

Eq. (48) $$\left(\frac{dT}{dt}\right)_{\varphi=1} = \varphi \cdot exp\left[\frac{Ea}{R}\left(\frac{1}{(T)_{\varphi=1}} - \frac{1}{T}\right)\right] \cdot \left(\frac{dT}{dt}\right)_{\varphi>1}$$

where, $\left(\frac{dT}{dt}\right)_{\varphi>1}$ is the experimental temperature-rise rate ($K \cdot s^{-1}$).

Eq. (49) $$\left(\frac{dnG}{dt}\right)_{max,\varphi=1} = \varphi \cdot exp\left[\frac{Ea}{R} \cdot \left(\frac{1}{T_M} - \frac{1}{T_{MAD}}\right)\right] \cdot \left(\frac{dG}{dt}\right)_{max,\varphi>1}$$

where, T_{M} is the experimental temperature at which the maximum gas generation rate was achieved (K), T_{MAD} is the value of this temperature after correction (K), and $\left(\frac{\mathrm{d}G}{\mathrm{d}t}\right)_{\max,\varphi>1}$ is the experimental maximum gas production rate (mol·s^{-1}).

3.4 Methods and Procedures

This section focuses on the methods and procedures of conducting experiments in the RSST and the APTAC. The chemicals used in this work are summarized in Section 3.4.1, and the procedures in Section 3.4.2.

3.4.1 Chemicals

Ammonium nitrate (NH_4NO_3, VWR, ACS Grade, 99.9% assay), sodium sulfate (Na_2SO_4, Aldrich, ACS Reagent, 99+%), potassium chloride (KCl, Sigma, powder, Bio Reagent, 99.0+%), sodium bicarbonate ($NaHCO_3$, Aldrich, ACS Grade, 99.7+% assay), potassium carbonate (K_2CO_3, Mallinckrodt, ACS Grade, Granular), ammonium sulfate ($(NH_4)_2SO_4$, J. T. Baker Inc., ACS Grade, 99.8% assay), barium nitrate ($Ba(NO_3)_2$, Sigma Aldrich, ACS Reagent, 99+%), sodium nitrate ($NaNO_3$, Sigma Aldrich, ACS Reagent, 97+%), and ferric sulfate (or iron(III) sulfate, $Fe_2(SO_4)_3$, EM Science, 97+%) were used without further purification.

Nitrogen (Acetylene Oxygen Co., Compressed nitrogen, DOT classification 2.2) was used to pressurize the RSST pressure containment vessel before each experiment.

Fine sand (silica, SiO_2, VWR, 99+%) was used for mixing with AN samples in the APTAC.

3.4.2 Experimental Procedures

In the RSST, glass test cells with 10 mL in volume were used in all the experiments. To study the thermal decomposition of pure AN, in a typical experiment, 3.5 g of powdered AN was weighed. To study the effect of different additives, 3.5 g of powdered AN was mixed well with various amounts of the additives in a solid form and loaded into the cell. The mixture in the test cell was then shaken in all directions for approximately 10 minutes in order to mix the sample thoroughly. By comparing the data obtained for the mixture with pure AN data, it is easy to differentiate between the chemicals that mitigate the explosion (inhibitors) and those that intensify the explosion (promoters). To study the effect of different conditions, the operating condition for each experiment varies. By comparing the data obtained for AN decomposition under various conditions, the safe storage conditions were identified. The generally used operating conditions are introduced in the next paragraph; this applies to all experiments in the RSST in this work, unless otherwise specified by using other conditions in order to study the condition-dependent AN decomposition. Each experiment was repeated at least twice.

A heating rate of 2 °C·min^{-1} was used for temperatures up to 150 °C; 1 °C·min^{-1} was used for temperatures from 150 °C to 180 °C; and 0.5 °C·min^{-1} was used for

temperatures from 180 °C up to 340 °C. The reason behind choosing such heating rates is that at lower temperatures, higher heating rates accelerate the reaction rate and reduce the experiment time. At higher temperatures, close to "onset" temperature, lower heating rates allow a more accurate detection of the "onset" data. The shutdown temperature and pressure limits were set to 410 °C, and 400 psig (2.9 MPa), respectively. Once the shutdown criteria are exceeded, the heater power supply automatically stops, and the system keeps recording the data until the temperature drops to the cool down temperature of 40 °C. A backpressure of 187 psig (1.4 MPa) was applied using a gas which was composed of 98.47% nitrogen and 1.53% oxygen. On the one hand, the initial pressure can be used to minimize vaporization and material loss from the sample cell. Moreover, the initial pressure can be used to simulate high-pressure conditions, for example, confined space or self-confinement at the bottom of an AN pile. To give a rough estimation, based on the pressure (P = 187 psig = 1.39 MPa) used in this study and the density of AN (ρ = 1.725 g·cm^{-3} = 1725 kg·m^{-3}), the height of an AN pile (h) that will create a pressure of 187 psig at the bottom is calculated using equation $P = \rho gh$, where g = 9.81 m·s^{-2}. The result shows that an AN pile of 82 m in height will generate an internal pressure of 187 psig at the bottom.

In the APTAC, glass test cells with 100 mL in volume were used in all the experiments. The desired sample size was weighted and placed into the test cell. In order for the solid sample to be mixed well, the test cell loaded with sample was shaken in all directions for ten minutes. The sample was mixed with 5 g of sand (SiO_2) (unless otherwise specified) to increase the volume of the sample for easier temperature

measurement, and to reduce the temperature increase rate to protect the equipment. In most of the sections of this work, Heat-Wait- Search (HWS) mode was used. An initial pad pressure (nitrogen) of 187 psia (1289.32 kPa) was applied to both the test cell and the containment vessel; the initial heating rate was 10 °C·min^{-1} from ambient temperature to 100 °C; subsequently, the Heat-Wait-Search (HWS) mode was turned on. The temperature step-increment was 10 °C, and the exotherm limit was 0.05 °C·min^{-1}. The shutdown criteria were temperature ≥410 °C or self-heating rate ≥400 °C·min^{-1} or pressure reached ≥1087.5 psi or pressure-rise rate ≥1087.5 psi·min^{-1}, or a pressure difference between the pressure vessel and the cell of 217.5 psi. This applied to all experiments conducted in the APTAC unless otherwise specifically stated. In the isothermal mode tests, the sample was heated to the pre-determined temperature and then kept constant for a certain period of time, usually 2,000 min, to detect the “onset” temperature.

4. THERMAL STABILITY OF AMMONIUM NITRATE WITH SODIUM SULFATE AND POTASSIUM CHLORIDE [*]

The first step of this research was to screen AN with additives. Since the objective of this work is to mitigate the explosion risks of AN as fertilizers, only inorganic salts that can be used as fertilizers were chosen as additives for this study. In this section, sodium sulfate (Na_2SO_4) and potassium chloride (KCl), both being fertilizers, were chosen to be mixed with AN and studied as additives. To be specific, this section starts with the thermal stability of pure AN, which serves a foundation for the discussions in later subsections, including calorimetry experiments and theoretical analysis. Then, various amounts of single additive (sodium sulfate and potassium chloride) were mixed with AN and tested in the RSST and the APTAC, with thermodynamic and kinetic parameters calculated and compared with the results of pure AN. Further, sodium sulfate and potassium chloride were mixed together with AN, and the experimental results were compared with the experiments stated earlier in this section, along with the discussion of the synergistic effect. Later on, the mechanisms of AN decomposition with sodium sulfate and potassium chloride were illustrated. Last but not least, mathematical models were proposed to predict the adiabatic temperature rise.

---

[*] Part of this section is reprinted with permission from "Ammonium nitrate thermal decomposition with additives" by Z. Han, S. Sachdeva, M. Papadaki and M. S. Mannan, 2015. *Journal of Loss Prevention in the Process Industries*, 35, 307-315, Copyright 2014 by Elsevier and from "Effects of inhibitor and promoter mixtures on ammonium nitrate fertilizer explosion hazards" by Z. Han, S. Sachdeva, M. Papadaki and M. S. Mannan, 2015. *Thermochimica Acta*, 624, 69-75, Copyright 2015 by Elsevier.

4.1 Thermal Stability of Pure AN

In this section, the thermal decomposition of pure AN in the RSST and the APTAC is described. In literature, AN studies using the RSST or the APTAC have not been reported.

4.1.1 Experimental Results of Pure AN in the RSST

In a typical AN experiment using the RSST, 3.5 g of powdered AN was weighed and loaded into the cell. The temperature *vs*. time, self-heating rate *vs*. temperature, pressure *vs*. time, and pressure-rise rate *vs*. temperature profiles are shown in Figure 8 for all the three replicate tests. As can be seen from Figure 8, the three replicate tests for AN are not identical. In all the cases, the "onset" temperatures obtained are relatively close, around 200 °C, but the time to "onset" is different. The reason behind this could be that AN was tested in solid form and the RSST has only one thermocouple which is located at the center of the loaded cell. For solids, the heating rate and heat distribution within the sample might not be homogeneous. But the overall trends and critical parameters are similar.

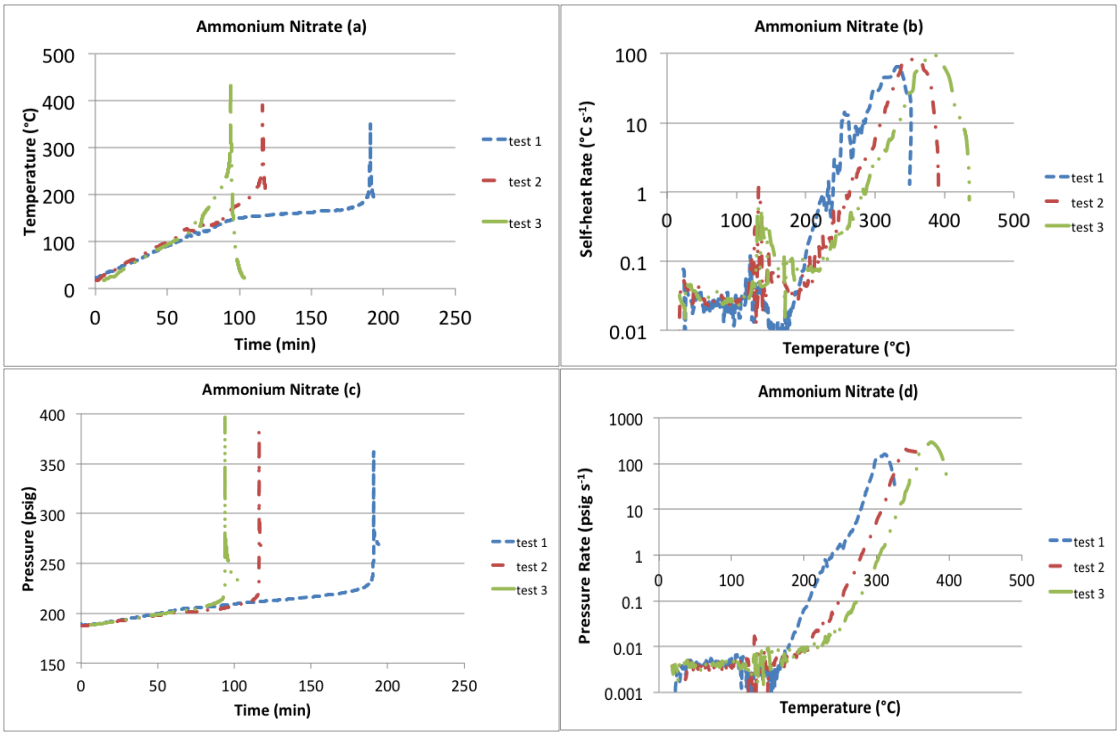

Figure 8. The thermal decomposition of AN (a) Temperature profile (b) Self-heating rate (c) Pressure profile (d) Pressure rate

Based on Figure 8*(a)*, for all the three tests, at 125 °C, an endotherm appears where the temperature decreases by approximately 5 °C, and then it starts to increase again to the point where the exothermic reaction occurs. However, the pressure profile from Figure 8*(c)* does not show a corresponding increase or decrease, indicating that no gas generation was involved in this stage of the process. Based on the RSST measurement, when the temperature reached around 200 °C, both the temperature and the pressure started to increase dramatically. This can be seen more clearly from the logarithmic plot of the self-heating rate profile and pressure-rise rate profile, which are

shown in Figure 8*(b)* and Figure 8*(d)*, respectively. The exothermic reaction started very rapidly, generating gas and vapor accordingly.

In this study, the "onset" temperature is defined from the self-heating rate profile, as shown in Figure 9. A tangent is drawn to the curve where the self-heating rate starts to increase, and then a straight line is drawn on the end of the temperature rate curve before the temperature starts to increase rapidly. The temperature at the intersection of these two lines is defined as the "onset" temperature. For pure AN, the "onset" temperature was determined to be 200 (±10) °C from the three replicate tests. The "onset" pressure, which was the pressure when the "onset" temperature was detected, was determined to be 217 (±11) psig. The maximum self-heating rate, $(dT/dt)_{max}$, was determined from the self-heating rate data. In solid sample tests, the maximum self-heating rate was reached before the shutdown of the experiment.

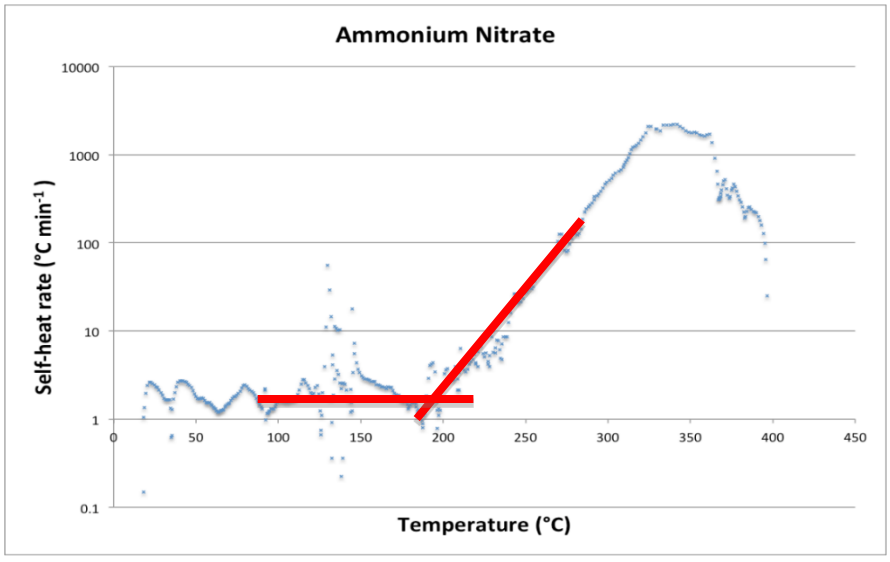

Figure 9. Determining the "onset" temperature

All the important parameters obtained from the analysis of the experimental data are summarized in Table 4. In this table, the temperature and pressure at the detected "onset" are the respective values when the self-heating rate starts to increase as described in the previous paragraph. The average maximum self-heating rate was 82 (±17) °C·s^{-1}, which occurred at 347 (±17) °C.

Table 4. Pure AN experimental data in the RSST

Test No.	1	2	3	Avg.
T_o (°C)	190	200	210	200 (±10)
P_o (psig)	230	211	210	217 (±11)
$(dT/dt)_{max}$ (°C·s^{-1})	65	82	98	82 (±17)
$(dP/dt)_{max}$ (psig·s^{-1})	160	207	293	220 (±67)
T_{max} (°C)	318	343	381	347 (±17)
T_f (°C)	352	391	436	393 (±42)
$-\Delta H_{rxn}$ (kJ·mol^{-1})	27	32	38	32 (±5)
E_a (kJ·mol^{-1})	62	64	72	66 (±5)

(Note: the maximum rate of pressure-rise is reached earlier than the maximum self-heating rate, and the temperature at $(dP/dt)_{max}$ is 4-7 °C lower than that of $(dT/dt)_{max}$)

Oxley *et al.* [22] scanned pure AN using DSC at 20 °C·min^{-1} from 50 °C to 450 °C. The results showed that there were two endotherms and one exotherm followed by another endotherm. The first endotherm happened at 125 °C, which is also detected by RSST in this work, as a result of the phase change of AN from phase II to phase I. The second endotherm occurred at 169 °C due to the melting of AN. The exotherm was

about 100 °C wide, with an exothermic maximum at 326 °C. In this work, the average temperature at maximum self-heating rate was observed at 347 (±17) °C. Sun *et al.* [24] have found that using the DSC, in the exothermic peak, the heat flow increases very slowly and gradually with the temperature increasing in the range of 190–232 °C, and increases sharply above 232 °C, which agrees with the results obtained in this study.

4.1.2 Calculation

The thermodynamic and kinetic parameters associated with AN decomposition are calculated based on the equations given in Section 3.3. In this study, φ was calculated to be 1.2; the heat capacity of AN is C_p=1.74 J·g^{-1}·K^{-1} [5]; T_o is the "onset" temperature determined from the previous section; and T_f is identified from the data. Then ΔT_{ad}^{mes} , ΔT_{ad}, and ΔH_{rxn} are obtained accordingly. ΔH_{rxn} for each test is listed in Table 4.

The theory of the n^{th} order reaction model of Townsend and Tou [99] was employed for analyzing the decomposition of pure AN. Assuming the AN decomposition reaction was a 1st order reaction, which agrees with the literature [56], and the reaction occurred in a closed system with constant volume, negligible pressure change, and an adiabatic environment. Following the steps in Section 3.3.1, Eq. (31) and Eq. (33) reduce to Eq. (50) and Eq. (51):

Eq. (50) $$k = \frac{dT}{dt} \cdot \frac{1}{T_f - T}$$

Eq. (51) $$\ln k = \ln A - \frac{E_a}{RT}$$

The plot of an AN 1st order reaction model, ln *k vs*. -1000/*T* profile, is shown in Figure 10 as an example. A straight line was fitted for the selected data points of each data set, between the "onset" temperature (T_o) and the final temperature (T_f) when the reaction completed. The results, with R^2=0.95-0.98, indicate that the assumption of a 1st order reaction is valid at these conditions. The pre-exponential factor (*A*) and activation energy (E_a) are then obtained from the fitted line. The activation energy is also summarized in Table 4. The average activation energy was 66 (±5) kJ·mol^{-1}, and the heat of reaction was –32 (±5) kJ·mol^{-1}, which is comparable to the literature value [56].

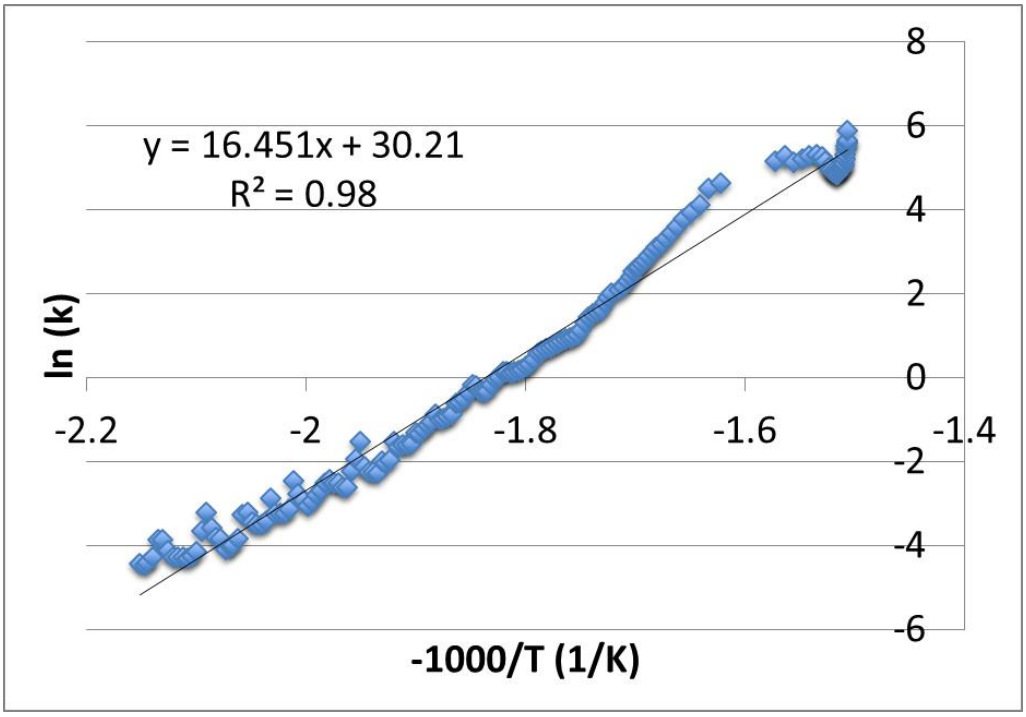

Figure 10. AN first order reaction decomposition model

4.1.3 Thermal Stability of Pure AN in the APTAC

To study the decomposition of AN in the APTAC, pure AN was well mixed with sand, and placed into the test cell. Sand was used to increase the volume of the sample for easier temperature measurement, and to reduce the temperature increase rate to protect the equipment. In order to mix the solid sample thoroughly, the test cell loaded with the sample was shaken in all directions for ten minutes. In the APTAC, initial pad pressure (nitrogen) was applied to the test cell and the containment vessel.

The experiments of pure AN were conducted under various conditions as described in later sections, and the "onset" temperature was approximately 220 °C using the employed operating conditions, which is higher than the "onset" temperature obtained from the RSST, 200 °C. This is caused by the smaller sample size (*i.e.*, 1 g) in the APTAC, while the RSST uses 3.5 g of AN. Besides, the sand mixed with AN in the APTAC also plays a role in the detected "onset" temperature. The details of pure AN decomposition in the APTAC are described in various subsections later on for easier comparison.

4.2 Effect of Sodium Sulfate and Potassium Chloride as Additive for AN Respectively

As can be seen from Figure 9, the "onset" temperature of AN decomposition is 200 (±10) °C (T_o = 200 °C for AN). When AN is mixed with additives, if the "onset"

temperature is greater than 210 °C (the upper limit of the "onset" temperature of AN), the additive is defined as an inhibitor as it delays the "onset" temperature (T_o > 210 °C for inhibitors); if the "onset" is less than 190 °C (the lower limit of the "onset" temperature of AN), the additive is a type of promoter (T_o < 190 °C for promoters).

The effects of two additives, sodium sulfate and potassium chloride, were studied in this section, separately. Sodium sulfate is an inhibitor for AN, and potassium chloride is a promoter. Both the RSST and the APTAC were used to study the decomposition of the mixtures at various concentrations.

4.2.1 Sodium Sulfate as Inhibitor

Janzen and Bettany [105] have applied sodium sulfate on crops to test the release rate of sulfur, which shows that sodium sulfate can be used as fertilizer. Since the objective of this work is to study the effects of different types of additives on thermal decomposition of AN while maintaining its agricultural benefit, only inorganic salts that can be used as fertilizers have been chosen as additives for this study.

4.2.1.1 Sodium Sulfate Experiments in the RSST

Using the RSST, in order to study the effect of sodium sulfate, pure solid AN (3.5 g) was mixed with various concentrations of sodium sulfate (Na_2SO_4), including 1.1 wt.% (0.04 g), 1.7 wt.% (0.06 g), 2.8 wt.% (0.1 g), 5.4 wt.% (0.2 g), 7.9 wt.% (0.3 g),

10.3 wt.% (0.4 g), 12.5 wt.% (0.5 g), 22.2 wt.% (1 g), and 36.4 wt.% (2 g). In this work, 2.8 wt.% is defined as 0.1 g of inhibitor in the total mass of the mixture, which is 3.6 g. Each experiment was repeated three times. The parameters obtained from each experiment are summarized in Table 5. The temperature *vs*. time profile, the self-heating rate *vs*. temperature profile, and the enlarged self-heating rate *vs*. temperature profile of selected concentrations are shown in Figure 11*(a)*, Figure 11*(b)*, and Figure 11*(c)* respectively. In the figures, the plots of the pure AN thermal decomposition data are also given as a reference, to enable easier comparisons.

Table 5. AN mixture with sodium sulfate at various concentrations

wt.% of Na_2SO_4	Na_2SO_4 (g)	T_o (°C)	P_o (psig)	$(dT/dt)_{max}$ (°C·s^{-1})	$(dP/dt)_{max}$ (psi·s^{-1})	T_{max} (°C)
	Pure AN	200 (±10)	217 (±11)	82 (±17)	220 (±67)	347 (±17)
1.13	0.04	240 (±7)	211 (±3)	166 (±12)	508 (±64)	394 (±4)
1.69	0.06	248 (±10)	212 (±4)	119 (±20)	492 (±52)	387 (±6)
2.78	0.1	250 (±8)	211 (±3)	115 (±16)	398 (±164)	381 (±4)
5.41	0.2	255 (±5)	211 (±5)	132 (±22)	423 (±152)	392 (±8)
7.89	0.3	260 (±3)	214 (±3)	110 (±16)	318 (±48)	377 (±12)
10.26	0.4	263 (±4)	215 (±7)	113 (±19)	240 (±30)	379 (±12)
12.50	0.5	268 (±1)	213 (±4)	107 (±8)	228 (±14)	388 (±5)
22.22	1	275 (±2)	216 (±6)	68 (±10)	129 (±25)	394 (±15)
36.36	2	276 (±2)	223 (±17)	19 (±7)	52 (±20)	377 (±10)

(Note: each test contains 3.5 g of AN)

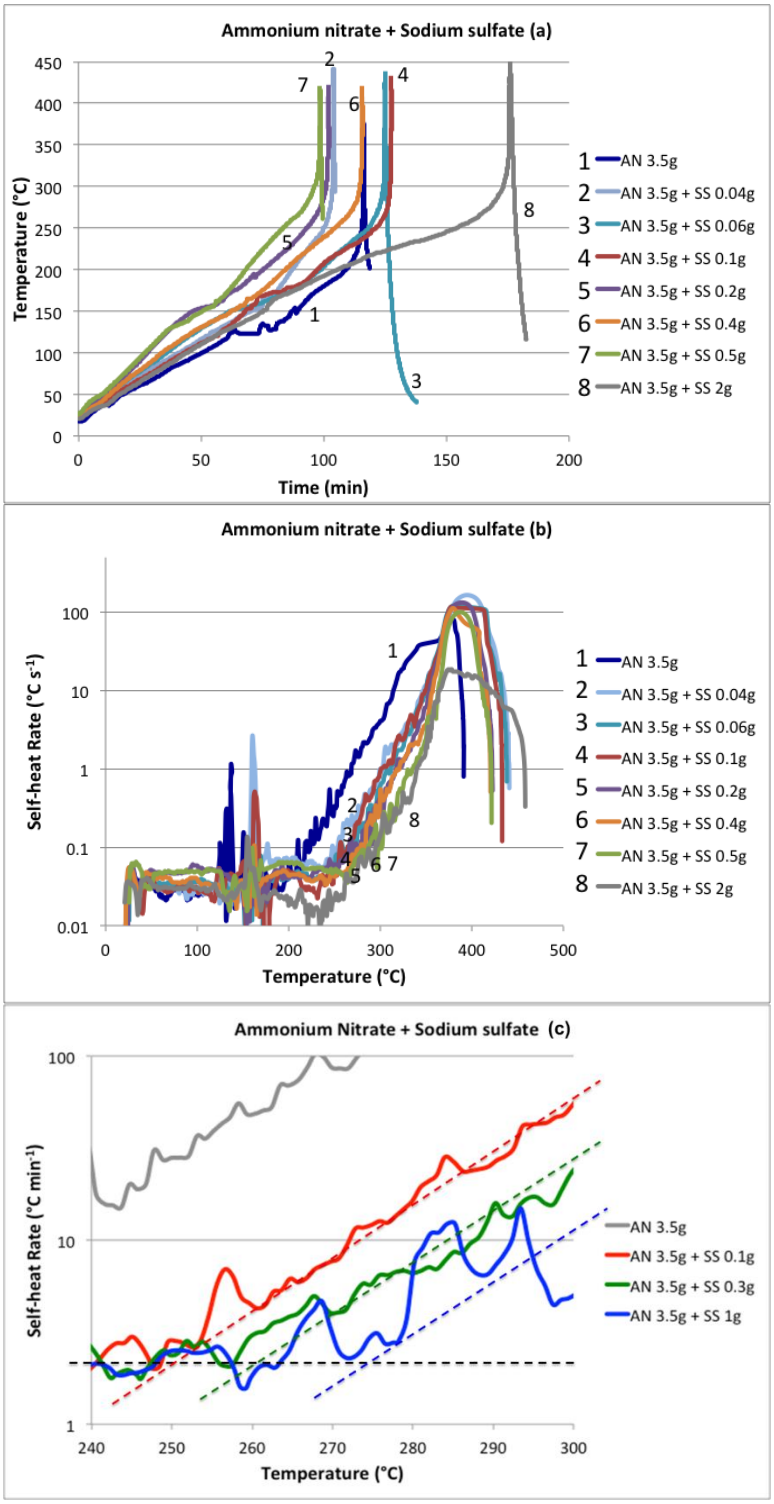

Figure 11. The thermal decomposition of AN and Na_2SO_4 at various concentrations (a) Temperature profile (b) Self-heating rate (c) Enlarged self-heating rate profile

To describe the analysis of a typical experimental set of data, details of AN mixture with 2.8 wt.% of Na_2SO_4 (3.5 g AN + 0.1 g Na_2SO_4) are discussed here. The temperature *vs*. time profiles and the self-heating rate *vs*. temperature profiles of the three replicate experiments are shown in Figure 12*(a)* and Figure 12(*b)*, respectively. Since the melting point of Na_2SO_4 is 884 °C, much higher than the temperature range of this work, there was a residue remaining in the test cell after each test.

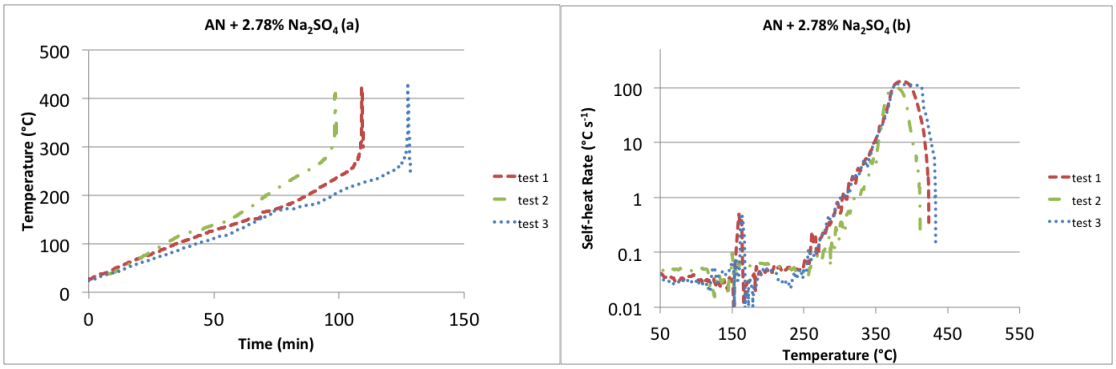

Figure 12. The thermal decomposition of AN with 2.78 wt.% of Na_2SO_4 (a) Temperature profile (b) Self-heating rate

From Figure 12*(a)*, it can be seen that the temperature curve increases smoothly. As can be seen in Figure 12*(b)*, there is a slight difference (~16 °C) in the "onset" temperature for the three replicate tests, but the temperatures at the maximum self-heating rate are similar. The "onset" temperature was 250 (±8) °C, with the maximum self-heating rate of 115 (±16) $°C \cdot s^{-1}$, which occurred at 381 (±4) °C. The "onset" pressure was 211 (±3) psig. The heat of reaction was determined to be –29 (±3) $kJ \cdot mol^{-1}$, and the activation energy was 178 (±14) $kJ \cdot mol^{-1}$.

On comparison of the results obtained for the mixture of AN with 2.8 wt.% of Na_2SO_4 against pure AN, it was found that the "onset" temperature increased by approximately 50 °C and the temperature at maximum self-heating rate increased by about 34 °C. The heat of reaction decreases by around 3 $kJ \cdot mol^{-1}$, and the activation energy increases by 36 $kJ \cdot mol^{-1}$. This shows that the addition of Na_2SO_4 delays the "onset" of runaway behavior of AN.

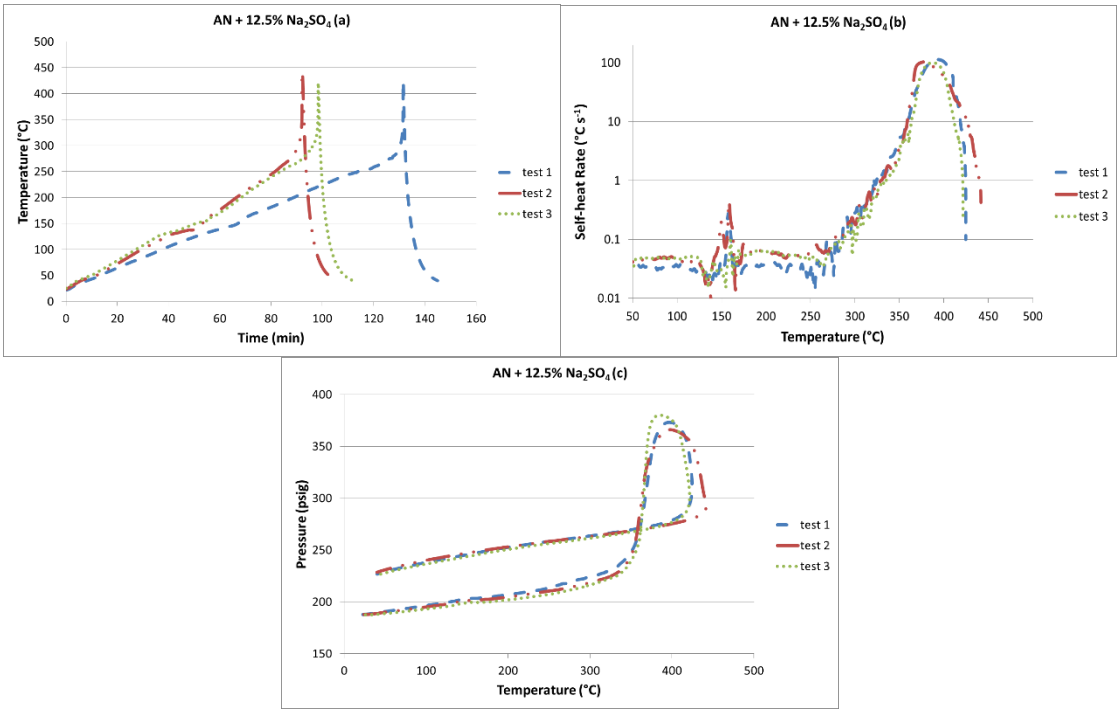

Figure 13. The thermal decomposition of AN with 12.5 wt.% of Na_2SO_4 (a) Temperature profile (b) Self-heating rate (c) Pressure *vs*. temperature

Another example is AN mixture with 12.5 wt.% of Na_2SO_4 (3.5 g AN + 0.5 g Na_2SO_4). The temperature *vs*. time profiles, the self-heating rate *vs*. temperature profiles,

and the pressure *vs*. temperature profiles of the three replicate experiments are shown in Figure 13*(a)*, Figure 13(*b)*, and Figure 13*(c)* respectively. The final temperature was 429 (±11) °C. The rest of the experimental parameters are summarized in Table 5.

The pressure *vs*. temperature profile, Figure 13*(c)*, of the three replicate tests gave very similar results for pressures below 320 psig and temperatures below 400 °C, which means that those three measurements in RSST had very good repeatability for pressure and temperature. Above 320 psig and 400 °C, repeatability between the three tests drops slightly. This is because the reaction rates were very fast, and RSST could not record the data fast enough. The RSST collects data every 30 s or every time the temperature, or pressure changes by 2 °C, or 2 psi, respectively [106]. However, if the reaction occurs too fast, the equipment is not able to track data at the intervals mentioned above. For example, when the reaction was experiencing the maximum self-heating rate (*i.e.*, the reaction occurs most violently), the RSST would only record one data point for every 5 °C, while in other periods, the RSST was able to record several data points for an increase in temperature of 1 °C. Thus, the pressure or temperature profiles during the maximum self-heating rate for replicate tests is unlikely to have exactly the same data points recorded. Moreover, both the solid and the gas phases were not thermally homogeneous, thus, the measured temperatures were the local temperatures at the position of the thermocouple and not the temperature of the whole solid or gas. This may explain the differences in the measured data.

Among all the concentrations of AN mixture with sodium sulfate, the severity of the runaway does not change much if the added mass of sodium sulfate is less than 0.5 g.

However, a clear trend of its reduction was observed as higher concentrations is used. Thus, sodium sulfate acts as an inhibitor.

Table 5 summarizes all the data for each concentration of the sodium sulfate including “onset” temperature, “onset” pressure, temperature at maximum self-heating rate, maximum self-heating rate, and maximum pressure-rise rate. It can be concluded from Figure 14, the comparison of those parameters, that in general, the addition of Na_2SO_4 will result in a higher “onset” temperature and temperature at maximum self-heating rate than pure AN. A little addition of Na_2SO_4 can increase the “onset” temperature a lot, and more Na_2SO_4 will result in higher “onset” temperature. For example, Na_2SO_4 raised the decomposition “onset” of AN by 40 °C for AN mixture with 1.1 wt.% Na_2SO_4, 48 °C for 1.7 wt.% Na_2SO_4, and 76 °C for 36.4 wt.% Na_2SO_4. However, the curve of the “onset” temperature *vs*. concentration plot has a small slope, meaning that a large amount of Na_2SO_4 would have similar results as a small amount of Na_2SO_4 regarding to the “onset” temperature, *e.g.*, 1.1 wt.% of Na_2SO_4 mixed with AN can increase the “onset” temperature by 40 °C. This is very fortunate, because, having to deal with a fertilizer, it is desirable for a small quantity of an inhibitor to have a large impact on the decomposition “onset”, thus rendering the fertilizer safer, without altering much of its composition. However, the recorded temperatures do not allow the accurate correlation of the effect of inhibitor concentration on the decomposition “onset”, because at the maximum rates temperatures change too fast for the recording capacity of the RSST as can be seen from the curves in Figure 14, for instance, which have been using

only the few raw data points. Nevertheless, there is clear evidence that sodium sulfate is a good inhibitor for AN.

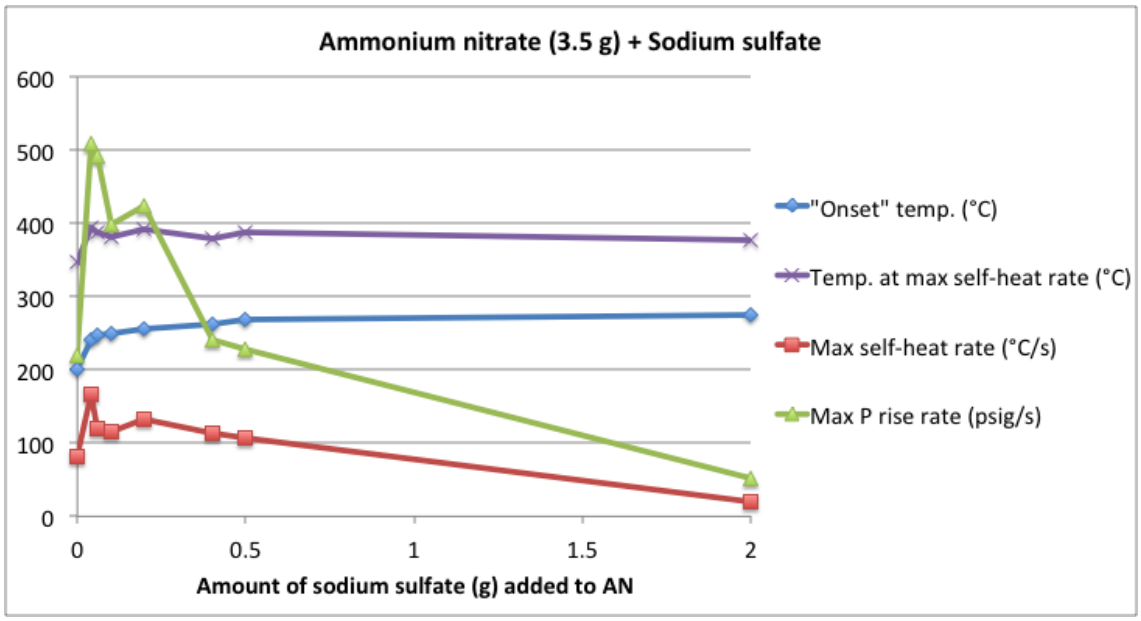

Figure 14. Comparison of the mixtures of AN with various concentrations of sodium sulfate

Similar results have been obtained using a DSC [22] where it is reported that Na_2SO_4 raised the decomposition exotherm of AN by 7 °C for AN mixture with 5wt.% Na_2SO_4, and 23 °C for 20 wt.% Na_2SO_4. Contrary to our observation that a substantial increase in Na_2SO_4 quantity did not have a proportional effect of the "onset" temperature rise, they found that quadruplication of Na_2SO_4 resulted in over tripled increase of the "onset" temperature rise. However, as reported earlier, the mass employed in RSST tests makes those results more reliable than those of DSC. In any case, more accurate

measurements are needed before any firm conclusions are drawn regarding the correlation between "onset" temperature rise and inhibitor concentration.

4.2.1.2 Sodium Sulfate Experiments in the APTAC

In the APTAC, to study the effect of sodium sulfate on the decomposition of AN, 1 g of AN was mixed thoroughly with various amounts of Na_2SO_4 and 5 g of sand, and placed into the test cell.

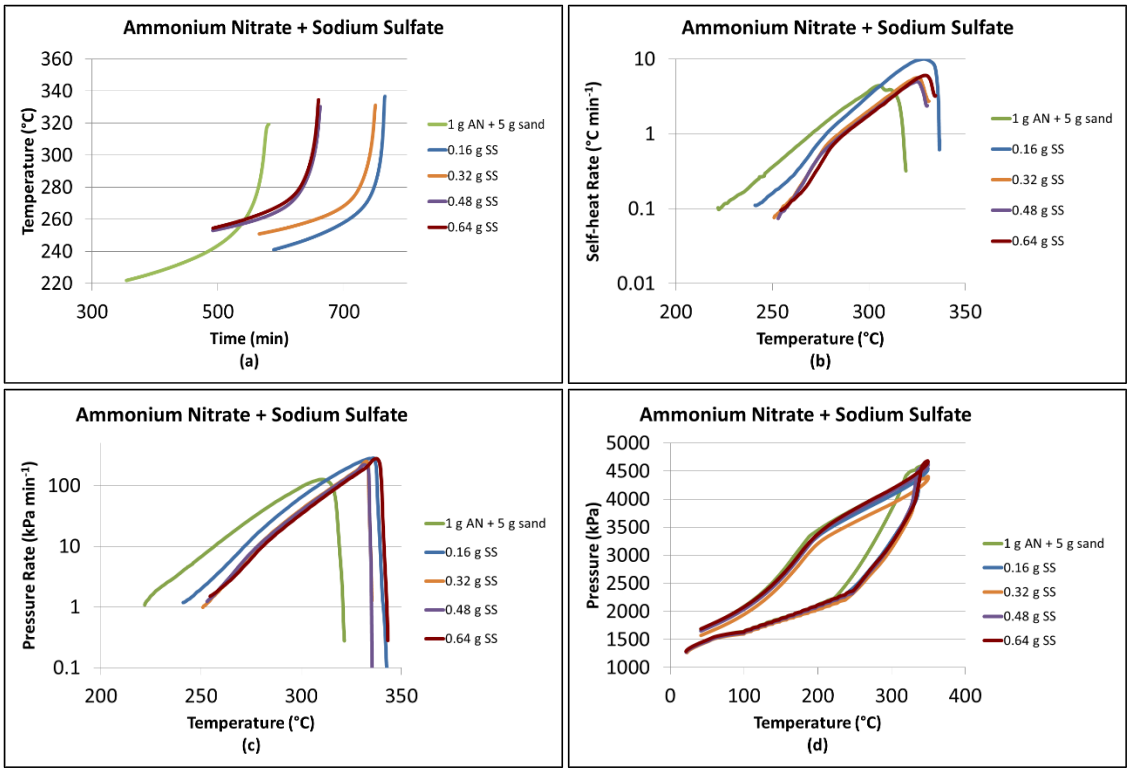

Figure 15. AN decomposition with sodium sulfate in the APTAC (a) Temperature *vs.* time profile (b) Self-heating rate *vs.* temperature profile (c) Pressure-rise rate *vs.* temperature profile (d) Pressure *vs.* temperature profile

Table 6. Experimental results of AN decomposition with sodium sulfate in the APTAC

Na_2SO_4 (g)	Pure AN	0.16	0.32	0.48	0.64
T_o (°C)	220	241	251	253	255
$(dT/dt)_{max}$ (°C·min^{-1})	4	10	6	5	6
T_{max} (°C)	306	329	325	325	329
T_f (°C)	322	343	335	335	343
P_o (kPa)	2223	2340	2360	2419	2465
$(dP/dt)_{max}$ (kPa·min^{-1})	127	285	251	221	280
P_{max} (kPa)	4102	4117	4109	4175	4309
P_f (kPa)	4450	4496	4311	4510	4620
P_c (kPa)	1687	1656	1573	1651	1689
$t_{runaway}$ (min)	252	176	185	171	168

(Note: each test contains 1 g of AN + 5 g of sand; P_c was obtained at 20 °C)

Various amounts of Na_2SO_4 were added into AN, including 13.8 wt.% (0.16 g), 24.2 wt.% (0.32 g), 32.4 wt.% (0.48 g), and 39.0 wt.% (0.64 g). The results are reported in Figure 15 and Table 6.

It can be concluded that with more Na_2SO_4 in the mixture, the "onset" temperature increases and the maximum self-heating rate decreases, showing that Na_2SO_4 is a good inhibitor for AN. However, with only a little addition of Na_2SO_4, the "onset" temperature can be increased a lot. The other parameters are similar, meaning that a small amount of Na_2SO_4 is good for AN, while more Na_2SO_4 is not necessary for the safe storage of AN.

4.2.2 Potassium Chloride as Promoter

Using the RSST, another additive, potassium chloride (KCl), was used to study the runaway behavior of AN. Mixtures of AN (3.5 g) with 2.8 wt.% (0.1 g), 5.4 wt.% (0.2 g), 7.9 wt.% (0.3 g), 11.4 wt.% (0.45 g), 12.5 wt.% (0.5 g), and 22.2 wt.% (1g) KCl were tested. Each experiment was repeated three times. The parameters obtained from experiments are summarized in Table 7.

Table 7. AN mixture with potassium chloride at various concentrations

wt.% of KCl	KCl (g)	T_o (°C)	P_o (psig)	$(dT/dt)_{max}$ (°C·s^{-1})	$(dP/dt)_{max}$ (psi·s^{-1})	T_{max} (°C)
	Pure AN	200 (±10)	217 (±11)	82 (±17)	220 (±67)	347 (±17)
2.8	0.1	194 (±2)	205 (±1)	332 (±35)	782 (±278)	301 (±2)
5.4	0.2	196 (±3)	207 (±4)	290 (±65)	692 (±306)	323 (±18)
7.9	0.3	196 (±2)	208 (±2)	373 (±32)	1453 (±352)	309 (±10)
11.4	0.45	180 (±5)	206 (±1)	420 (±20)	1287 (±122)	292 (±6)
12.5	0.5	152 (±9)	203 (±1)	490 (±96)	1134 (±294)	295 (±15)
22.2	1	145 (±8)	201 (±2)	503 (±65)	1067 (±266)	302 (±3)

(Note: each test contains 3.5 g of AN)

The experimental data obtained from AN mixture with 2.8 wt.% of KCl (3.5 g AN + 0.1 g KCl) is discussed here; the same analysis was performed for all samples. The temperature *vs*. time profile and self-heating rate *vs*. temperature profile are shown in Figure 16*(a)* and Figure 16*(b)*, respectively.

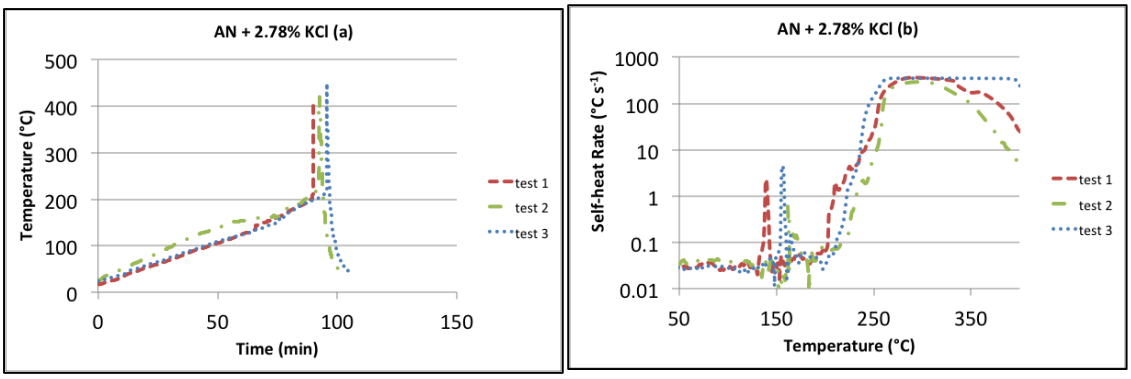

Figure 16. The thermal decomposition of AN with 2.78 wt.% of KCl (a) Temperature profile (b) Self-heating rate

As can be seen the presence of KCl tends to induce the thermal decomposition of AN at a lower temperature compared with that of pure AN. There is a slight difference for the three replicate tests. The "onset" temperature obtained was 194 (±2) °C, with the maximum self-heating rate of 332 (±35) °C·s^{-1}, which occurred at 301 (±2) °C. The "onset" pressure was 205 (±1) psig and the maximum pressure-rise rate was 782 (±278) psi·s^{-1}. The heat of reaction was –39 (±3) kJ·mol^{-1}, and the activation energy was 206 (±33) kJ·mol^{-1}. The large standard deviation might be caused by the deficiency of the RSST in recording data when the reaction occurs too fast. In the RSST, during temperature, or pressure changes data is supposed to be recorded every 30 s, 2 °C, and 2 psi [106]. However, if the reaction occurs too fast, the equipment is not capable to track data at the intervals mentioned above. For example, when the reaction occurs most violently, the RSST can only record one data point for every 5 °C, while in other periods, the RSST is capable to record several data points for an increase in temperature

of 1 °C. Thus, the data during the maximum self-heating rate for replicate tests may not have exactly the same data points recorded.

On comparison of the results obtained for the mixture of AN with KCl, against pure AN, it was found that the "onset" temperature decreased by 6 °C. Although the "onset" temperature is 194 (±2) °C, which is not lower than 190 °C, making it not confident to conclude that KCl is a promoter, the mixtures with other concentrations clearly show that the presence of KCl decreases the "onset" temperature of AN by more than 10 °C. Moreover, the temperature at maximum self-heating rate decreased by 42 °C. The maximum temperature and pressure-rise rates of AN with KCl also increases severely. This shows that the addition of KCl advances the "onset" of runaway behavior of AN and generates heat at a higher rate.

Another concentration, 12.5 wt.% KCl in the mixture (3.5 g AN + 0.5 g Na_2SO_4), was also reported here. The temperature *vs*. time profile is shown in Figure 17*(a)* and the self-heating rate as a function of temperature is shown in Figure 17*(b)*. In Figure 17*(b)*, each point represents a data point collected by the computer. In addition to the data from the three replicate tests, pure AN data and pure KCl data are also shown as reference in Figure 17. When the AN decomposition became measurable, its rate was so fast that the RSST could not record fast enough the temperature as the temperature typically rose by over 10 °C in 60 ms; the instrument software projected these data and calculated a self-heating rate for the mixture above 10,000 °C·min^{-1}. Consequently, for those measurements only a few data points were recorded for the temperature range of 250-500 °C as shown in Figure 17*(b)*.

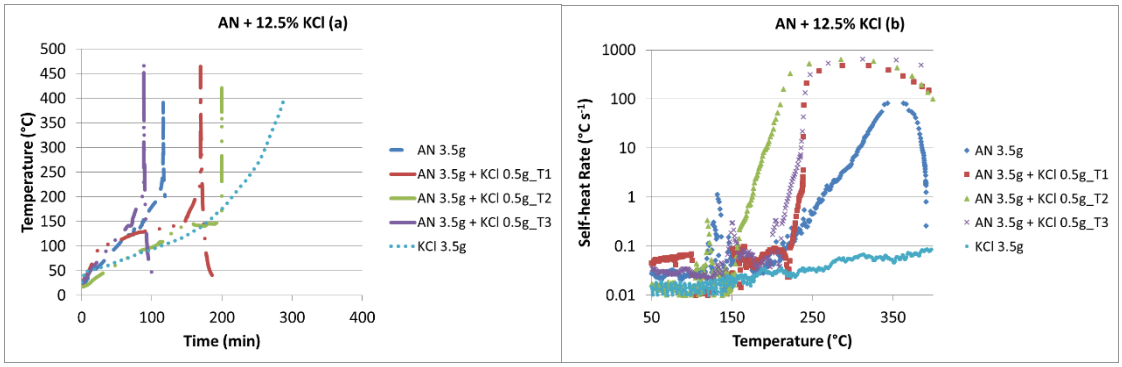

Figure 17. The thermal decomposition of AN with 12.5 wt.% of KCl (a) Temperature profile (b) Self-heating rate

From Figure 17*(a)*, it is obvious that when AN was mixed with 12.5 wt.% of KCl, when the sample was heated up to approximately 150 °C, there was a sudden increase in the rate of temperature rise, which was much larger than the pre-set temperature-increase-rate (1 °C·min^{-1}). This means there was a fast reaction starting at 150 °C, which was then followed by a much faster reaction after 200 °C. Looking at the data of pure KCl from Figure 17*(b)*, it can be seen that after 150 °C, the self-heating rate was higher than the pre-set temperature-increase-rate supplied by the heater from the RSST. This phenomenon may explain the sudden increase in the self-heating rate at 150 °C for the mixture. More work needs to be done to explain the behavior of the mixture.

Using the data in Table 7, "onset" temperature, temperature at maximum self-heating rate, and maximum self-heating rate *vs*. concentration profiles are plotted in Figure 18.

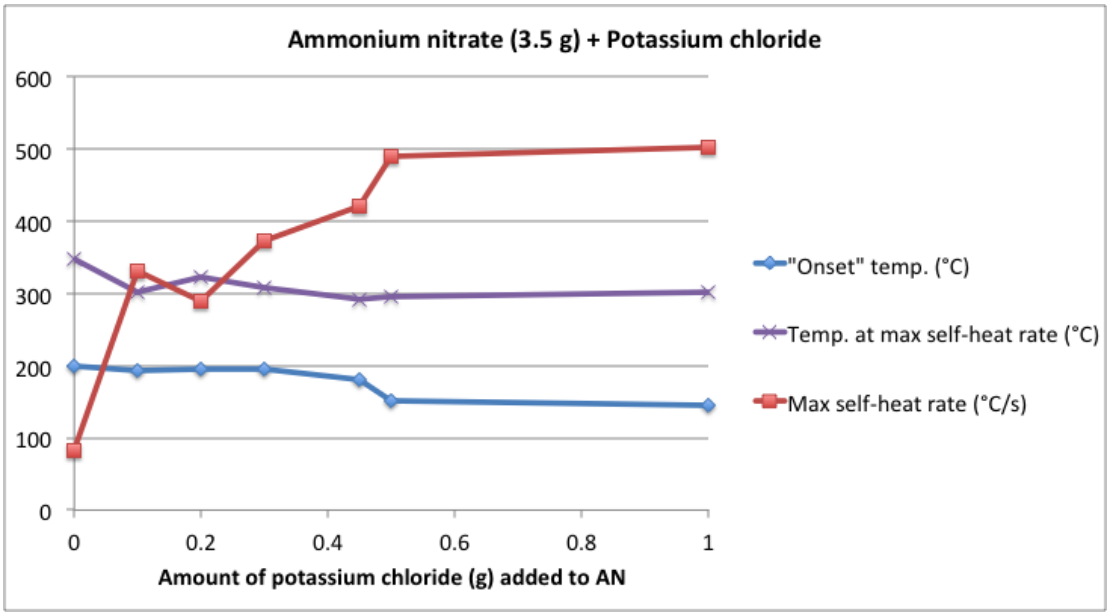

Figure 18. Comparison of the mixtures of AN with various concentrations of potassium chloride

It is observed that the addition of KCl resulted in a lower "onset" temperature and temperature at maximum self-heating rate than that of pure AN. The more KCl mass in the mixture the lower the "onset" temperature. In general, the mixture with a higher concentration of KCl has a higher value of maximum self-heating rate than the mixture with a lower concentration of KCl. The maximum self-heating rates of all the mixtures occur at almost the same temperature range, around 290 °C to 310 °C, which is approximately 40 °C lower than that temperature of pure AN. It is worth noting that the "onset" temperature changes a lot when the weight of KCl exceeds 0.4 g, beyond which point the "onset" temperature drops faster than that of the mixture with less KCl; and the maximum self-heating rate increases faster when the weight of KCl exceeds 0.2 g. This needs to be further studied by equipment with higher accuracy and the reason behind it

needs to be researched. However, it can be concluded that potassium chloride is a promoter for AN thermal decomposition.

Other works in literature have shown that KCl has a strong promoting effect. Oxley *et al.* [22] found that KCl lowered the exotherm of AN by about 70 °C using a DSC. Li and Koseki [48] found that the exotherm was lowered by approximately 75 °C using a C80, where samples of 500 mg were used.

4.2.3 Comparison between Inhibitor and Promoter using the APTAC

The effect of sodium sulfate as an inhibitor and potassium chloride as a promoter on the decomposition of AN was compared in the APTAC, 1 g of AN was mixed thoroughly with 0.16 g of additive and 5 g of sand, and placed into the test cell.

The temperature *vs*. time profile, self-heating rate *vs*. temperature profile, pressure-rise rate *vs*. temperature profile, and the pressure *vs*. temperature profile are plotted in Figure 19. The parameters are summarized in Table 8 and Table 9.

From Figure 19*(a)*, the temperature *vs*. time profile, it can be concluded that when AN is mixed with KCl, the decomposition occurs at a lower temperature (approximately 200 °C) than that of pure AN (approximately 220 °C), while when AN is mixed with Na_2SO_4, the decomposition occurs at higher temperature (approximately 240 °C). It is also concluded that the time to complete the reaction for AN mixture with KCl is shorter than others. Figure 19*(b)*, the self-heating rate *vs*. temperature profile, shows that the addition of KCl resulted in a much higher maximum self-heating rate, while the

addition of Na_2SO_4 resulted in a lower maximum self-heating rate than pure AN. Figure 19*(c)*, the pressure-rise rate *vs*. temperature profile, shows that the addition of KCl resulted in a much higher pressure-rise rate, while the addition of Na_2SO_4 resulted in a lower pressure-rise rate than pure AN. Figure 19*(d)*, the pressure *vs*. temperature profile, shows that the adiabatic temperature rise of AN mixture with KCl was the largest, followed by pure AN, and the AN mixture with Na_2SO_4 had the smallest adiabatic temperature rise.

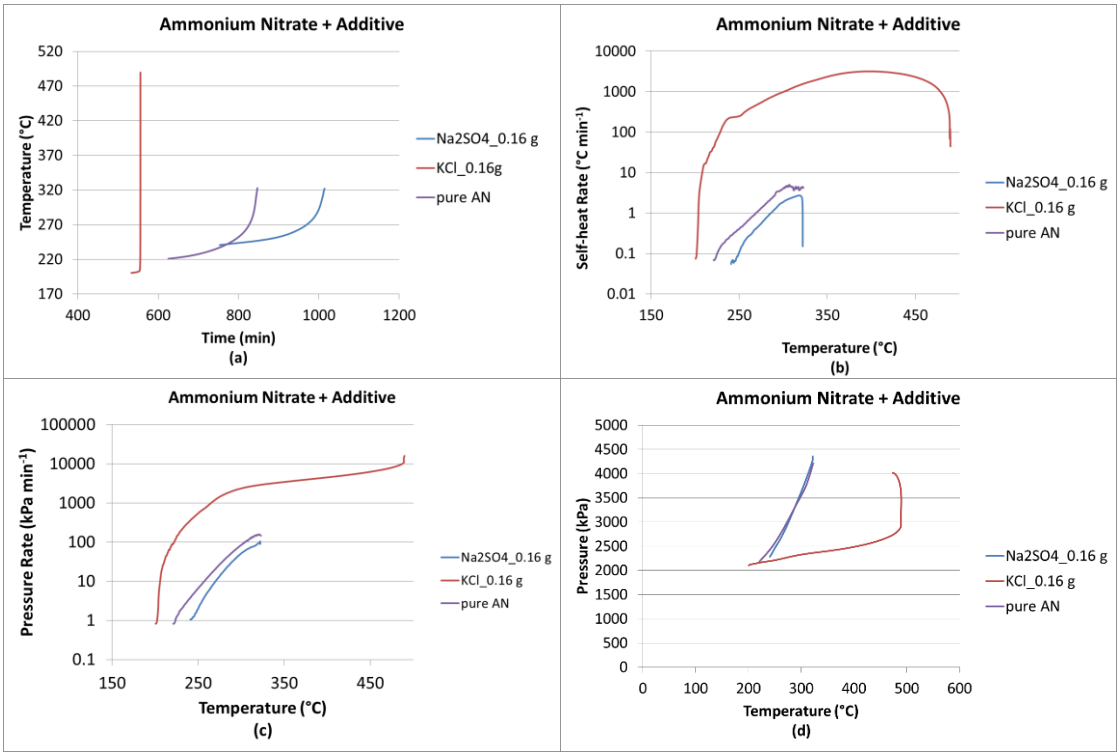

Figure 19. AN decomposition with additives in the APTAC (a) Temperature *vs*. time profile (b) Self-heating rate *vs*. temperature profile (c) Pressure-rise rate *vs*. temperature profile (d) Pressure *vs*. temperature profile

Table 8. Experimental results of AN decomposition with additives in the APTAC: Temperature

Additive (g)	T_o (°C)	$(dT/dt)_{max}$ (°C·min^{-1})	T_{max} (°C)	T_f (°C)	$t_{runaway}$ (min)
Pure AN	221	4.98	307	323	222
0.16 Na_2SO_4	241	2.73	318	322	261
0.16 KCl	200	3190	394	490	23

(Note: each test contains 1 g of AN + 5 g of sand)

Table 9. Experimental results of AN decomposition with additives in the APTAC: Pressure

Additive (g)	P_o (kPa)	$(dP/dt)_{max}$ (kPa·min^{-1})	P_{max} (kPa)	P_f (kPa)	P_c (kPa)
Pure AN	2184	157	4128	4216	1628
0.16 Na_2SO_4	2286	104	4311	4355	1646
0.16 KCl	2102	16070	3504	4019	1616

(Note: each test contains 1 g of AN + 5 g of sand; P_c was obtained at 20 °C)

Therefore, KCl hugely promotes the decomposition of AN, and Na_2SO_4 inhibits AN decomposition. It agrees with the experimental results obtained in the RSST. The AN mixtures with Na_2SO_4 in other concentrations were discussed in Section 4.2.1.2.

4.3 Effect of the Mixture of Sodium Sulfate and Potassium Chloride as Additive Together

In AN storage, there are usually other materials stored nearby, which could potentially come in contact with or contaminate AN. In order to study the effect on AN in the presence of mixed materials (both an inhibitor and a promoter), sodium sulfate and potassium chloride, both in small quantities, were mixed with AN.

The main objective of the research presented in this section focuses on the synergistic effect of an inhibitor and a promoter on AN decomposition. The RSST was used in the study of the runaway behavior of AN in the presence of a promoter (KCl) and an inhibitor (Na_2SO_4) together, and it was compared with the behavior of AN with each additive separately. It was found that when both additives were mixed, Na_2SO_4 induced a rise in the decomposition "onset" temperature. The presence of KCl, however, induced a more violent decomposition worsening all other parameters.

4.3.1 Experimental Results – Sodium Sulfate and Potassium Chloride Mixture as Additive

To study the effect of sodium sulfate and potassium chloride together as additives, each compound of the sample to be tested (inhibitor and/or promoter and AN) was weighed and loaded into the test cell where it was then mixed by vigorous shaking

until the sample was well mixed, confirmed by visual observation and verified by the good repeatability of identical experiments.

In all tests, 3.5 g of solid AN were employed. Equal quantities of each of the two additives (sodium sulfate and potassium chloride) were added, *i.e.*, 0.25 g and 0.5 g in two different measurements. Three identical measurements were performed in each composition to ensure good repeatability. Measurements with the respective quantity of each additive separately were also performed.

Two different mixture concentrations as mentioned in the previous section, 3.5 g AN + 0.25 g Na_2SO_4 + 0.25 g KCl and 3.5 g AN + 0.5 g Na_2SO_4 + 0.5 g KCl, were tested and the results are plotted in Figure 20. The total mass of additives in the former experiment was 0.5 g, which equals to the one of the masses of a single additive in the previous sections; in the latter experiment 1 g of additives had been used, *i.e.*, 0.5 g of Na_2SO_4 and 0.5 g of KCl together with 3.5 g of AN. Figure 20*(a-c)* shows the temperature *vs*. time profile, the self-heating rate *vs*. temperature profile, and the pressure-rise rate *vs*. temperature profile, respectively. There are three curves shown in each figure: the respective curve of pure AN as well as those of each of the aforementioned mixtures. As can be seen in Figure 20, there are relatively few points collected at higher self-heating rates.

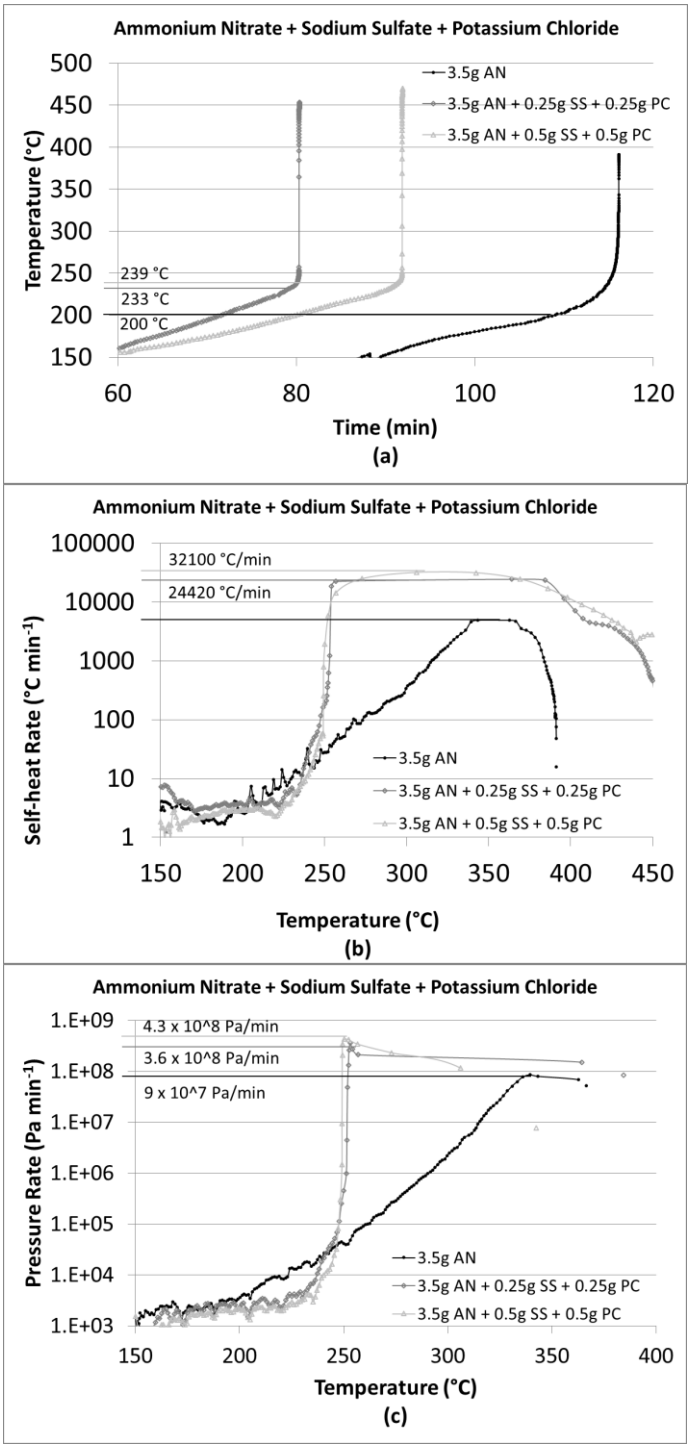

Figure 20. The thermal decomposition of AN, using Na_2SO_4 and KCl as additives (a) Temperature profile (b) Self-heating rate (c) Pressure-rise rate. (●)Pure AN (△) AN with 0.25 g of each additive and (△) AN with 0.5 g of each additive

As can be seen in Figure 20*(a)*, when both Na_2SO_4 and KCl were mixed with AN, the "onset" temperature was higher than that of the pure AN, where the "onset" temperature was determined in the way as reported in Section 4.1.1. Moreover, although the "onset" temperature increased by approximately 30 °C, the maximum temperature reached, T_f , increased by 60 °C as compared to that of pure AN decomposition. Therefore it was expected that the reaction pathways were different in each case. When Na_2SO_4 was used in isolation the "onset" temperature increased while the temperature increase dropped. On the contrary, the addition of KCl had the opposite effect on both parameters, *i.e.*, "onset" temperature dropped and temperature rise increased. In that aspect, when both Na_2SO_4 and KCl were used, Na_2SO_4 seemed to have only one inhibiting effect, *i.e.*, a rather strong effect on the runaway "onset", while KCl had a stronger effect on the runaway severity. It also appears that all other inhibiting effects that Na_2SO_4 induced when used as a single additive were overwritten by the presence of KCl. As shown in Figure 20*(b)*, when both Na_2SO_4 and KCl were added, the "onset" temperatures and maximum self-heating rates were both higher than those of the pure AN, but the self-heating rates also increased faster. Figure 20*(c)* shows that the "onset" temperatures and maximum pressure-rise rates were higher when Na_2SO_4 and KCl were mixed with AN. The values of each of the important parameters used to characterize the thermal decomposition with the associated error are summarized in Table 10 . In every column the highest and the lowest values are highlighted for an easiest comparison.

Table 10. Parameters of thermal decomposition of AN with Na_2SO_4 and KCl added in equal mass

Mass of Na_2SO_4+KCl (g (mol%))	T_o (°C)	$(dT/dt)_{max}$ (°C·s^{-1})	T_{max} (°C)	T_f (°C)	T_f-T_o (°C)	P_o (Pa)	$(dP/dt)_{max}$ (Pa·s^{-1})
0.25+0.25 (3.61+6.87)	231 (±3)	468 (±86)	344 (±1)	478 (±35)	247	$1.5\cdot10^6$ ($\pm5\cdot10^3$)	$6.3\cdot10^6$ ($\pm5\cdot10^5$)
0.5+0.5 (6.53+12.44)	237 (±3)	**637** (±144)	343 (±1)	**490** (±28)	253	$1.5\cdot10^6$ ($\pm5\cdot10^3$)	$\mathbf{9.9\cdot10^6}$ ($\pm4\cdot10^6$)
0.5+0.0 (7.45+0)	**268** (±1)	107 (±8)	**388** (±5)	429 (±11)	**161**	$1.6\cdot10^6$ ($\pm1\cdot10^5$)	$1.6\cdot10^6$ ($\pm1\cdot10^5$)
0.0+0.5 (0+13.31)	**152** (±9)	596 (±92)	**295** (±15)	453 (±28)	**301**	$1.5\cdot10^6$ ($\pm1\cdot10^5$)	$7.8\cdot10^6$ ($\pm2\cdot10^6$)
0.0+0.0	200 (±10)	**82** (±17)	347 (±17)	**393** (±42)	193	$1.6\cdot10^6$ ($\pm2\cdot10^5$)	$\mathbf{1.5\cdot10^6}$ ($\pm5\cdot10^5$)

(Note: each test contains 3.5 g of AN)

4.3.2 Discussion of the Synergistic Effect

The impact of Na_2SO_4 and KCl together on AN as reported in the previous section, and some of the experimental results from Section 4.2.1 and Section 4.2.2, are summarized in Table 10, in which the mass of each additive is shown in the first column and its mole percentile in the mixture in parentheses in the same column. Each experiment was performed using the same quantity of AN, 3.5 g. The results show that the presence of Na_2SO_4 and KCl together increased the "onset" temperature of AN, which lowered the possibility of AN decomposition. However, it also increased the

maximum self-heating rate, the maximum pressure-rise rate, and the maximum temperature, which increases the consequences of AN decomposition should it occur. As can be seen from a comparison of each value with the effect that the pure additives have on AN decomposition, Na_2SO_4 increases T_o and reduces the adiabatic temperature rise (T_f - T_o), while it leaves practically unaffected both the maximum self-heating rate and the maximum pressure-rise rate (within the experimental error). On the other hand, the addition of KCl alone reduces T_o while it has a significant effect on the values of all other parameters. The addition of both additives improved from a safety point of view, only the T_o value, while the maximum self-heating rate and pressure-rise rate increased. In safety studies, quantities are usually expressed in mass units; however, to study the mechanisms of chemical reactions, moles is a more meaningful unit to use, thus the molar percentile of each additive is shown in the first column in Table 10. As can be seen the quantity of KCl which has been added is about twice as much as that of Na_2SO_4.

Figure 21 shows a comparison of the data in Table 10, *i.e.*, pure AN data with and without additives. Figure 21*(a)* shows a comparison of the "onset" temperature, temperature at maximum self-heating rate, and maximum temperature reached. Figure 21*(b)* shows a comparison of the maximum self-heating rate and maximum pressure-rise rate. In each figure, the corresponding parameters of pure AN are plotted in straight dashed lines for easier comparison.

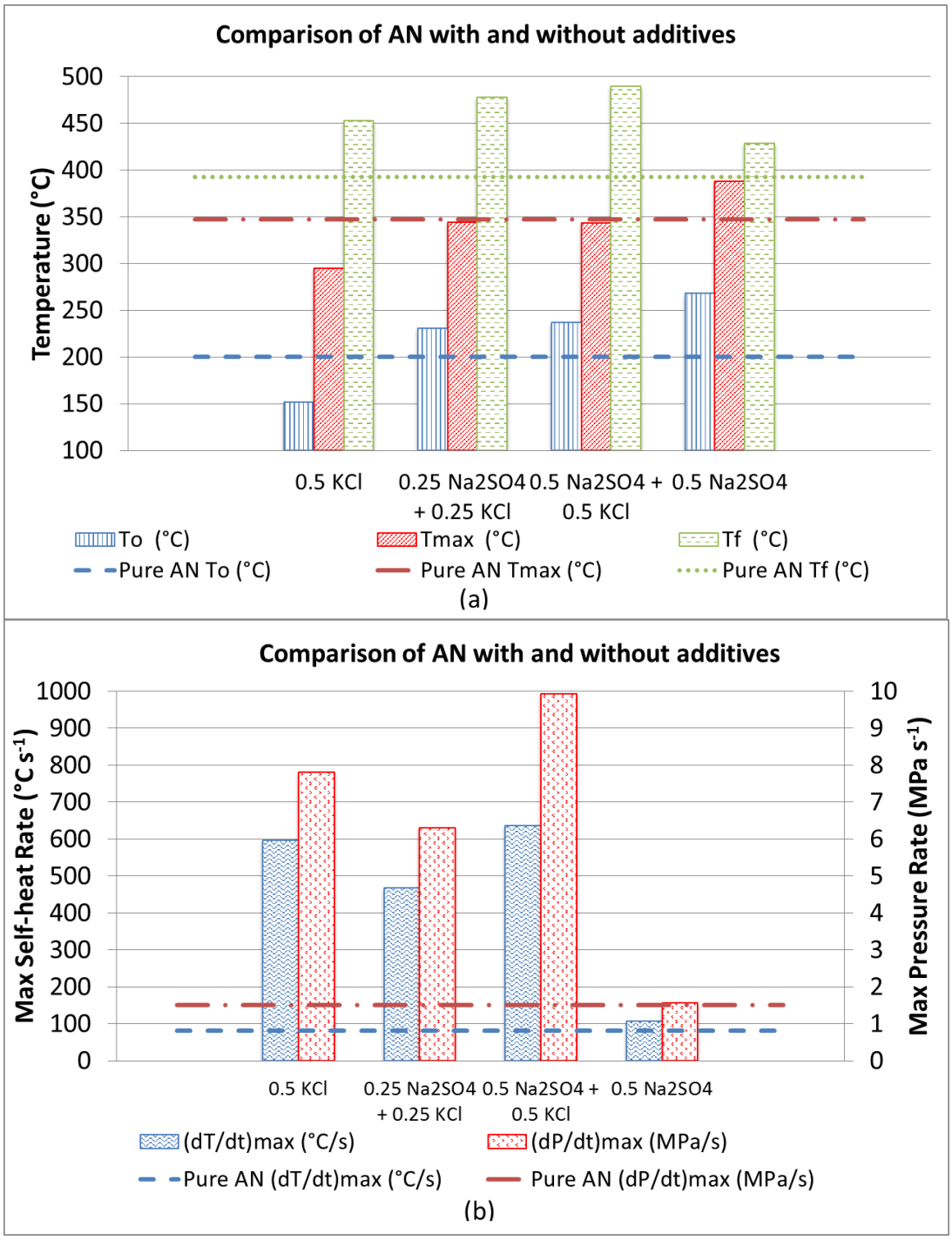

Figure 21. Comparison of AN with and without additives (a) "onset" temperature (T_o), temperature at maximum self-heating rate (T_{max}), and maximum temperature (T_f) (b) maximum self-heating rate $((dT/dt)_{max})$ and maximum pressure-rise rate $((dP/dt)_{max})$

Figure 21*(a)* shows that for the samples tested in this work, the presence of KCl alone led to a lower "onset" temperature than that of pure AN, and the presence of Na_2SO_4 resulted in a higher "onset" temperature than that of pure AN irrespectively of whether or not KCl was present in the sample. When equal masses of Na_2SO_4 and KCl were mixed with AN, the temperatures at maximum self-heating rate were almost the same as pure AN. For all the samples with additive, the maximum temperatures reached during the reaction were higher than those of pure AN, although for the measurement of AN mixture with pure Na_2SO_4 the increase of T_f was smaller than the respective increase of T_o. The overall adiabatic temperature rise in the case of Na_2SO_4 addition was the lowest compared to all other measurements, even those of pure AN. Na_2SO_4 always resulted in higher "onset" temperatures. As can be seen in Figure 21*(b)* the presence of KCl dramatically increased the maximum self-heating rate, the maximum pressure-rise rate, and T_f, and when present in larger quantities its effect as promoter was higher. Higher molar concentration of KCl in general resulted in higher maximum self-heating rates and maximum pressure-rise rates. This is better shown in Figure 22, where each sample is heated from ambient temperature and the pressure increases with temperature, once the decomposition reaction occurs, non-condensable gaseous products are generated and pressure starts to increase faster, when the reaction completes the temperature cools down and the pressure drops, and the pressure after cooling down is higher than the initial pressure due to the non-condensable gas products. As can be seen in Figure 22, the presence of KCl in the sample induces a more violent decomposition reaction.

It is evident that to avoid AN explosions, AN should be separately stored from promoters, even when inhibitors are also present.

To understand this behavior, it is important to discuss the potential mechanism of AN decomposition with the two additives, both separately and together. The next section discusses the mechanism behind the behavior.

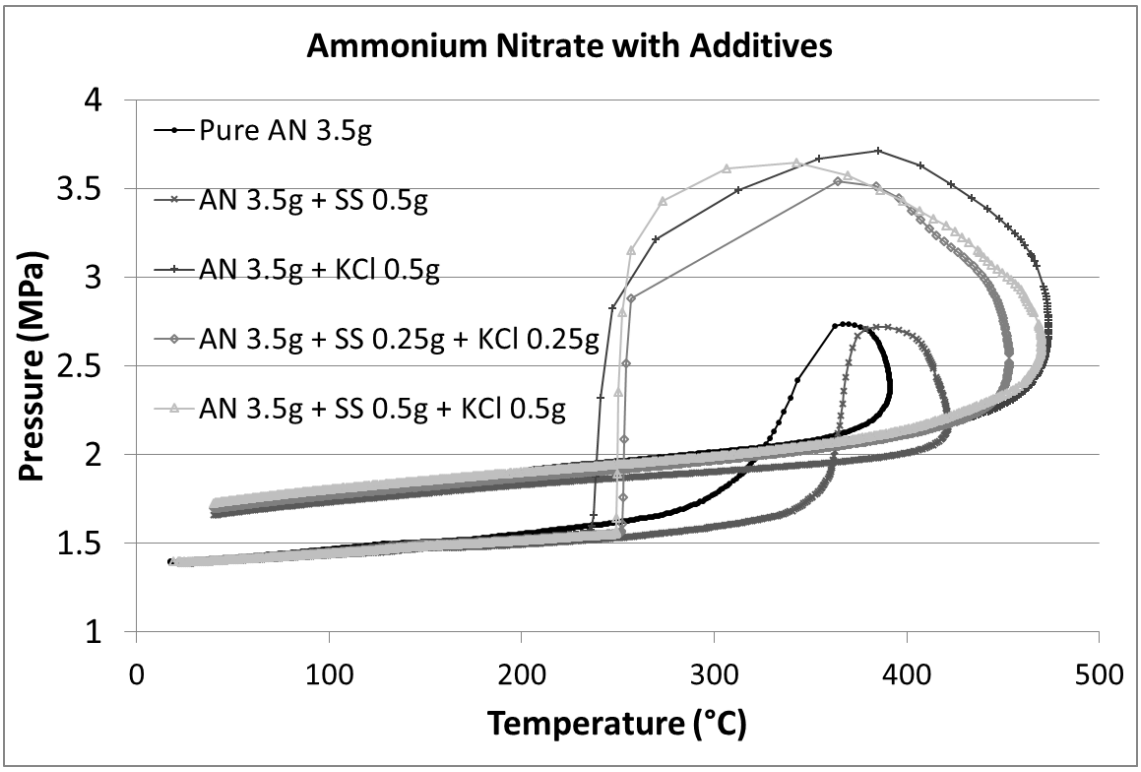

Figure 22. The pressure *vs*. temperature profile of the thermal decomposition of AN with different additives

4.4 Mechanisms of AN Decomposition with the Inhibitor and Promoter

4.4.1 Sodium Sulfate as Inhibitor

When Na_2SO_4 is mixed with AN as an additive, the salt is partially or totally dissolved in the water produced by the decomposition reaction of AN, giving the respective ion. However, HSO_4^- is a weak acid, SO_4^{2-} reacts with water according to reaction Eq. (52) (hydrolysis) to produce HSO_4^- and liberating OH^- thus increasing the solution pH.

Eq. (52) $SO_4^{2-} + H_2O \rightleftharpoons HSO_4^- + OH^-$

Reactions Eq. (2) and Eq. (3) produce NH_3 and water via a reversible and a practically irreversible reaction, respectively.

In an aqueous environment NH_3 formed by reaction Eq. (2) acts as a weak basis as shown in Eq. (53).

Eq. (53) $NH_3 + H_2O \rightleftharpoons NH_4^+ + OH^-$

In an alkaline or a less acidic environment the equilibrium of reaction Eq. (53) is shifted to the left, increasing the concentration of the non-associated NH_3, shifting on its turn to the left the equilibrium of reaction Eq. (2) and thus inhibiting one of the major paths of NH_4NO_3 decomposition, also reducing HNO_3 formation. The extent to which this mechanism affects the decomposition depends on the equilibrium constant of each of reactions Eq. (2), Eq. (52) and Eq. (53) and the concentration of water formed by reaction Eq. (3).

On the other hand, KCl, is the salt of a strong acid and a strong base, thus when dissolved in water practically leaves its pH unaffected.

Although the solution pH during reaction was not possible to measure, according to Oxley *et al.* [22], solutions containing SO_4^{2-} result in pH values in the range of 4–5, and it is more basic than nitrate. According to them Na_2SO_4 acts as an inhibitor due to the following rationale. The anion SO_4^{2-} functions as a conjugate base of weak acids, as can be seen in reaction Eq. (54) [22]. The SO_4^{2-} is basic and it forms NH_3 and H_2SO_4 in the presence of NH_4^+. Based on reaction Eq. (11), HNO_3 reacts with acid, including NH_4^+, H_3O^+, or HNO_3, and produce NO_2^+. Subsequently, NO_2^+ further reacts with NH_3 as described in reaction Eq. (12), and it is the controlling step of the AN decomposition reaction. According to AN decomposition mechanism introduced in Section 1.5, there is always more NH_3 than NO_2^+ in the system, therefore, the amount of NO_2^+ determines the rate of AN decomposition. In other words, with less NO_2^+, AN decomposition is mitigated. The behavior of Na_2SO_4 as an inhibitor for AN agrees with the theory that the acidity of the additive affects AN thermal stability [55, 107].

Eq. (54) $\quad 2NH_4^+ + SO_4^{2-} \rightarrow 2NH_3 + H_2SO_4$

The presence of SO_4^{2-} ions mitigate AN decomposition and the rationale is as follows. Based on reaction Eq. (11), NH_4^+ produces NO_2^+, and based on reaction Eq. (54), one SO_4^{2-} consumes two NH_4^+, thus reducing the generation of NO_2^+. This means that the presence of SO_4^{2-} reduces the amount of NO_2^+. As stated earlier, less NO_2^+ reduces the severity of AN decomposition, thus, inhibiting AN decomposition.

Another mechanism and rationale with a new reaction scheme is as follows. Na_2SO_4 as a slightly basic species reacts with HNO_3 to produce a slightly acidic stable $NaHSO_4$ species as well as the non-reactive $NaNO_3$, as reported in reaction Eq. (55). Nitric acid (HNO_3) is then strongly removed by this simple reaction and consequently NO_2^+ is much less present to produce decomposition reactions of AN, based on reactions Eq. (11) and Eq. (12). It is concluded that sodium sulfate added to AN plays the role of a scavenger for nitric acid reactive species, reducing the presence of reactive NO_2^+. As stated earlier, less NO_2^+ reduces the severity of AN decomposition.

Eq. (55) $Na_2SO_4 + HNO_3 \rightarrow NaHSO_4 + NaNO_3$

4.4.2 Potassium Chloride as Promoter

When KCl is mixed with AN as an additive, it acts as a promoter. According to MacNeil *et al.* [54], one plausible explanation of the decomposition mechanism of the mixture of AN and hydrochloric acid is the one proposed next. Reaction Eq. (12) is substituted by reaction Eq. (56). Moreover, reactions Eq. (57) and Eq. (58) are expected to occur. The ion NO_2^+ and NH_3 are activated by Cl^- and H^+, therefore, the generation rate of $[NH_3NO_2^+]$ at lower temperatures is increased. The activation energy of the reaction Eq. (12) is also decreased [24].

Eq. (56) $NH_3 + H^+ = NH_4^+ *$

Eq. (57) $NO_2^+ + Cl^- \rightarrow NO_2Cl$

Eq. (58) $NO_2Cl + NH_4^+ \rightarrow [NH_3NO_2^+] + H^+ + Cl^-$

Another conceivable reaction path of the decomposition of the mixture of AN and Cl^- is listed in reactions Eq. (59), Eq. (60), and Eq. (61) as proposed by Li and Koseki [42]. In Eq. (61), the generation rate of N_2 and HCl is fast.

Eq. (59) $NO_2^+ + Cl^- \rightarrow NO_2 + Cl$

Eq. (60) $Cl + Cl \rightarrow Cl_2$

Eq. (61) $Cl_2 + NH_3 \rightarrow [NH_2Cl] \xrightarrow{fast} N_2 + HCl$

Another mechanism and rationale is explained here [108]. In the mixtures of AN and KCl, the reaction Eq. (62) predominates, more so above 200 °C.

Eq. (62) $5NH_4NO_3 \rightarrow 4N_2 + 9H_2O + 2HNO_3$

When AN is mixed with 10% KCl, the molar ratio of N_2O/N_2 in the decomposition products is 3:1 at 165 °C, 1:1 at 205 °C, and 1:4 at 295 °C [108]. This ratio does not change with acidity, but increases with pressure. The results show strong auto-catalytic effects. The rate of decomposition during the induction period is similar to that of pure AN. The acidity of the mixture during the induction period will increase with the evaporation of NH_3, and the auto-catalyzing components (mainly Cl_2 and NOCl) will be generated, at the same time the induction period is shortened considerably. The reaction rate increases fast to a maximum value and then falls off. The induction period is approximately 75 minutes at 175 °C and 28 minutes at 220 °C. The maximum reaction rate increases with acidity and pressure. In the pressure range of 2-125 cm Hg, the reaction rate appears to increase proportionally with pressure, $\frac{-d(AN)}{dt} = cP$. The activation energy of the decomposition of AN or of AN+KCl is about 30 $kcal \cdot mol^{-1}$ [108], which agrees with the results in this work as reported in Section 4.2.2.

AN and gaseous chlorine react violently, even when the nitrate is solid. The reaction is perceptible at 140 °C. The reaction rate starts to increase fast after AN dissolves in the water formed during the reaction, with the decomposition gas containing mainly N_2O. The activation energy is about 10 kcal·mol^{-1} [108].

4.4.3 The Mixture of Sodium Sulfate and Potassium Chloride as Additive

Based on the results of our work, it can be concluded that when Na_2SO_4 and KCl were mixed together with AN, Na_2SO_4 played a dominant role at the first stages of decomposition, inhibiting AN decomposition, possibly by reducing the rate of HNO_3 generation via reaction Eq. (2) and reducing the amount of NO_2^+, as explained before; however, at higher temperatures, the equilibrium of endothermic reaction Eq. (2) was shifted to the right and HNO_3 generation increased. Once this occurred, the reaction ran away and KCl was accelerating the decomposition, potentially via the mechanism proposed by Sun *et al.* [24] or Li and Koseki [42], thus playing a dominant role over Na_2SO_4. However, in order to test whether it is autocatalytic reaction more research is required. In fact, the mechanism of such fast reactions can be thoroughly studied by intensive research involving computational chemistry, backed up by complex and extensive experimental work.

Reaction Eq. (54) indicates that 0.5 mol SO_4^{2-} reacts with 1 mol AN; and reactions Eq. (56), Eq. (57), and Eq. (58) show that 1 mol Cl^- reacts with 1 mol AN. As the molar mass of Na_2SO_4 is approximately twice that of KCl, when equal masses of

Na_2SO_4 and KCl were mixed with AN, the mole number of KCl was approximately twice that of Na_2SO_4. When equal masses of Na_2SO_4 and KCl were mixed with AN, the temperatures at maximum self-heating rate were almost the same as that of pure AN. It is thus plausible that the mitigating effect of SO_4^{2-} on AN counteracts the promoting effect of Cl^-.

4.5 Models to Predict Experimental Results

Except for the mixture of AN with Na_2SO_4 and KCl reported in Section 4.3.1, a few more experiments have been conducted as summarized in Table 11 and Table 12, where the key parameters are reported, such as the mole fraction of the additive, the "onset" temperature, the "onset" pressure, the temperature at maximum self-heating rate, maximum self-heating rate, maximum pressure-rise rate, and the final temperature. The data were used to build up the models explained in this section.

Table 11. Experimental results of AN mixture with Na_2SO_4 and KCl (1)

Mass (g)		Molar mass (mol)		mol%		T_o	P_o	T_{max}
Na_2SO_4	KCl	Na_2SO_4	KCl	Na_2SO_4	KCl	(°C)	(MPa)	(°C)
0	0	0	0	0	0	200	1.6	347
0.25	0.13	0.00176	0.00176	3.73	3.73	231	1.5	317
0.25	0.25	0.00176	0.00335	3.61	6.87	231	1.5	335
0.5	0.5	0.00352	0.00671	6.53	12.44	237	1.5	343
0.5	0.26	0.00352	0.00352	6.93	6.93	240	1.6	340
0.25	0	0.00176	0	3.87	0	257	1.5	391
0	0.13	0	0.00176	0	3.87	194	1.5	301
0	0.26	0	0.00352	0	7.45	196	1.5	317

Table 12. Experimental results of AN mixture with Na_2SO_4 and KCl (2)

Mass (g)		Molar mass (mol)		mol%		$(dT/dt)_{max}$	$(dP/dt)_{max}$	T_f
Na_2SO_4	KCl	Na_2SO_4	KCl	Na_2SO_4	KCl	(°C·s^{-1})	(MPa·s^{-1})	(°C)
0	0	0	0	0	0	82	1.5	393
0.25	0.13	0.00176	0.00176	3.73	3.73	613	6.8	450
0.25	0.25	0.00176	0.00335	3.61	6.87	468	6.4	478
0.5	0.5	0.00352	0.00671	6.53	12.44	637	10	490
0.5	0.26	0.00352	0.00352	6.93	6.93	865	8.8	470
0.25	0	0.00176	0	3.87	0	165	2.5	443
0	0.13	0	0.00176	0	3.87	332	5.5	427
0	0.26	0	0.00352	0	7.45	467	8.7	416

4.5.1 Prediction of T_{final} - T_{onset}

Adiabatic temperature rise ($T_f - T_o$) is closely related with the heat of reaction, therefore this section reports a model to predict the adiabatic temperature rise of AN with additives.

When Na_2SO_4 is added into AN as an inhibitor, the adiabatic temperature rise ($T_f - T_o$) can be expressed as a function of the mole fraction of Na_2SO_4 in the mixture, $T_f - T_o$ = f (mol% of Na_2SO_4). Based on the data shown in Table 5, the difference between the ($T_f - T_o$) of the mixture and the ($T_f - T_o$) of pure AN versus the mole fraction of Na_2SO_4 is plotted in Figure 23, which shows the function of data correlation.

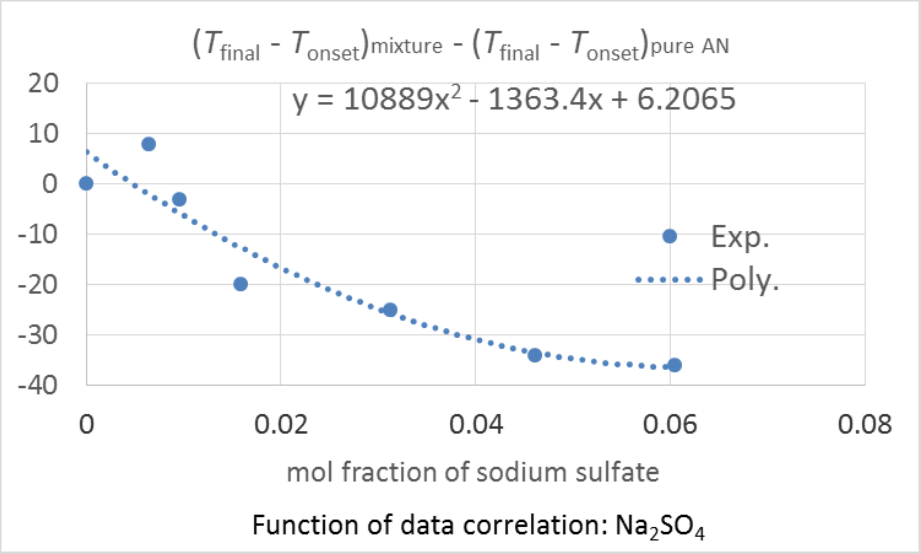

Figure 23. Prediction of ($T_f - T_o$) of AN mixture with Na_2SO_4

A polynomial fitting of the curve is shown in Eq. (63), which is fitted according to experimental measurements.

Eq. (63) $y(Na_2SO_4) - (T_f - T_o)_{\text{pure AN}} = 10889x^2_{Na2SO4} - 1363.4x_{Na2SO4} + 6.2065$

When KCl is added into AN as a promoter, the adiabatic temperature rise ($T_f - T_o$) is a function of the mole fraction of KCl in the mixture, $T_f - T_o$ = f (mol% of KCl). Based on the data shown in Table 7, the difference between the ($T_f - T_o$) of the mixture and the ($T_f - T_o$) of pure AN versus the mole fraction of KCl is plotted in Figure 24. A linear fitting of the curve is shown in Eq. (64).

Eq. (64) $y(KCl) - (T_f - T_o)_{\text{pure AN}} = 578.82x_{KCl} - 0.8555$

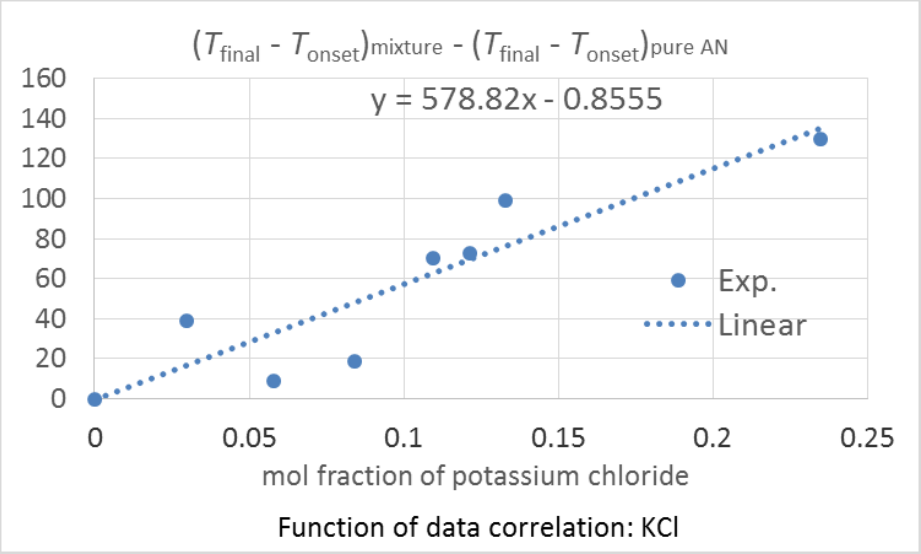

Figure 24. Prediction of ($T_f - T_o$) of AN mixture with KCl

When Na_2SO_4 and KCl are added into AN together as additive, it is assumed that the difference between the ($T_f - T_o$) of the mixture and the ($T_f - T_o$) of pure AN is the combination of the contribution of Na_2SO_4 and KCl. That is to say, for the dual-mixture system, the predicted adiabatic temperature rise can be assumed to be $y(\text{mixture}) =$ contribution of Na_2SO_4 + contribution of KCl, as shown in Eq. (65), which can be used to predict the behavior of the binary mixtures using the functions created in Eq. (63) and Eq. (64).

Eq. (65) $y(\text{mixture}) = 10889x_{Na2SO4}^2 - 1363.4x_{Na2SO4} + 6.2065 + 578.82x_{KCl} - 0.8555 + (T_f - T_o)_{\text{pure AN}} = 10889x_{Na2SO4}^2 - 1363.4x_{Na2SO4} + 6.2065 + 578.82x_{KCl} - 0.8555 + 393 - 200 = 10889x_{Na2SO4}^2 - 1363.4x_{Na2SO4} + 578.82x_{KCl} + 198.351$

In order to confirm the assumption, the predicted data are compared with other experimental data in the following paragraph, where those data were not used to propose the Eq. (63), Eq. (64), or Eq. (65).

There are nine tests of AN with various amount of additive in Table 11 and Table 12, where the experimental adiabatic temperature rise ($T_f - T_o$) of these tests can be obtained. Accordingly, for the nine mixtures, the predicted adiabatic temperature rise can be calculated from Eq. (65). The experimental adiabatic temperature rise (as y-axis) *vs*. the calculated predicted adiabatic temperature rise (as x-axis) is shown in Figure 25. Ideally, the data should fit the linear fitting of y=x, and now the linear fitting is y=1.1x, which means that the model fits the experiments well.

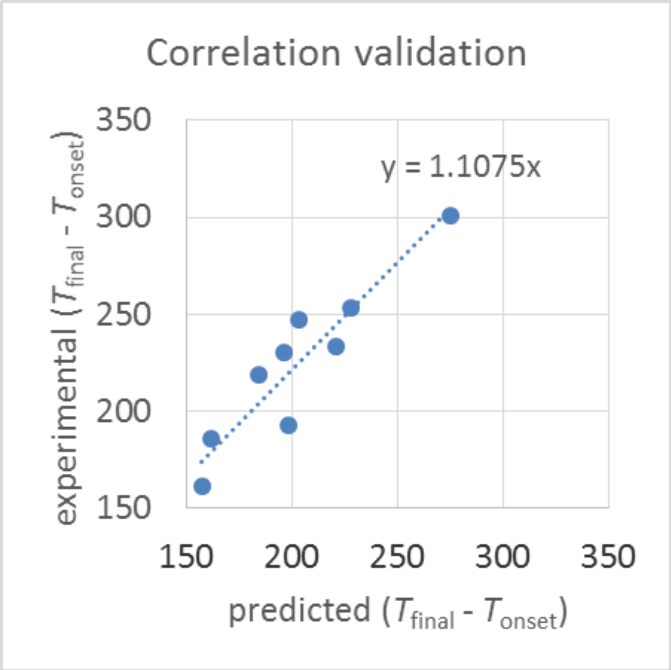

Figure 25. The comparison between the experimental ($T_f - T_o$) and the predicted ($T_f - T_o$) with model

4.5.2 Prediction of T_{max} - T_{onset}

Similarly, this section reports a model to predict the ($T_{max} - T_o$) of AN with additives.

When Na_2SO_4 is added into AN as an inhibitor, the ($T_{max} - T_o$) is a function of the mole fraction of Na_2SO_4 in the mixture, $T_{max} - T_o$ = f (mol% of Na_2SO_4). Based on the data shown in Table 5, the difference between the ($T_{max} - T_o$) of the mixture and the ($T_{max} - T_o$) of pure AN versus the mole fraction of Na_2SO_4 is plotted in Figure 26, which shows the function of data correlation. A polynomial fitting of the curve is shown in Eq. (66), which is fitted according to experimental measurements.

Eq. (66) $y(Na_2SO_4) - (T_{max} - T_o)_{pure\ AN} = 6594.4x^2_{Na2SO4} - 928.94x_{Na2SO4} + 3.5052$

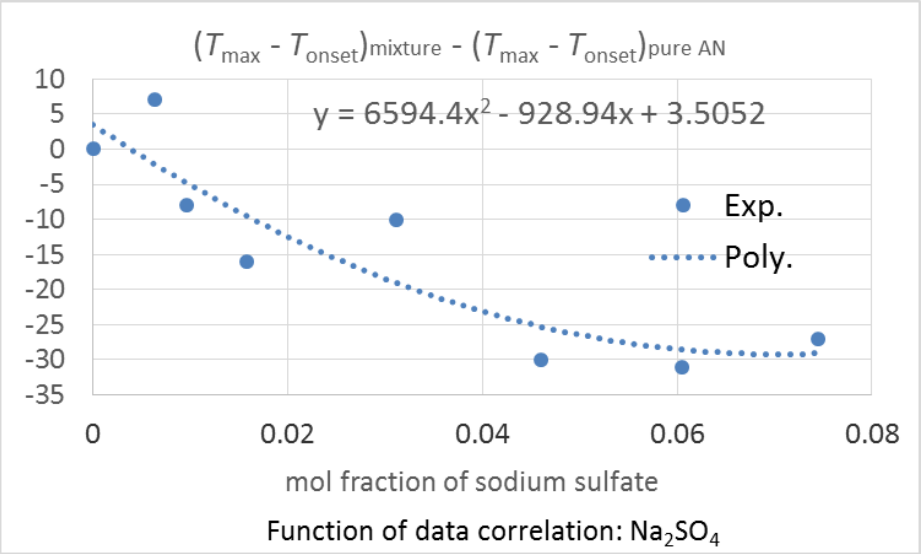

Figure 26. Prediction of ($T_{max} - T_o$) of AN mixture with Na_2SO_4

When KCl is added into AN as a promoter, the adiabatic temperature rise ($T_{max} - T_o$) is a function of the mole fraction of KCl in the mixture, $T_{max} - T_o$ = f (mol% of KCl). Based on the data shown in Table 7, the difference between the ($T_{max} - T_o$) of the mixture and the ($T_{max} - T_o$) of pure AN versus the mole fraction of KCl is plotted in Figure 27. A linear fitting of the curve is shown in Eq. (67).

Eq. (67) $y(KCl) - (T_{max} - T_o)_{pure\ AN} = 221.89x_{KCl} - 46.274$

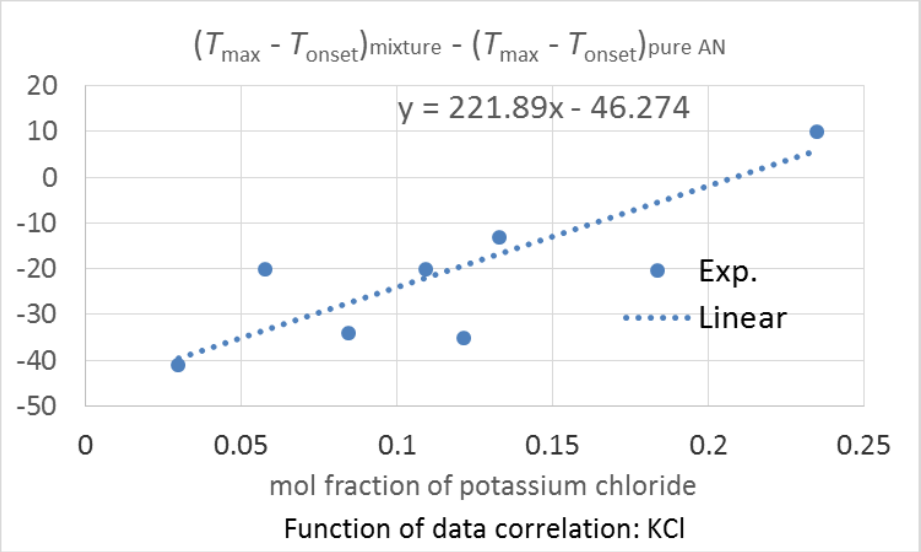

Figure 27. Prediction of ($T_{max} - T_o$) of AN mixture with KCl

When Na_2SO_4 and KCl are added into AN together as additive, it is assumed that the difference between the ($T_{max} - T_o$) of the mixture and the ($T_{max} - T_o$) of pure AN is the combination of the contribution of Na_2SO_4 and KCl. That is to say, for the dual-mixture system, the predicted ($T_{max} - T_o$) can be assumed to be y(mixture) = contribution of Na_2SO_4 + contribution of KCl, as shown in Eq. (68).

Eq. (68) $y(mixture) = 6594.4x_{Na2SO4}^2 - 928.94x_{Na2SO4} + 3.5052 + 221.89x_{KCl} - 46.274 + (T_{max} - T_o)_{pure\ AN} = 6594.4x_{Na2SO4}^2 - 928.94x_{Na2SO4} + 3.5052 + 221.89x_{KCl} - 46.274 + 347 - 200 = 6594.4x_{Na2SO4}^2 - 928.94x_{Na2SO4} + 221.89x_{KCl} + 104.2312$

In order to confirm the assumption, the predicted data is compared with the new experimental data in the following paragraph.

Based on Table 11 and Table 12, where the parameters (such as the mole fraction of the additive, the "onset" temperature, and the temperature at maximum self-heating rate) are summarized, for the nine tests of AN with various amount of additive, the experimental ($T_{max} - T_o$) can be obtained. Accordingly, for the nine mixtures, the predicted ($T_{max} - T_o$) can be calculated from Eq. (68). The experimental ($T_{max} - T_o$) (as y-axis) *vs*. the calculated predicted ($T_{max} - T_o$) (as x-axis) is shown in Figure 28. Ideally, the data should fit the linear fitting of y=x, and now the linear fitting is y=1.0x, which means that the model fits the experiments well.

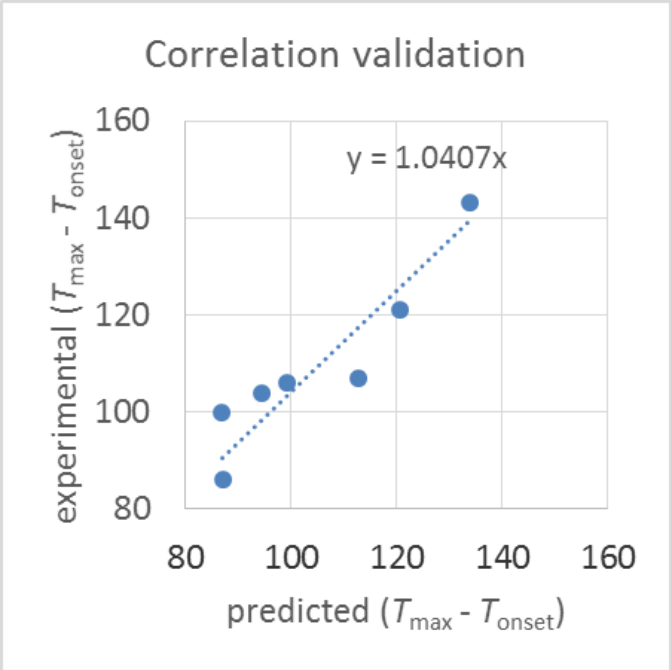

Figure 28. The comparison between the experimental ($T_{max} - T_o$) and the predicted ($T_{max} - T_o$) with model

4.6 Conclusions

In this section, the RSST and the APTAC were used to study the effects of two additives, an inhibitor (sodium sulfate), a promoter (potassium chloride), and the mixture of an inhibitor and a promoter (sodium sulfate and potassium chloride), using different concentrations of the additives.

The "onset" temperature of pure AN has been determined to be approximately 200 °C in pure solid form in the RSST and 220 °C in the APTAC. The decomposition behavior of AN is similar to the results reported in literature using DSC. It can be concluded from this work that the presence of additives influences the "onset" temperature, the rate of decomposition, and the maximum temperature and pressure developed during AN decomposition.

To be specific, in the RSST, when Na_2SO_4 is mixed with AN, it helps mitigate AN decomposition by increasing the "onset" temperature and temperature at maximum self-heating rate, decreasing the heat of reaction, and increasing the activation energy. For example, the "onset" temperature is 268 (±1) °C when AN is mixed with 12.5 wt.% of sodium sulfate, which is higher than that of pure AN, 200 (±10) °C. However, when AN is mixed with KCl, it acts as a promoter as it decreases the "onset" temperature and temperature at maximum self-heating rate, increases the maximum rate of temperature rise as well as the maximum rate of pressure-rise, and increases the heat of reaction, thus, making AN decomposition start earlier and generate heat faster. For example, the

"onset" temperature is 152 (±9) °C when AN is mixed with 12.5 wt.% of potassium chloride.

When sodium sulfate and potassium chloride are mixed together with AN, the "onset" temperature is increased, inhibiting the decomposition; however, the maximum self-heating rate and pressure-rise rate are also increased, and the severity of decomposition increases. The mitigating effect of SO_4^{2-} on AN is likely to counteract the promoting effect of Cl^-. Different researchers proposed decomposition mechanisms to explain the behavior of the mixture when the two additives are added to AN.

Models were proposed to predict the adiabatic temperate rise and the difference between the temperature at maximum self-heating rate and the "onset" temperature, for sodium sulfate and potassium chloride as additive both together and separately, which agree well with experimental data.

It becomes evident though that to avoid AN explosions, AN should be separately stored from promoters, even when inhibitors are also present.

5. CONDITION-DEPENDENT THERMAL DECOMPOSITION OF AMMONIUM NITRATE [*]

In order to the advance the understanding of the effect of different conditions on the decomposition of AN and furthering the use of this particular knowledge to mitigate these risks to make AN storage and use inherently safer, it is important to study the conditions which affect the AN thermal decomposition. The conditions that were studied in this section include the presence of additives, confinement, heating rate, temperature, thermal history, and sample size. Those conditions were studied using the heating ramp mode in the RSST and the HWS mode in the APTAC. The thermodynamic and kinetic parameters were analyzed, and the data were corrected based on thermal inertia factor to provide more accurate results. In addition, the APTAC isothermal mode was used to study the decomposition of pure AN. Thus, safe storage conditions for AN were identified.

[*] Part of this section is reprinted with permission from "Ammonium nitrate thermal decomposition with additives" by Z. Han, S. Sachdeva, M. Papadaki and M. S. Mannan, 2015. *Journal of Loss Prevention in the Process Industries,* 35, 307-315, Copyright 2014 by Elsevier and from "Calorimetry studies of ammonium nitrate – Effect of inhibitors, confinement, and heating rate" by Z. Han, S. Sachdeva, M. Papadaki and M. S. Mannan, 2015. *Journal of Loss Prevention in the Process Industries*, 38, 234-242, Copyright 2015 by Elsevier and from "Study on Mitigating Ammonium Nitrate Fertiliser Explosion Hazards" by Z. Han, A. Pineda, S. Sachdeva, M. Papadaki and M. S. Mannan, 2014. In *Proceeding of the Hazard 24 Conference*. Edinburgh, UK. Copyright 2014 by IChemE.

5.1 Effect of Additives

Apart from the additives studied in Section 4, *i.e.*, sodium sulfate and potassium chloride, the effects of more additives were analyzed in order to systematically understand how their presence affects the thermal stability of AN.

5.1.1 Runaway Behavior of AN with Water

The effect of water on the decomposition of AN is discussed in this section. When water vaporizes, a large amount of steam is generated and resulting in pressure build-up in a confined space. For example, in the RSST, if 3.6 g of water (3.6 mL and 0.20 mol of water) vaporizes in the containment vessel, the pressure generated by the evaporation of water can be calculated from steam tables.

In the RSST, a solution of AN was prepared and tested by fully mixing 3.35 g of AN in 4.18 g of water (AN mixture with 55.5 wt.% water), the molar ratio of which was 1:5.54 (AN : water), which could fully dissolve AN. The solubility of AN in 100 g water is 150 g at 20 °C, the molar ratio of which is 1:2.96 (AN : water). Polymer coated magnetic stirrer bars were used in this test to make sure the solution was homogeneous. This could produce a more homogeneous sample, reducing the inhomogeneity caused by the pure solid. At 187 psig (1.4 MPa), the boiling point of water is 195 °C. The temperature *vs*. time profile and self-heating rate *vs*. temperature profile for the three replicate tests are shown in Figure 29*(a)* and Figure 29*(b)*, respectively. As can be seen

from Figure 29, for the three replicate tests, two of the curves are identical and one of them still has a different time to "onset". Also the standard deviation between maximum self-heating rates is smaller than that of the solid sample. The "onset" temperature was around 251 (±10) °C. The maximum self-heating rate was 108 (±20) °C·s^{-1}, which occurred at 402 (±2) °C. More detailed data for each experiment are summarized in Table 13. It can be concluded from these results that there is no clear advantage of mixing AN with water to get repeatable times to "onset". However, it can be seen that it delayed the "onset" temperature. The unproved repeatability of these tests can probably be attributed to a better measurement of sample temperature due to it being in a liquid, rather than a solid phase.

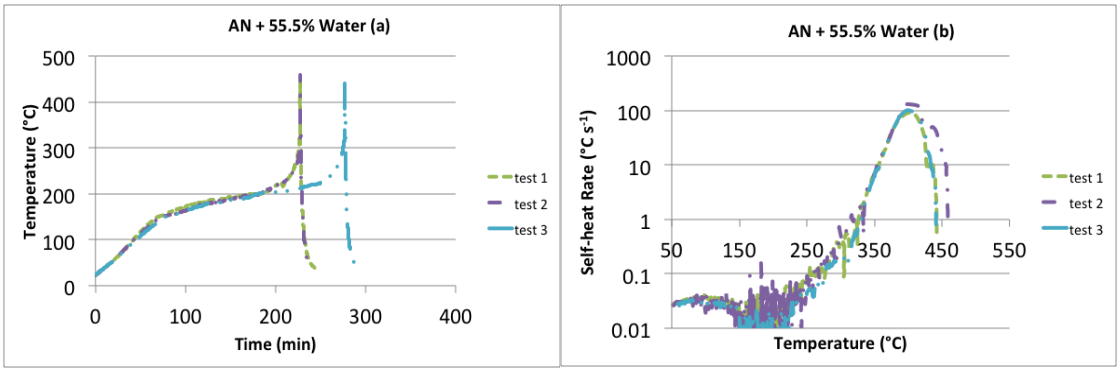

Figure 29. The thermal decomposition of AN with water (a) Temperature profile (b) Self-heating rate

Table 13. AN in aqueous solution experimental data

Test No.	T_o (°C)	P_o (psig)	$(dT/dt)_{max}$ (°C·s^{-1})	T_{max} (°C)	T_f (°C)	$-\Delta H_{rxn}$ (kJ·mol^{-1})	E_a (kJ·mol^{-1})
1	240	231	92	403	442	33.86	132.77
2	253	216	131	403	459	34.53	161.57
3	260	221	102	399	441	30.34	150.54
Avg.	251 (±10)	223 (±8)	108 (±20)	402 (±2)	447 (±10)	32.91 (±2.25)	148.29 (±14.54)

(Note: the maximum rate of pressure-rise was reached earlier than the maximum rate of temperature rise, and the temperature at $(dP/dt)_{max}$ was 6-10 °C lower than that of $(dT/dt)_{max}$)

Analyzing the kinetic parameters for AN decomposition in a solution, following the procedure described in Section 4.1.2, the heat of reaction and activation energy in Table 13 were obtained. The average heat of reaction was -32.91 (±2) kJ·mol^{-1}, and the average activation energy was 148.29 (±14) kJ·mol^{-1}.

5.1.2 Runaway Behavior of AN with Sodium Sulfate in Water Solution

The effect of sodium sulfate as an inhibitor for solid AN has been studied in Section 4.2.1; in this section the effect of sodium sulfate as an inhibitor in a water solution using the RSST, is further studied. 3.35 g of pure solid AN was mixed with 0.48 g of sodium sulfate, with the concentration of Na_2SO_4 in the solid mixture being 12.5 wt.%, and the mixture was then dissolved in 5.96 g of water. The temperature *vs*. time profiles, the self-heating rate *vs*. temperature profiles, and the pressure-rise rate *vs*.

temperature profiles of the three replicate tests are shown in Figure 30*(a)(b)(c)*, respectively. For easier comparison, Figure 30 also gives the plots of pure solid AN decomposition (3.5 g), solid AN mixture with 2.8 wt.% Na_2SO_4 (3.5 g AN + 0.1 g Na_2SO_4) , solid AN mixture with 12.5 wt.% Na_2SO_4 (3.5 g AN + 0.5 g Na_2SO_4), and AN in a water solution. For the AN mixture with Na_2SO_4 in a water solution, the "onset" temperature was 259 (±4) °C, with the maximum self-heating rate of 100 (±9) °C·s^{-1}, which occurred at 390 (±5) °C. The "onset" pressure was 218 (±2) psig and the maximum pressure-rise rate was 211 (±63) psi·s^{-1}. The final temperature was observed at 426 (±4) °C.

From Figure 30*(a)*, for all the experiments in water solutions, the time to reach "onset" was longer than that of solid samples. In water solutions, the final temperature of AN mixture with Na_2SO_4 was lower than that of pure AN in water. Figure 30*(b)* shows that in water solutions, the "onset" temperature of AN mixture with Na_2SO_4 was higher than that of pure AN in water, indicating Na_2SO_4 could delay AN decomposition in water solution as well. Comparing AN mixture with 12.5 wt.% Na_2SO_4 in water with the solid mixture of the same concentration, the "onset" temperatures of the solution was lower than that of solid mixture, which was 268 (±1) °C. However, the experimental results of AN mixture with 12.5 wt.% Na_2SO_4 with or without water are quite close to each other, therefore the water effect needs to be further studied. Figure 30*(c)* shows that the pressure-rise rate was not affected by the presence of water for AN mixture with 12.5 wt.% Na_2SO_4 under the experimental conditions of this work. In water solutions, AN mixture with 12.5 wt.% Na_2SO_4 delayed the pressure increase rate compared to pure AN

water solution. It can be concluded that there is not an obvious effect of water on the AN mixture with Na_2SO_4. More work is needed to understand the reasons behind it.

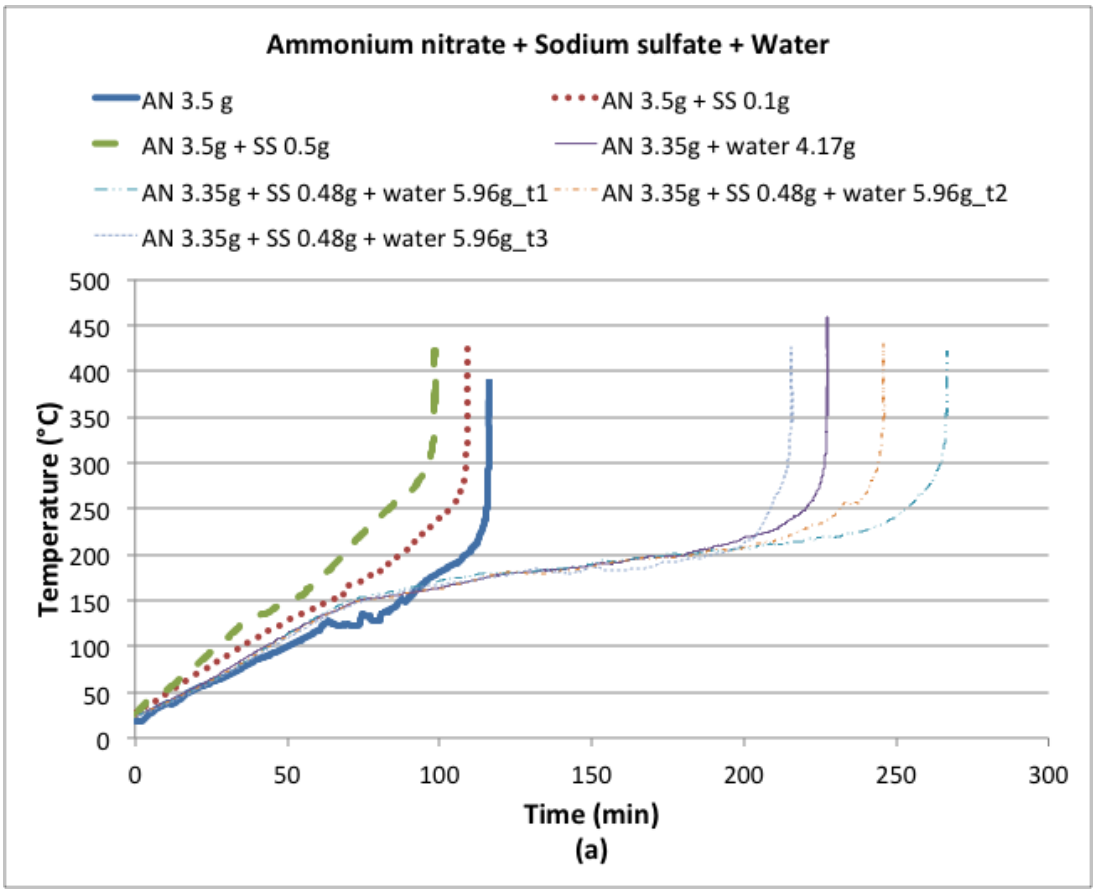

Figure 30. The thermal decomposition of AN and Na_2SO_4 in water solution at various concentrations (a) Temperature profile (b) Self-heating rate profile (c) Pressure-rise rate profile

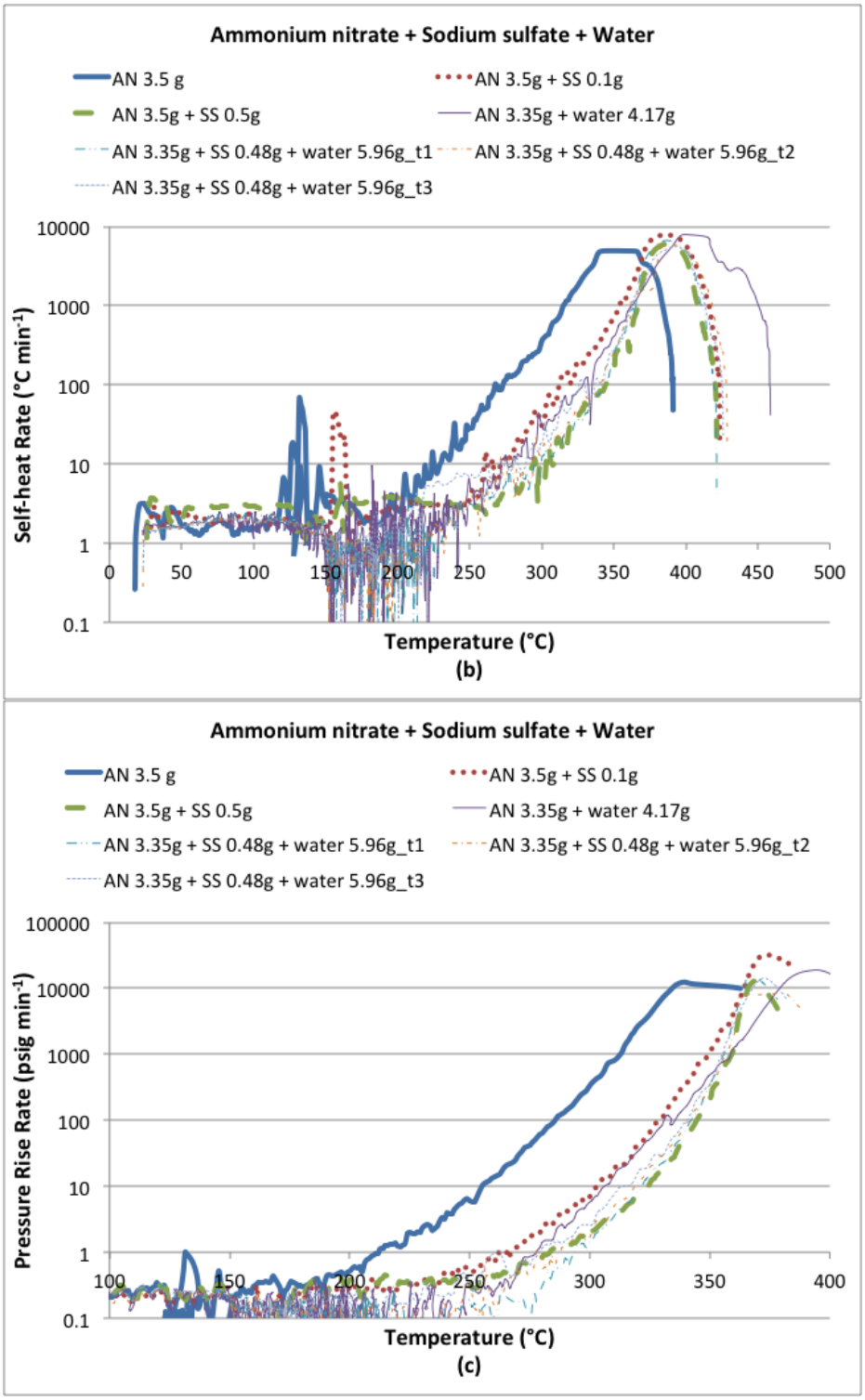

Figure 30 Continued.

5.1.3 Runaway Behavior of AN with Sodium Bicarbonate, Potassium Carbonate, and Ammonium Sulfate

In order to mitigate AN hazards, other inhibitors were mixed with AN to reduce its explosivity. Since AN is used as fertilizer, such additives should be ideally beneficial, or at least not harmful to crops. This section reports the findings of the effect of inhibitors, including sodium bicarbonate, potassium carbonate, and ammonium sulfate. All of the three selected additives are commercial fertilizers [5, 109, 110], and they have never been studied systematically. Here the inhibitors were determined based on "onset" temperature as reported in Section 4.2, *e.g.*, the additive is defined as an inhibitor if it delays the "onset" temperature (T_o > 210 °C for inhibitors).

Pure solid AN (3.5 g) was mixed with two concentrations of each additive, *i.e.*, 2.8 wt.% (3.5 g of AN with 0.1 g of inhibitor) and 12.5 wt.% (3.5 g of AN with 0.5 g of inhibitor). The temperature *vs*. time profiles and the self-heating rate *vs*. temperature profiles of the decomposition of the three mixtures are reported in Figure 31, Figure 32, and Figure 33, and pure AN experimental data are provided as a reference in each figure. The experimental data are summarized in Table 14, which also reports the average T_o, $(dT/dt)_{max}$, T_{max}, and T_f for pure AN under 187 psig (1.4 MPa) initial pressure. The molar concentration of each additive is provided in Table 14 as well.

Table 14. Effect of inhibitors on AN decomposition

Amount of inhibitor added to AN (g)	Mass concentration of additive (wt.%)	Molar concentration of additive (mol%)	T_o (°C)	$(dT/dt)_{max}$ (°C·s^{-1})	T_{max} (°C)	T_f (°C)
pure AN	-	-	200	82	347	393
0.1 $NaHCO_3$	2.8	2.65	250	110	407	448
0.5 $NaHCO_3$	12.5	12.0	265	124	440	470
0.1 K_2CO_3	2.8	1.63	260	113	414	457
0.5 K_2CO_3	12.5	7.65	270	134	418	484
0.1 $(NH_4)_2SO_4$	2.8	1.70	247	162	421	459
0.5 $(NH_4)_2SO_4$	12.5	7.97	260	228	420	465

(Note: each test contains 3.5 g of AN)

Sodium bicarbonate ($NaHCO_3$) was first mixed with AN as an additive, and the results are shown in Figure 31, where the major parameters are marked. The melting point of $NaHCO_3$, has been reported both as 270 °C [111] and 300 °C [112] in literature. On comparison of the results obtained for the mixture of AN and $NaHCO_3$ against pure AN, it is concluded that the T_o increased by 50 °C for the AN mixture with 2.8 wt.% (2.65 mol%) $NaHCO_3$, and 65 °C for 12.5 wt.% (12.0 mol%) $NaHCO_3$. The T_{max} increased by 60 °C for the AN mixture with 2.8 wt.% (2.65 mol%) $NaHCO_3$, and about 90 °C for 12.5 wt.% (12.0 mol%) $NaHCO_3$. Similar results have been obtained using a DSC [22] which shows that $NaHCO_3$ raised the decomposition exotherm of AN by 22 °C for the AN mixture with 4.5 mol% $NaHCO_3$, and 52 °C for 16 mol% $NaHCO_3$. The

RSST gives a higher temperature rise most likely because the generated heat in the DSC is smaller as it employs a smaller sample.

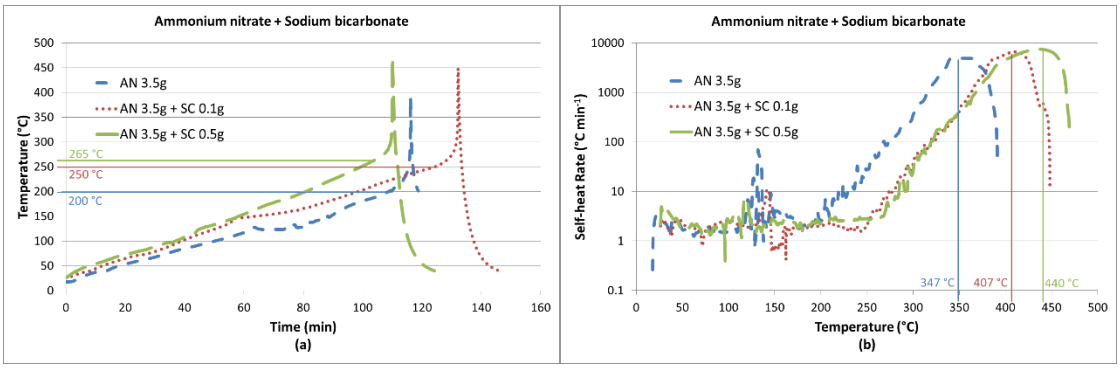

Figure 31. The thermal decomposition of AN and $NaHCO_3$ at various concentrations (a) Temperature profile (b) Self-heating rate profile

Potassium carbonate (K_2CO_3) was also mixed with AN, and the results are shown in Figure 32. The melting point of K_2CO_3 is 891 °C [5]. On comparison of the results obtained for the mixture of AN and K_2CO_3 against pure AN, it is concluded that the T_o increased by 60 °C for the AN mixture with 2.8 wt.% (1.63 mol%) K_2CO_3, and 70 °C for 12.5 wt.% (7.65 mol%) K_2CO_3. The T_{max} increased by 67 °C for the AN mixture with 2.8 wt.% (1.63 mol%) K_2CO_3, and 71 °C for 12.5 wt.% (7.65 mol%) K_2CO_3. Similar results have been observed in a DSC [22], where K_2CO_3 raised the decomposition exotherm of AN by 25 °C for the AN mixture with 2.8 mol% K_2CO_3, and 48 °C for 10 mol% K_2CO_3.

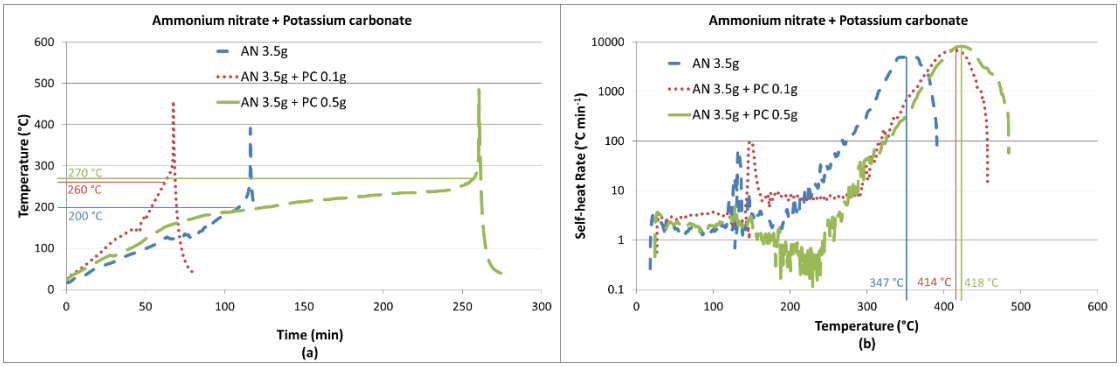

Figure 32. The thermal decomposition of AN and K_2CO_3 at various concentrations (a) Temperature profile (b) Self-heating rate profile

The above-mentioned two additives are both carbonates. AN thermal stability is affected by the acidity of the additive, which changes the decomposition mechanism [113]. Addition of weak acids and weak acid salts causes an increase in AN decomposition, and salts in which the anion is more basic than nitrate cause a reduction in AN decomposition rate [113]. Wood and Wise proposed that AN decomposition was catalyzed by nitric acid [107], which is one of AN decomposition products at 170 °C. One potential explanation could be that solutions containing CO_3^{2-} yield pH values in the range 7.4–8.3 [22], and it is more basic than NO_3^-. When carbonate is mixed with AN as an additive, the CO_3^{2-} is basic and forms H_2CO_3 in the presence of nitric acid, which is unstable and decomposes to water and carbon dioxide gas, thus, reducing the amount of nitric acid. In this way, the AN decomposition is mitigated.

Finally, ammonium sulfate [$(NH_4)_2SO_4$], was mixed with AN, and the results are shown in Figure 33. The melting point of $(NH_4)_2SO_4$ is between 511 to 515 °C in closed systems; however, it melts with decomposition at 280 °C in open systems [5]. After each

test there was residue left in the cell, but the mass of the residue was always less than that of the initial mass of $(NH_4)_2SO_4$ employed in the respective test. Therefore, it is believed that some $(NH_4)_2SO_4$ had also decomposed under the conditions of this research. On comparison of the results obtained for the mixture of AN and $(NH_4)_2SO_4$ against pure AN, it is concluded that the T_o increased by approximately 50 °C for the AN mixture with 2.8 wt.% (1.70 mol%) $(NH_4)_2SO_4$, and 60 °C for 12.5 wt.% (7.97 mol%) $(NH_4)_2SO_4$. The T_{max} increased by around 70 °C for the AN mixture with both 2.8 wt.% (1.70 mol%) and 12.5 wt.% (7.97 mol%) $(NH_4)_2SO_4$. Using a DSC [22], $(NH_4)_2SO_4$ raised the decomposition exotherm of AN by 11 °C for the AN mixture with 2.9 mol% $(NH_4)_2SO_4$, and 22 °C for 11 mol% $(NH_4)_2SO_4$.

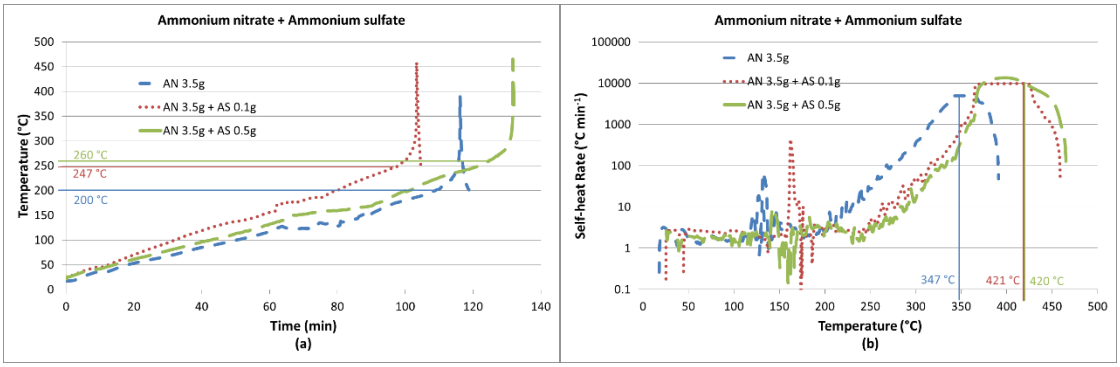

Figure 33. The thermal decomposition of AN and $(NH_4)_2SO_4$ at various concentrations (a) Temperature profile (b) Self-heating rate profile

Considering sodium sulfate (Na_2SO_4) as an inhibitor for AN as discussed in Section 4.2.1, the T_o increased by 50 °C for the AN mixture with 2.8 wt.% Na_2SO_4, and 68 °C for 12.5 wt.% Na_2SO_4. The T_{max} increased by around 40 °C for the AN mixtures

with both 2.8 wt.% and 12.5 wt.% Na_2SO_4. Thus, although the increase of T_o was approximately the same for either additive, the increase of T_{max} with $(NH_4)_2SO_4$ was almost twice as much as the one with Na_2SO_4. This difference may be related with the pH of the solution due to hydrolysis. In the presence of water (product of the decomposition) the mixture pH is higher in the case of the former additive, which is a salt of a weak base and a rather strong acid, as opposed to the second which is a salt of a strong base and a rather strong acid.

On the other hand, according to Oxley *et al.* [22], solutions containing SO_4^{2-} produce pH values in the range 4–5, and it is more basic than nitrate, whose pH values are in the range 3–4. When sulfate is mixed with AN as an additive, the anion SO_4^{2-} functions as a conjugate base of weak acids, which forms H_2SO_4 in the presence of NH_4^+, and decreases AN decomposition rate [113], thus, inhibiting AN decomposition [22].

It can be concluded from the results that the presence of each of the three inhibitors increased the T_o of pure AN, and the AN mixture with 12.5 wt.% of inhibitor had a higher T_o than the mixture with 2.8 wt.% of inhibitor. This shows that more inhibitor can result in a higher T_o. Therefore, the addition of these inhibitors delays the "onset" of the runaway behavior of AN, and they are good inhibitors for AN.

5.1.4 Potassium Carbonate as Additive in the APTAC

Potassium carbonate was mixed with AN and tested in the APTAC. 1 g of AN was mixed thoroughly with various amounts of K_2CO_3 and 5 g of sand, and placed into the test cell.

The amount of K_2CO_3 added into AN was 0.16 g, 0.32 g, and 0.48 g, respectively. The results are reported in Figure 34 and Table 15.

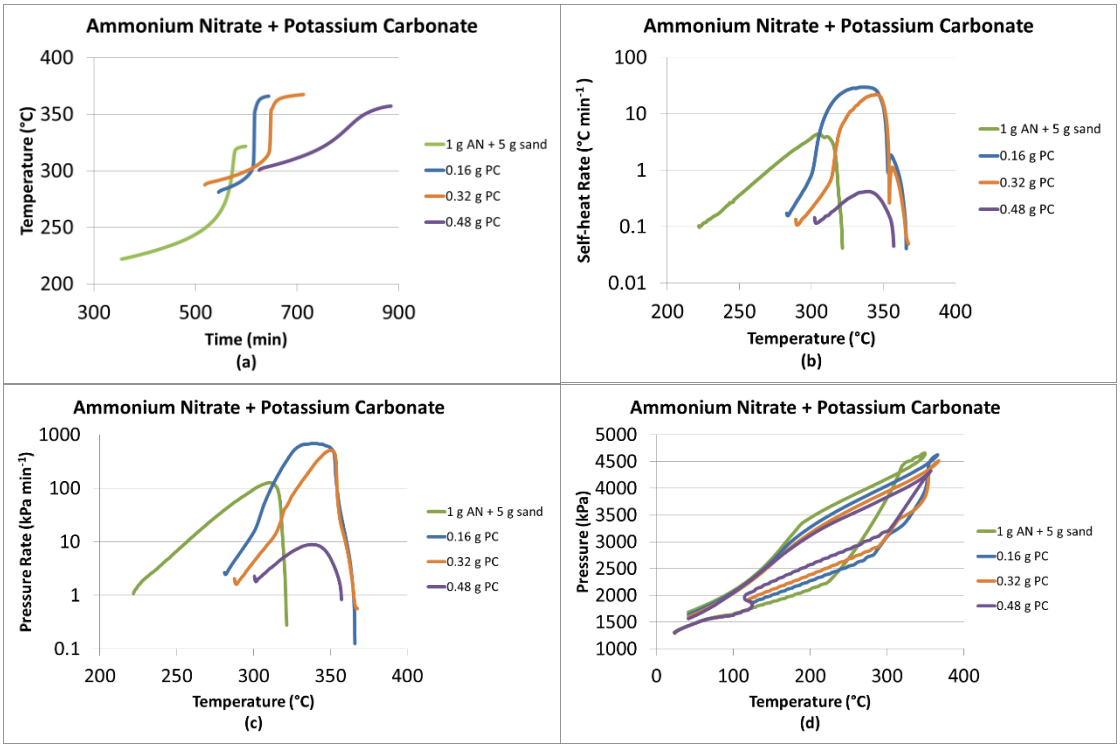

Figure 34. AN decomposition with potassium carbonate in the APTAC (a) Temperature *vs*. time profile (b) Self-heating rate *vs*. temperature profile (c) Pressure-rise rate *vs*. temperature profile (d) Pressure *vs*. temperature profile

Table 15. Experimental results of AN decomposition with potassium carbonate in the APTAC

K_2CO_3 (g)	Pure AN	0.16	0.32	0.48
T_o (°C)	220	281	288	301
$(dT/dt)_{max}$ (°C·min^{-1})	4	30	22	0.4
T_{max} (°C)	306	337	345	340
T_f (°C)	322	366	367	357
P_o (kPa)	2223	2746	2901	3199
$(dP/dt)_{max}$ (kPa·min^{-1})	127	688	511	8.89
P_{max} (kPa)	4102	3658	3866	3956
P_f (kPa)	4450	4625	4516	4327
P_c (kPa)	1687	1640	1601	1564
$t_{runaway}$ (min)	252	99	194	260

(Note: each test contains 1 g of AN + 5 g of sand; P_c was obtained at 20 °C)

It can be concluded that with more K_2CO_3 in the mixture, the "onset" temperature was increased, the maximum self-heating rate was decreased, the maximum pressure-rise rate was decreased, and the time to complete and reaction was increased. Therefore, K_2CO_3 is a good inhibitor for AN.

5.1.5 Comparison of More Additives

To study the effect of more additives mixed with AN, different chemicals were mixed with AN at two concentrations, *i.e.*, 3.5 g of AN with 0.1 g of single additive and 0.5 g of single additive, respectively. Apart from the tests described in Section 4.2 and

Section 5.1.2, preliminary results for other chemicals mixed with AN have been tested as well, such as barium nitrate, sodium nitrate, and ferric sulfate. Using the same methods as described above, the RSST experimental results for AN with those additives were obtained. Among all these chemicals, sodium bicarbonate and ferric sulfate are not fertilizers, but all the rest can be used as fertilizers.

The "onset" temperatures and temperatures at maximum self-heating rate are summarized in Figure 35, in which the additives include sodium sulfate (SS, Na_2SO_4), ammonium sulfate (AS, $(NH_4)_2SO_4$), barium nitrate (BN, $Ba(NO_3)_2$), sodium nitrate (SN, $NaNO_3$), sodium bicarbonate (SC, $NaHCO_3$), potassium carbonate (KC, K_2CO_3), potassium chloride (PC, KCl), and ferric sulfate (or iron(III) sulfate, FS, $Fe_2(SO_4)_3$). Based on the experimental data, it is concluded that Na_2SO_4, $(NH_4)_2SO_4$, $Ba(NO_3)_2$, $NaNO_3$, $NaHCO_3$, and K_2CO_3 are inhibitors, because when they were mixed with AN, both the "onset" temperature and temperature at maximum self-heating rate were higher than that of pure AN. On the contrary, KCl and $Fe_2(SO_4)_3$ are promoters, because their mixtures with AN resulted in lower "onset" temperature and temperature at maximum self-heating rate.

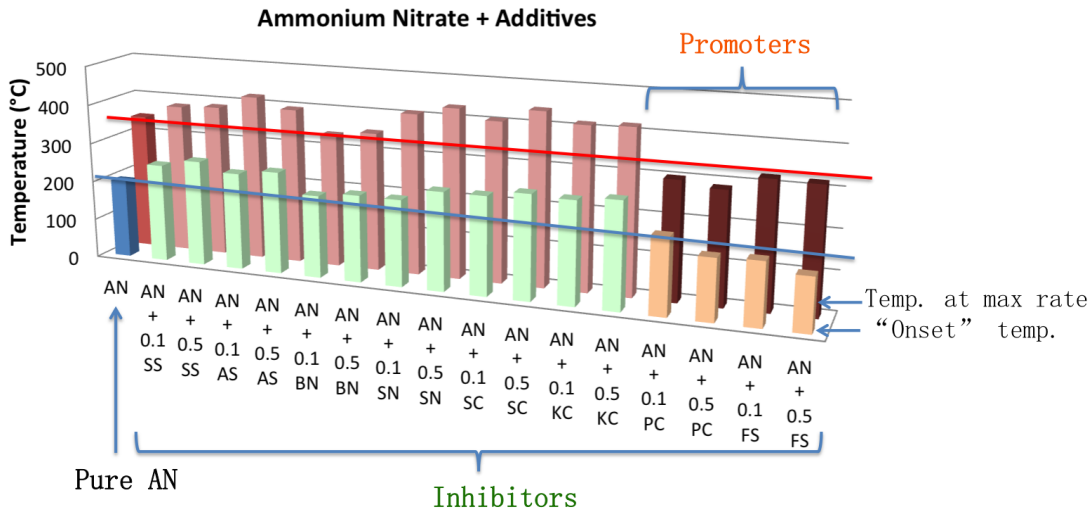

Figure 35. The "onset" temperature and temperature at maximum self-heating rate of AN mixtures with additives

5.2 Effect of Confinement

The issues of storing AN in confined spaces were addressed in Section 1.6. This section reports the effect of confinement on AN decomposition using the RSST and the APTAC. The different levels of confinement were studied by varying the initial pressures in the overhead space of the test cell.

5.2.1 Effect of Confinement – RSST Experiments

To study the effect of confinement, 3.5 g of solid AN sample was prepared and tested using the RSST. Before each test, nitrogen was applied to the containment vessel including the test cell, as an initial back pressure. Different initial pressures were applied

to the samples, including 109 psig (0.9 MPa), 150 psig (1.1 MPa), 180 psig (1.3 MPa), and 187 psig (1.4 MPa). Another test without pressurization was also conducted under ambient pressure to compare with the ones with confinement. This study presents AN behavior from ambient to high-pressure conditions, and thus, the effect of confinement on the decomposition of AN.

The results are presented in Figure 36, where the major parameters are marked. Figure 36*(a)*, the self-heating rate versus temperature profile, shows that with higher initial pressure, the T_o decreased slightly. From Figure 36*(b)*, the pressure rate versus temperature profile, it is concluded that with less confinement the "onset" occurred later, and the $(dP/dt)_{max}$ was lower. Based on Figure 36*(c)*, the pressure versus temperature profile, it is concluded that there was non-condensable gas generation after each reaction, because the pressure after each experiment (at ambient temperature), P_c, in the containment vessel was higher than the respective initial pressure (at ambient temperature). Figure 36*(d)*, the pressure-rise rate versus pressure profile, shows that with higher initial pressure, P_o, $(dP/dt)_{max}$, and P_{max} were all higher.

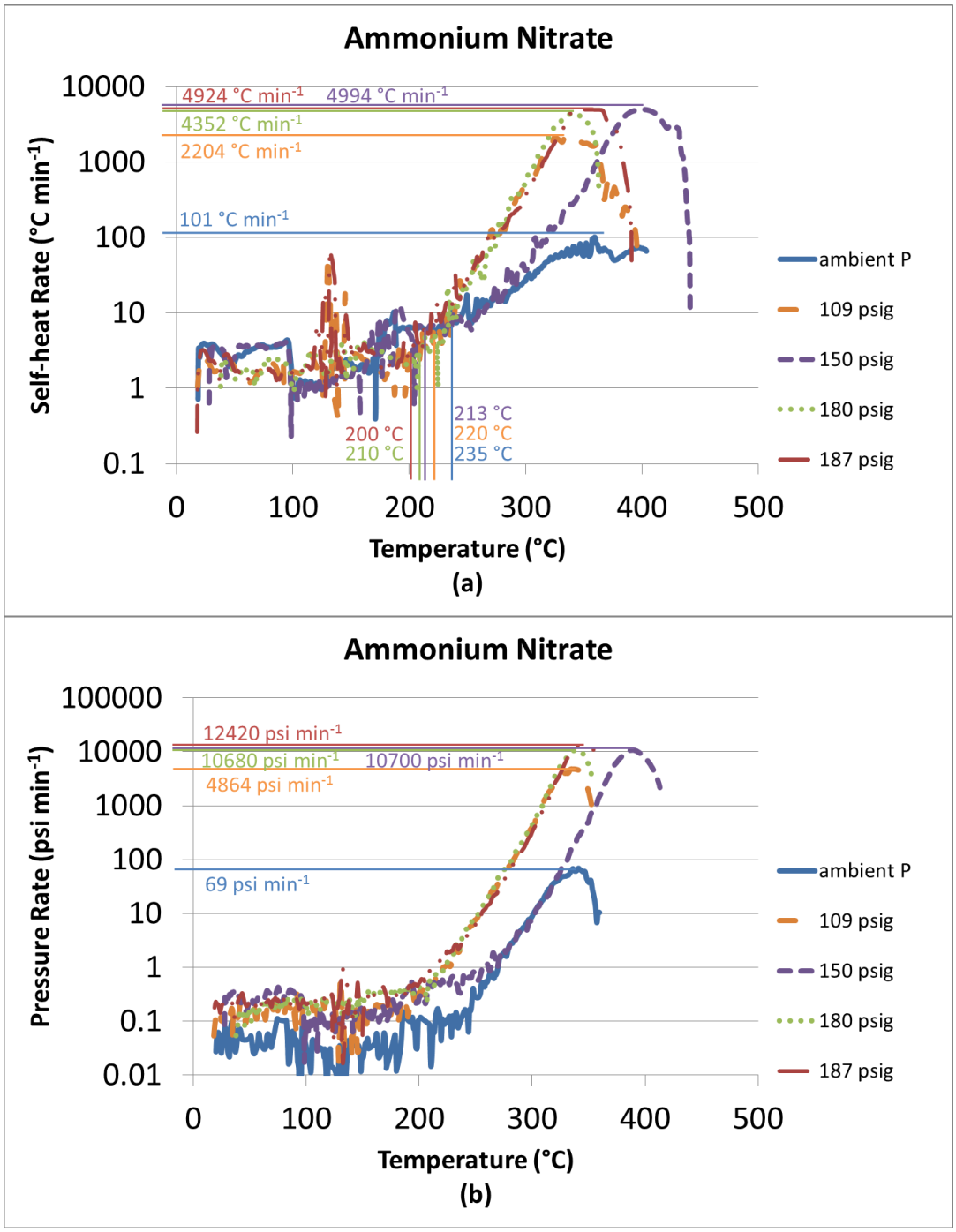

Figure 36. Effect of confinement (a) Self-heating rate profile (b) Pressure rate – temperature profile (c) Pressure – temperature profile (d) Pressure rate – pressure profile

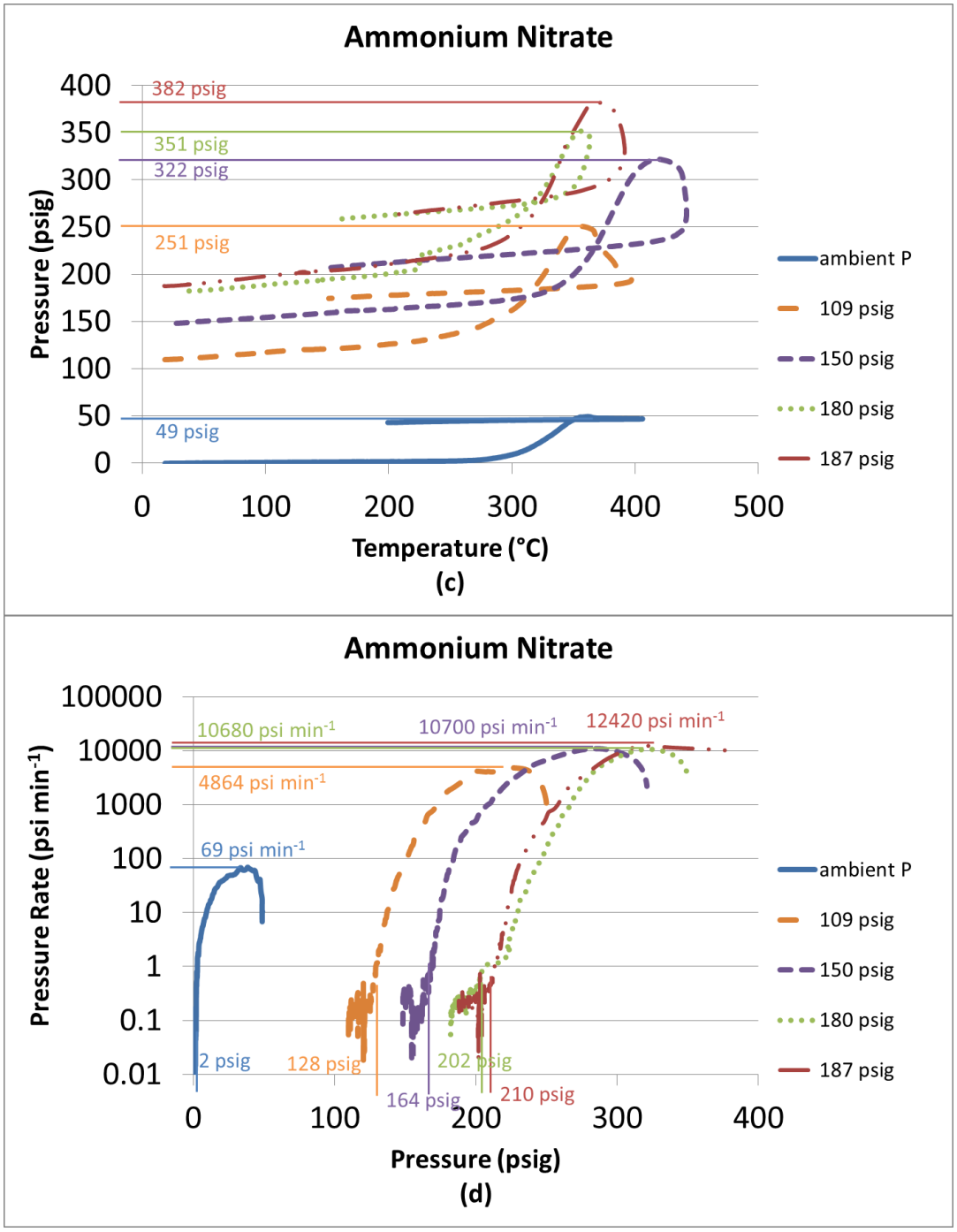

Figure 36 Continued.

The important parameters are summarized in Table 16. It is concluded that with increasing initial pressure, T_o decreased slightly, and $(dP/dt)_{max}$ increased dramatically. With increasing initial pressure, all P_o, P_{max}, P_f, and P_c were higher. There was non-condensable gas generation because, again, the pressure after each experiment (at ambient temperature), P_c, was higher than the initial pressure (at ambient temperature) in the containment vessel.

Table 16. Experimental data of various levels of confinement

No. of test	1	2	3	4	5
Initial pressure P_1 (psig)	ambient	109	150	180	187
T_o (°C)	235	220	213	210	200
$(dT/dt)_{max}$ (°C·s^{-1})	2	37	83	73	82
T_{max} (°C)	360	340	441	342	343
T_f (°C)	406	397	399	363	391
P_o (psig)	2	128	164	202	210
$(dP/dt)_{max}$ (psi·s^{-1})	1	81	178	178	207
P_{max} (psig)	39	221	289	319	322
P_f (psig)	49	251	322	351	382
P_c (psig)	34	157	192	236	254

(Note: each test contains 3.5 g of AN; P_c was obtained at 20 °C)

Since in one measurement, the pressure parameters, such as the slope of the pressure-rise due to heating, will be higher with a higher initial pressure, the normalized pressure parameters provide better comparisons. The pressure parameters can be

normalized using Eq. (69). The normalized parameters are summarized in Table 17. Based on the normalized maximum pressure-rise rate data, it can be concluded that higher initial pressure results in higher pressure-rise rates.

Eq. (69) $$P_{normalize} = \frac{P_{experiment}}{P_{initial}} \cdot \frac{T_{ambient}}{T_{experiment}}$$

where, $P_{\text{experiment}}$ is the experimental value obtained from the calorimeter, $T_{\text{experiment}}$ is the temperature when $P_{\text{experiment}}$ occurs, P_{initial} is the initial pressure applied to the containment vessel, and T_{ambient} is the ambient temperature when initial pressure is applied. T_{ambient} is 20 °C.

Table 17. Normalized pressure data of various levels of confinement

No. of test	1	2	3	4	5
Initial pressure P_1 (psig)	ambient	109	150	180	187
$P_{\text{o, normalize}}$	0.66	0.68	0.66	0.68	0.69
$(dP/dt)_{\text{max, normalize}}$	0.03	0.31	0.44	0.44	0.49
$P_{\text{max, normalize}}$	1.69	0.91	0.76	0.82	0.79
$P_{\text{f, normalize}}$	1.87	0.94	0.89	0.87	0.87

Assuming the gases in the experiments follow ideal gas law, $PV=nRT$, before the exothermic reaction, $P_1V=n_1RT_a$, and after the exothermic reaction, $P_cV=n_2RT_a$. Where P_1 is the initial back pressure, P_c is the pressure after cooling down, n_1 are the total moles of gas in the containment vessel before the reaction, n_2 are the moles of gas after

the reaction, V is the volume of the containment vessel ($3.5 \cdot 10^{-4}$ m^3), R is the gas constant (8.3145 $J \cdot mol^{-1} \cdot K^{-1}$), and T_a is ambient temperature (293 K).

In this study, n_1 is calculated based on $n_1 = P_1V/RT_a$, and $n_2 = n_1P_c/P_1$; both n_1 and n_2 are shown in Table 18. The generated moles of gas is defined as $n_{generate} = n_1 - n_2$. The net pressure-rise is defined as $P_{rise} = P_c - P_1$. $n_{generate}$ and P_{rise} can be calculated accordingly. Of course these results can be perceived as approximations only, especially for the measurements employing a large quantity of inert gases (large initial pressure). The calculated values presented in Table 18, show that there was a substantial generation of non-condensable gases; the different P_{rise} for each measurement indicates that different pathways were followed in each case; and it is obvious that with higher initial pressure, there was more gaseous product produced. There are three potential reasons behind this observation as explained here.

Table 18. Experimental analysis of various levels of confinement

No. of experiment	Initial pressure P_1 (psig)	P_{rise} (psi)	n_1 (mol)	n_2 (mol)	$n_{generate}$ (mol)
1	ambient	34	0.0146	0.0482	0.034
2	109	48	0.123	0.170	0.047
3	150	42	0.163	0.205	0.042
4	180	56	0.193	0.248	0.055
5	187	67	0.200	0.266	0.066

Firstly, the initial gas used in the containment vessel (nitrogen) plays a key role in affecting the reactions. In a similar study with hydroxylamine [114], it has been reported that the pressure increase and decomposition reaction rate were affected by the presence of nitrogen in the overhead space as the research conducted using nitrogen, argon, and air showed. Comparing the experiments in this work, it is clear that the presence of nitrogen increases the gaseous products of AN decomposition. AN decomposition under other gas environment needs to be further examined in order to identify whether it is only the high pressure or the kind of the gas employed which affects the decomposition. Secondly, the chemical effect as proposed in Table 19 [56], AN decomposition scheme consists of a series of gaseous reactions with the first one reversible and the subsequent practically irreversible [67]. Different macroscopic decomposition paths with various intermediate products have been proposed [59, 60]. If a gaseous reaction with a change of moles is conducted at different pressures, its equilibrium will be shifted according to Le Chatelier's principle. Third, the physical effect that higher pressure results in different behaviors also affect the experimental results. For instant, when gas disappears from the sample, it would take away heat, thus, different pressure results in different temperature gradient; in deflagration, the reaction zone is thinner with higher pressure, and the deflagration rate is therefore changed; and in detonation, the energy loss diminishes with higher level of confinement.

Table 19. Theoretical analysis of AN decomposition reactions and their moles of gaseous products

AN decomposition reactions	mol of gaseous products for 1 mol of AN	mol of gaseous products for 3.5 g of AN (0.044 mol)
$NH_4NO_3 \rightleftharpoons HNO_3 + NH_3$	1	0.044
$NH_4NO_3 \rightarrow N_2O + 2H_2O$	1	0.044
$NH_4NO_3 \rightarrow 1/2N_2 + NO + 2H_2O$	1.5	0.066
$NH_4NO_3 \rightarrow 3/4N_2 + 1/2NO_2 + 2H_2O$	1.25	0.055
$2NH_4NO_3 \rightarrow 2N_2\uparrow + O_2\uparrow + 4H_2O$	1.5	0.066
$8NH_4NO_3 \rightarrow 5N_2\uparrow + 4NO + 2NO_2\uparrow + 16H_2O$	1.375	0.061

In this study, 3.5 g of AN were tested in each experiment. The moles of 3.5 g of AN is calculated to be 0.044 mol, since its molar mass is 80.052 $g \cdot mol^{-1}$. The commonly accepted reactions of AN decomposition are listed in the first column of Table 19 [56], and the moles of gaseous products at ambient temperature for each reaction with 1 mol of AN are listed in the second column. Then the moles of gaseous products for 3.5 g of AN can be calculated by multiplying the second column by 0.044, and the results are shown in the third column in Table 19.

Considering the experimental errors and the error introduced by ideal gas in the containment vessel assumption, $n_{generate}$ in Table 18 for all the five experimental trials are relatively close to the values in the third column of Table 19. The development of a methodology which will enable the analysis of the decomposition products under each

initial pressure is expected to provide data which will also contribute towards the determination of AN decomposition pathways.

It is obvious that confinement is dangerous to AN, which should be avoided in AN storage and transportation.

5.2.2 Effect of Confinement – APTAC Experiments

The effect of confinement was further studied using the APTAC. 1 g of AN was mixed thoroughly with 5 g of sand, and placed into the test cell. The use of sand was to increase the volume of the sample for easier temperature measurement, and to reduce the temperature increase rate to protect the equipment. In order to mix the solid sample thoroughly, the test cell loaded with sample was shaken in all directions for ten minutes. Different initial pad pressures (nitrogen) were applied to different tests, including 120 psia, 140 psia, 160 psia, 180 psia, 187 psia, and 200 psia (*i.e.*, 827.37 kPa, 965.27 kPa, 1103.16 kPa, 1241.06 kPa, 1289.32 kPa, and 1378.95 kPa). By comparing the experimental results, it is concluded that the "onset" temperature doesn't change a lot, but the pressure increases with increasing initial pressure.

To give an example, the experimental results of 140 psia (965.27 kPa) initial pressure is presented here to explain how each parameter is determined. The temperature *vs*. time profile is provided in Figure 37. Once the temperature reached 100 °C, HWS mode was started. When the temperature reached 226 °C, the APTAC switched to adiabatic mode because the temperature rise rate exceeded 0.05 °C·min^{-1} in the wait

step. Now 226 °C is determined to be the "onset" temperature. The corresponding "onset" pressure was 1725 kPa, $(dT/dt)_{max}$=5.6 °C·min^{-1}, $(dP/dt)_{max}$=155 kPa·min^{-1}, T_{max}=316 °C, P_{max}=3565 kPa, T_f=333 °C, P_f=3920 kPa, and P_c=187 psi (1289.32 kPa).

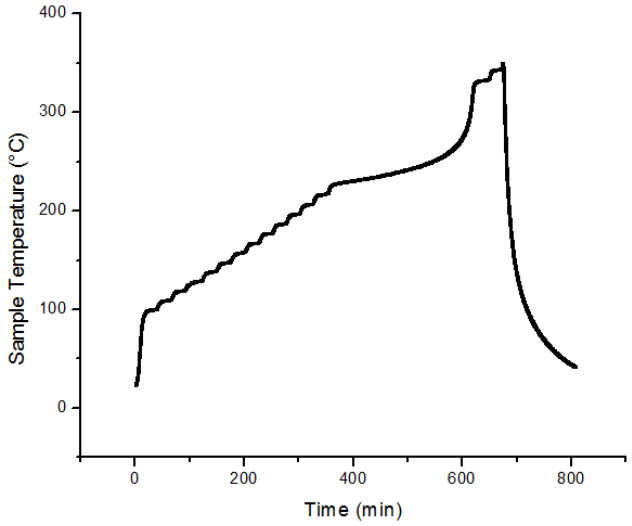

Figure 37. The thermal decomposition of AN under 140 psia in the APTAC

The experimental data of all the tests under various pressures are summarized in Table 20. However, the "onset" temperatures were obtained from the raw experimental data, which could not be a good representative of the real situation. Although the temperature rise rate was greater than 0.05 °C·min^{-1}, the pre-set threshold for the equipment to switch to adiabatic mode, it could have been caused by the residual heat supply of the containment vessel from the heaters in the APTAC. The very slow temperature rise rate immediately after 226 °C could be an evidence. Therefore, another definition of the T_o and T_f is proposed here to better analyze the experimental data.

Table 20. Experimental data of AN decomposition under various initial pressures in the APTAC

$P_{initial}$ (psia)	T_o (°C)	$(dT/dt)_{max}$ (°C·min^{-1})	T_{max} (°C)	T_f (°C)	P_o (kPa)	$(dP/dt)_{max}$ (kPa·min^{-1})	P_{max} (kPa)	P_f (kPa)	P_c (psia)
120	227	8.8	313	330	1506	219	3238	3607	165
140	226	5.6	316	333	1725	155	3565	3920	187
160	214	13.9	299	334	1875	201	3777	4170	203
180	225	1.8	294	306	2157	50	3824	4169	217
187	220	4.4	306	322	2221	127	4102	4443	228
200	214	4.6	313	329	2351	148	4276	4680	238

(Note: each test contains 1 g of AN + 5 g of sand; P_c was obtained at 20 °C)

The self-heating rate *vs*. temperature profile, in Figure 38, shows that before the temperature started to increase rapidly, the temperature rise rate was relatively slow. Therefore, a tangent line was drawn along this curve, where the temperature rise rate was relatively slow; another tangent line was drawn where the temperature just started to rise rapidly. The intersection of the two lines was defined as the new "onset" temperature, T_o. And the final temperature, T_f, is defined as the intersection of the tangent line along the temperature rise and the tangent line of the curve where the temperature rise slowed down. Using the data of 140 psia (965.27 kPa) initial pressure as an example, T_o is plotted in Figure 38 and T_f is plotted in Figure 39. The corresponding pressures to those two temperatures are defined as P_o and P_f.

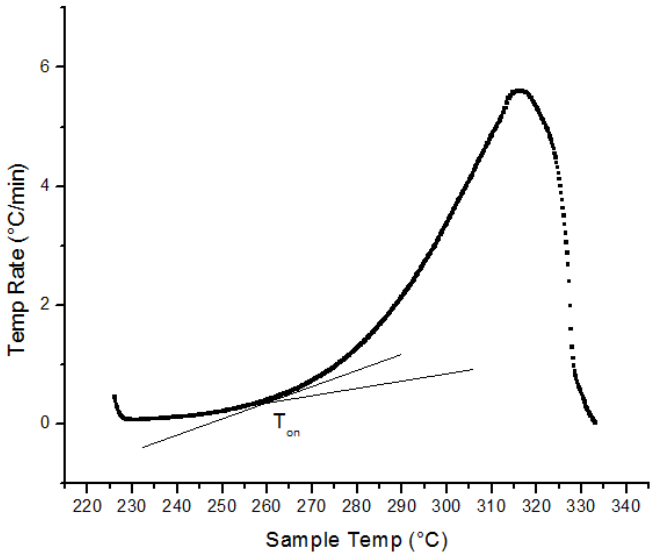

Figure 38. Alternative "onset" temperature from self-heating rate *vs*. temperature of AN decomposition under 140 psia in the APTAC

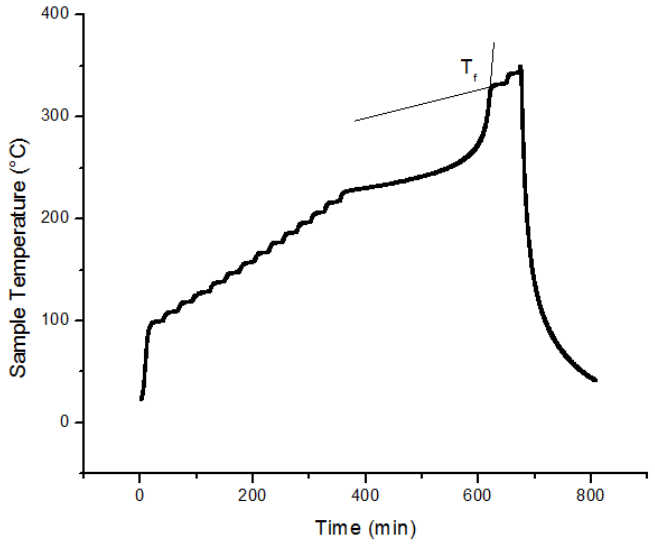

Figure 39. Alternative final temperature from temperature *vs*. time profile of AN decomposition under 140 psia in the APTAC

Analyzing the data points between the new T_o and the new T_f, the decomposition of AN can be described by the n^{th} order reaction model. Following similar procedure as reported in Section 4.1.2, the activation energy was calculated to be 208 kJ·mol^{-1}, and the R^2=0.9887 showing it was first order reaction. The results of the experiments under various initial pressures can be obtained, where the R^2 are between 0.96 – 1.00. The parameters using the new method to define T_o are summarized in Table 21.

Table 21. Updated experimental data of AN decomposition under various initial pressures in the APTAC

$P_{initial}$ (psig)	T_o (°C)	T_f (°C)	P_o (kPa)	P_f (kPa)	E_a (kJ·mol^{-1})	$t_{runaway}$ (min)
120	258	325	1991	3487	218	518
140	257	329	2146	3846	208	570
160	258	327	2416	4067	209	811
180	255	315	2716	4229	205	688
187	255	317	2778	4347	211	533
200	261	338	2850	4351	225	525

(Note: each test contains 1 g of AN + 5 g of sand)

On the other hand, since sand is mixed in the samples, the heat released by the decomposition of AN would not be used only to increase the temperature of AN itself. Therefore, the thermal inertia factor, φ factor, should be considered and the results should be corrected by φ factor. The thermal inertia factor is relatively large because the mass of sand was larger than that of AN, which would affect the heat of reaction, and the

final temperature. In the APTAC, there is temperature compensation in adiabatic mode in order to maintain the sample, test cell, and the nitrogen at the same temperature. Therefore in the calculation of φ, the test cell was ignored and only sand was taken into consideration. The heat capacity of AN and sand was C_{AN}=1.74 J·g^{-1}·K^{-1} and C_{sand}=1.03 J·g^{-1}·K^{-1}. To give an example of the φ factor correction calculation, the experiment under 140 psi is analyzed below.

$$\Delta T_{ad} = \varphi \cdot \Delta T_{ad}^{mes} = 3.95 \times (329 - 257) = 284.4°C$$

$$T_{f,\varphi} = T_{on} + \varphi \Delta T_{ad}^{mes} = 257 + 3.95 \times 72 = 541.4°C$$

$$-\Delta H_{rxn} = \frac{m \cdot C_p \cdot \Delta T_{ad}}{n_{rxn}} = \frac{1.01 \times 1.74 \times 284.4}{1.01/80.04} = 39.6 kJ/mol$$

$$T_{max,\varphi} = T_{on} + \varphi(T_{max} - T_{on}) = 257 + 3.95 \times (316 - 257) = 490°C$$

$$(\frac{dT}{dt})_{max,\varphi} = \varphi(\frac{dT}{dt})_{max} = 3.95 \times 5.6 = 22.12°C/min$$

$$\Delta n = n_{final} - n_{initial} = \frac{P_{final} \times V}{R \times T_{final}} - \frac{P_{initial} \times V}{R \times T_{initial}} = \frac{1289.37 \times 0.095}{8.314 \times 295.15} - \frac{985.65 \times 0.095}{8.314 \times 297.09} = 0.012$$

All the parameters of the experiments under various initial pressures after the φ factor correction are summarized in Table 22, including, ΔT_{ad}^{mes} , ΔT_{ad}, and ΔH_{rxn}.

To compare the results under different initial pressures, the “onset” temperature, “onset” pressure, activation energy, and heat of reaction changing with various initial pressures are compared in Figure 40.

Table 22. Experimental data of AN decomposition under various initial pressures in the APTAC after thermal inertia factor correction

$P_{initial}$ (psig)	φ	T_o (°C)	$(dT/dt)_{max, \varphi}$ (°C·min^{-1})	$T_{max, \varphi}$ (°C)	$T_{f, \varphi}$ (°C)	E_a (kJ·mol^{-1})	$-\Delta H_{rxn}$ (kJ·mol^{-1})	Δn (mol)
120	3.91	258	35	473	520	218	36	0.011
140	3.95	257	22	490	541	208	40	0.012
160	3.95	258	49	459	529	209	38	0.011
180	3.92	255	24	440	491	206	33	0.011
187	3.91	255	17	454	497	211	34	0.011
200	3.95	261	18	552	567	224	42	0.012

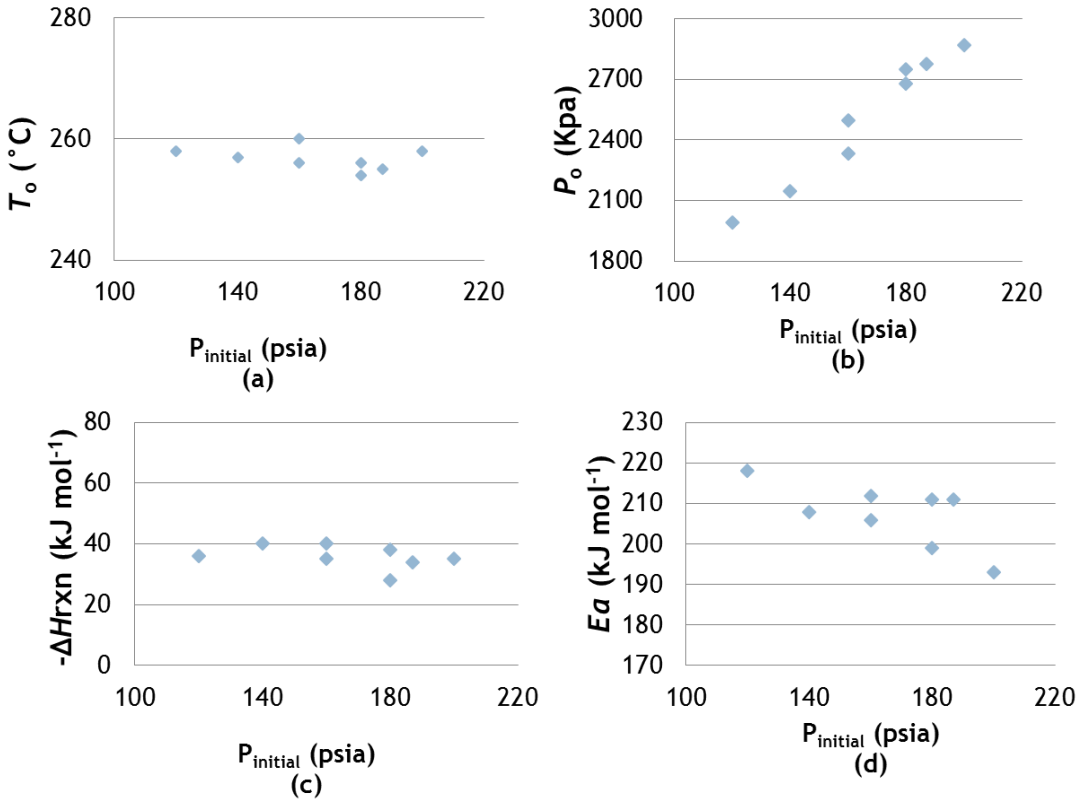

Figure 40. The effect of different initial pressures on AN thermal decomposition (a) "Onset" temperature (b) "Onset" pressure (c) Heat of reaction (d) Activation energy

Based on Figure 40, all the "onset" temperatures were in the range of 257±3 °C, and overall it was decreasing with increasing initial pressure, but not significantly. The activation energies were 205±13 kJ·mol^{-1}, and it was decreasing with increasing initial pressure. The heat of reaction was 37±3 kJ·mol^{-1}. The "onset" pressure was significantly increased with increasing initial pressure; however, it was caused by the different experimental conditions. Therefore, confinement should be avoided in AN storage and transportation.

5.3 Effect of Heating Rate

The issues of heating AN at different rates were addressed in Section 1.6. This section reports the effect of heating rate on AN decomposition using the RSST and the APTAC.

5.3.1 Effect of Heating Rate – RSST Experiments

To study the effect of heating rate, 3.5 g of solid AN sample was tested under two heating rates of 0.25 °C·min^{-1} and 2 °C·min^{-1} in the RSST. The self-heating rate *vs.* temperature profile and the pressure-rise rate *vs.* temperature profile are provided in Figure 41*(a)* and *(b)*, where the results of two replicate tests for each heating rate are shown. The major parameters are marked in the figures as well.

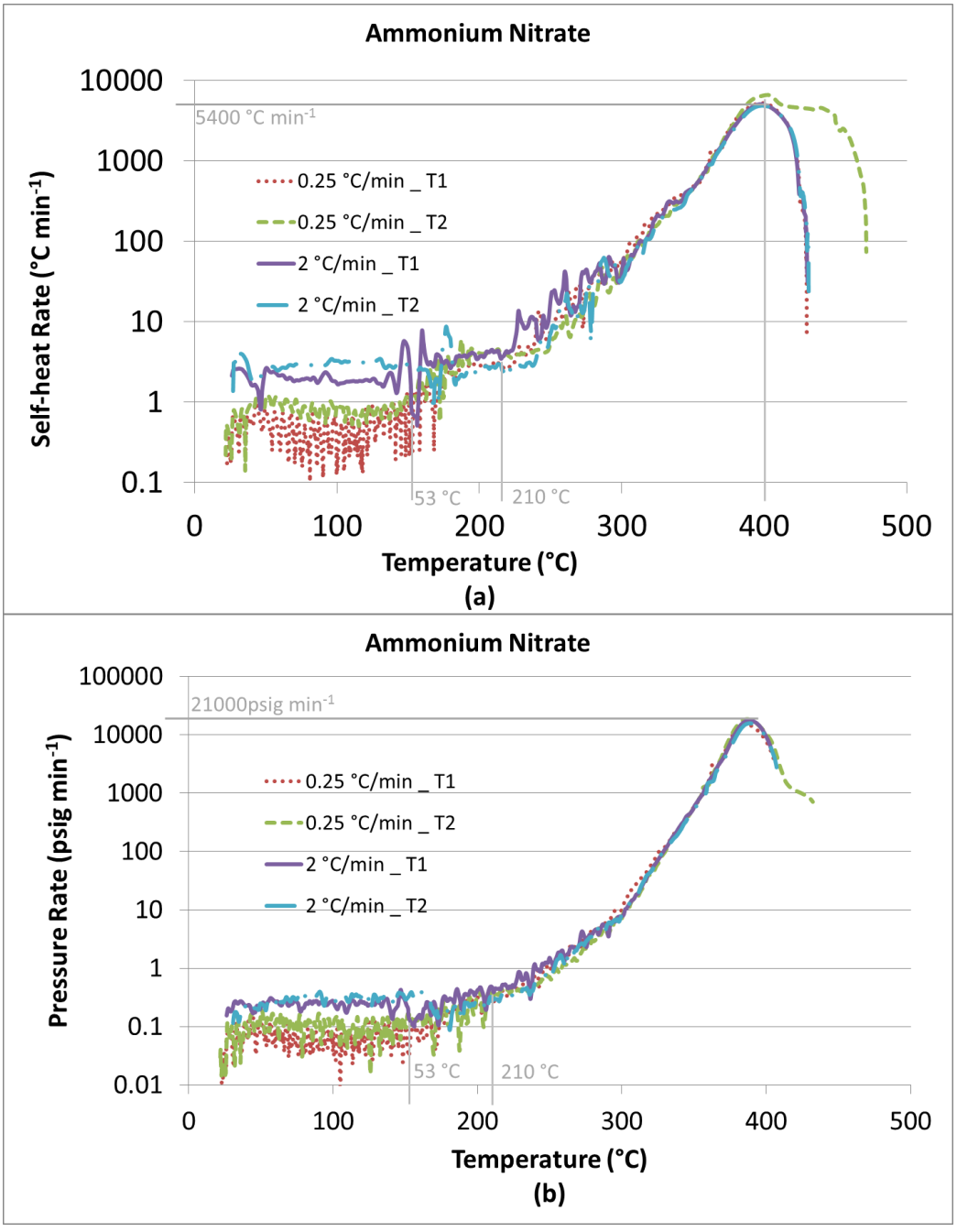

Figure 41. The thermal decomposition of AN under different heating rates (a) Self-heating rate profile (b) Pressure-rise rate profile

As shown in Figure 41*(a)*, when the pre-set heating rate was 0.25 °C·min^{-1}, the self-heating rate was lower than 1 °C·min^{-1} for the two replicate samples from ambient temperature to approximately 150 °C; then the self-heating rate increased to around 2 °C·min^{-1} and it remained at this value until the runaway reaction occurred. On the other hand, when the pre-set heating rate was 2 °C·min^{-1}, the self-heating rate was about 2 °C·min^{-1} from ambient temperature to 200 °C. As can be seen in Figure 41*(b)*, when the pre-set heating rate was 0.25 °C·min^{-1}, the pressure-rise rate was smaller than that of the samples with a pre-set heating rate of 2 °C·min^{-1}, up to around 150 °C; after that temperature, the pressure-rise rate started to increase. For all four tests conducted with the two pre-set heating rates, the pressure-rise rate profiles were similar after around 170 °C; after this temperature, the pressure started rising faster. After 200 °C, there was a steep increase in the pressure-rise rate.

According to Feick and Hainer, at 170 °C, AN will decompose endothermically [9], generating HNO_3 and NH_3; this could result in an increase in pressure but not in temperature. In such a case, the heater of the RSST would continue to compensate for the heat needed for the endothermic reaction to ensure that the self-heating rate follows the pre-set value.

It is plausible that a reaction or phase transition occurred at around 150 °C followed by a violent decomposition reaction after 200 °C. There are two potential causes of the event taking place at 150 °C. First, it could be a slow exothermic reaction, but whether it was self-sustaining reaction or autocatalytic reaction needs further research. Second, it might be an endothermic phase transition because in the temperature

range between 125 °C and 169 °C, the crystal structure of AN was cubic. According to Theoret and Sandorfy [115] at 125 °C there was a phase transition of AN from phase I to phase II. In this case, the temperature rise rate at 150 °C could fluctuate due to the heater, for the same reason as explained in the previous paragraph. The thermal effects at 150 °C could be caused by either the exothermic reaction or the endothermic phase transition; or they are both likely to occur simultaneously.

The important parameters are summarized in Table 23 and Table 24. When the pre-set heating rate was 0.25 °C·min^{-1}, two "onset" temperatures were detected. The first "onset" occurred at 153 (±1) °C when the self-heating rate started to increase slightly, but the decomposition was not violent; and the second "onset" occurred at 209 (±1) °C which led to a fast decomposition reaction, rapidly generating heat and gaseous products. When the pre-set heating rate was 2 °C·min^{-1}, only one "onset" was determined by the method employed in this work to define the "onset". The identified "onset" at this heating rate was 213 (±4) °C. The remaining parameters were similar under both heating rates. It is plausible that the pre-set heating rate of 2 °C·min^{-1} was too fast and concealed the mild exothermic reaction or endothermic phase transition at 150 °C. The temperature-rise rate caused by the sample self-heating after 150 °C, might be lower than 2 °C·min^{-1} up to around 213 °C, the "onset" temperature; after that, the self-heating rate was higher than 2 °C·min^{-1}. On the other hand, when the heating rate was 0.25 °C·min^{-1}, the rise of the temperature rate caused by sample decomposition after 150 °C was greater than 0.25 °C·min^{-1}, thus, the first "onset" peak was observed. Then, there

was a substantial increase in the self-heating rate later on at around 209 °C, when the second "onset" was observed.

Table 23. AN decomposition under different heating rates: Temperature

No. of experiment	Heating rate (°C·min^{-1})	First T_o (°C)	Second T_o (°C)	$(dT/dt)_{max}$ (°C·s^{-1})	T_{max} (°C)	T_f (°C)
0.25_T1	0.25	154	210	88	400	429
0.25_T2	0.25	152	208	109	404	472
2_T1	2	-	210	85	399	431
2_T2	2	-	216	81	398	431
0.25_Avg.	0.25	153±1	209±1	99±15	402±3	451±30
2_Avg.	2	-	213±4	83±3	399±1	431±0

(Note: each test contains 3.5 g of AN)

Table 24. AN decomposition under different heating rates: Pressure

No. of experiment	Heating rate (°C·min^{-1})	P_o (psig)	$(dP/dt)_{max}$ (psi·s^{-1})	P_{max} (psig)	P_f (psig)	P_c (psig)
0.25_T1	0.25	208	250	342	384	226
0.25_T2	0.25	207	305	355	404	228
2_T1	2	209	290	359	397	227
2_T2	2	206	265	350	389	225
0.25_Avg.	0.25	208±1	278±39	349±9	394±14	227±1
2_Avg.	2	208±2	278±18	355±6	393±6	226±1

(Note: each test contains 3.5 g of AN; P_c was obtained at 20 °C)

5.3.2 Effect of Heating Rate – APTAC Experiments

In the APTAC, 1 g of AN was mixed thoroughly with 5 g of sand, and placed into the test cell. Different heating rates were applied to the experiments, including 2 °C·min^{-1}, 3 °C·min^{-1}, 5 °C·min^{-1}, and 10 °C·min^{-1}. HWS mode stared at 100 °C. In order to study how the starting temperature of HWS affects the experimental results, another two experiments were conducted, *i.e.*, HWS started at 160 °C with a heating rate of 3 °C·min^{-1}, and HWS started at 180 °C with a heating rate of 5 °C·min^{-1}. The initial pressure of all the experiments in this section was 187 psia (1.3 MPa), which was achieved by applying nitrogen into the test cell.

The experimental results of the heating rate of 2 °C·min^{-1} are discussed here as an example to show how the results were analyzed. Using the same definition as reported in Section 5.2.2, the "onset" temperature is determined from the self-heating rate *vs*. temperature profile in Figure 42. The final temperature is determined from the temperature *vs*. time profile in Figure 43. The corresponding "onset" pressure and final pressure can be determined as well.

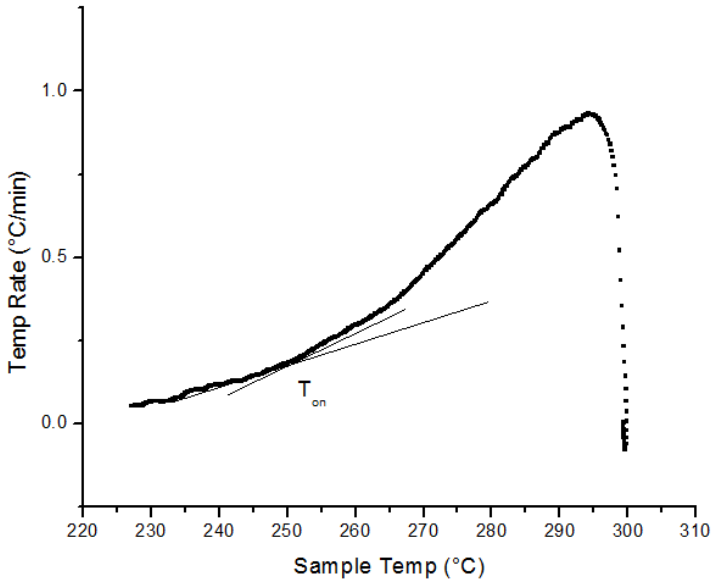

Figure 42. "Onset" temperature from self-heating rate *vs*. temperature of AN decomposition with 2 °C·min^{-1} heating rate in the APTAC

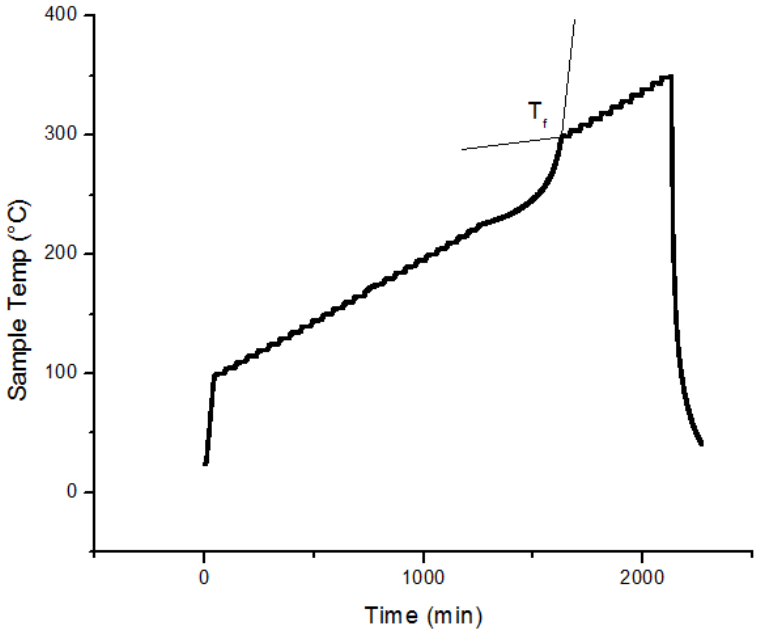

Figure 43. Final temperature from temperature *vs*. time profile of AN decomposition with 2 °C·min^{-1} heating rate in the APTAC

From Figure 42, the reaction started when the temperature reached 251 °C, therefore T_o = 251 °C and P_o = 2624.30 kPa. The maximum self-heating rate was $(dT/dt)_{max}$ = 1 °C·min^{-1} and it occurred when the temperature was T_{max} = 294 °C. The maximum pressure-rise rate was $(dP/dt)_{max}$ = 26 kPa·min^{-1}, which occurred when the pressure was P_{max} = 3760 kPa. When the reaction completed, the final temperature was T_f = 299 °C and the final pressure was P_f = 3994 kPa. When the reaction cooled down, the pressure was P_c = 1558 kPa (226 psia). The experimental results with the heating rate of 2 °C·min^{-1}, together with the results of other experiments, are summarized in Table 25.

Table 25. Experimental data of AN decomposition under various heating rates in the APTAC

No.	1	2	3	4	5	6
Heating rate (°C·min^{-1})	2	3	5	10	3	5
HWS (°C)	100	100	100	100	160	180
T_o (°C)	251	253	252	255	255	252
$(dT/dt)_{max}$ (°C·min^{-1})	1	2	3	4	19	12
T_{max} (°C)	294	293	298	306	320	310
T_f (°C)	299	305	310	317	326	322
P_o (kPa)	2624	2838	2810	2778	2656	2690
$(dP/dt)_{max}$ (kPa·min^{-1})	26	64	79	127	364	285
P_{max} (kPa)	3760	3984	4000	4102	3988	4011
P_f (kPa)	3994	4219	4219	4347	4242	4316

(Note: each test contains 1 g of AN + 5 g of sand)

Analyzing the data points between the T_o and the T_f, the decomposition of AN can be described by the n^{th} order reaction model. When first order reaction was assumed for the heating rate of 2 °C·min^{-1}, the R^2=0.98, showing it was first order reaction, and the activation energy was approximately 209 kJ·mol^{-1}. The results of other heating rates were calculated as well, and R^2 was between 0.97 – 1.00, which shows that the reactions followed first order reaction.

After thermal inertia factor, φ factor, correction, were performed using the same approach as described in Section 5.2.2. The results of all the experiments are summarized in Table 26.

Table 26. Experimental data of AN decomposition under various heating rates in the APTAC after thermal inertia factor correction

No.	1	2	3	4	5	6
Heating rate (°C·min^{-1})	2	3	5	10	3	5
HWS (°C)	100	100	100	100	160	180
φ	3.95	3.98	3.96	3.91	3.95	3.98
T_o (°C)	251	253	252	255	255	252
$(dT/dt)_{max,\varphi}$ (°C·min^{-1})	4	8	12	17	76	48
$T_{max,\varphi}$ (°C)	421	410	436	454	510	484
$T_{f,\varphi}$ (°C)	441	460	482	497	535	531
E_a (kJ·mol^{-1})	209	237	215	211	231	218
$-\Delta H_{rxn}$ (kJ·mol^{-1})	26	29	32	34	39	39
Δn (mol)	0.004	0.013	0.011	0.011	0.011	0.011

(Note: each test contains 1 g of AN + 5 g of sand)

Looking at the experiments with HWS starting at 100 °C under various heating rates, experiment No. 1 to 4, the impact of heating rate on AN decomposition is discussed here. It can be concluded that for the four experiments, T_o = 253±2 °C, T_{max} = 432±22 °C, T_f = 469±28 °C, P_o = 2731±107 kPa, P_{max} = 3931±171 kPa, P_f = 4170±177 kPa, E_a = 223±14 kJ·mol^{-1}, and -ΔH_{rxn} = 30±4 kJ·mol^{-1}. The "onset" temperature and activation energy was not significantly affected by heating rate. However, T_f, P_f, $(dT/dt)_{max}$, $(dP/dt)_{max}$, and -ΔH_{rxn} all increased with higher heating rate, especially $(dT/dt)_{max}$ and $(dP/dt)_{max}$. The self-heating *vs*. temperature profile in Figure 44 and the pressure-rise rate *vs*. temperature profile in Figure 45 clearly show that the maximum temperature and pressure-rise rate increase with faster heating rate. Based on Figure 44 and Figure 45, not only $(dT/dt)_{max}$ and $(dP/dt)_{max}$ were increasing with faster heating rate, but the self-heating rate and pressure-rise rate at each temperature were all higher with faster heating rate.

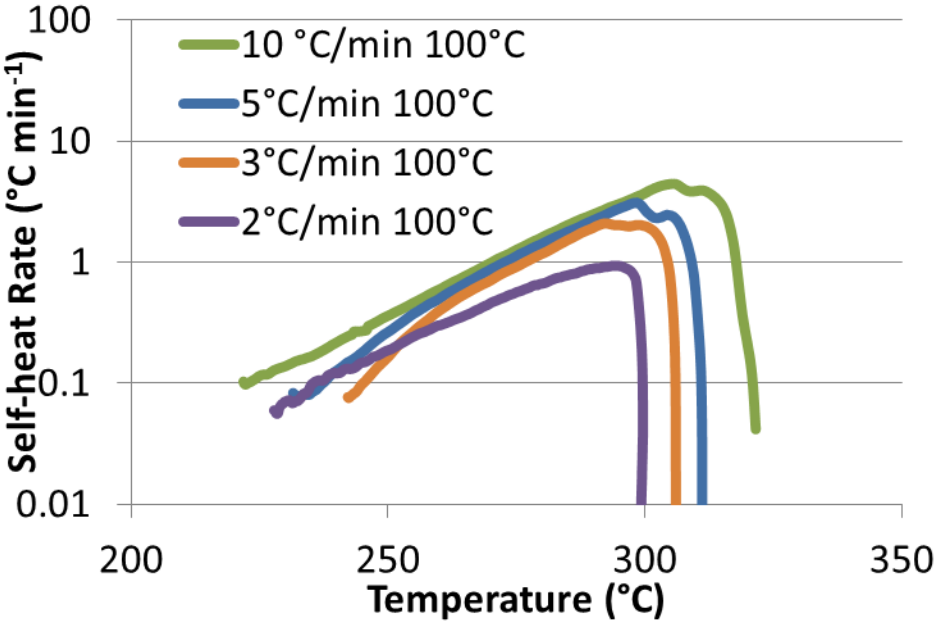

Figure 44. Self-heating rate *vs*. temperature profile of AN decomposition under various heating rates

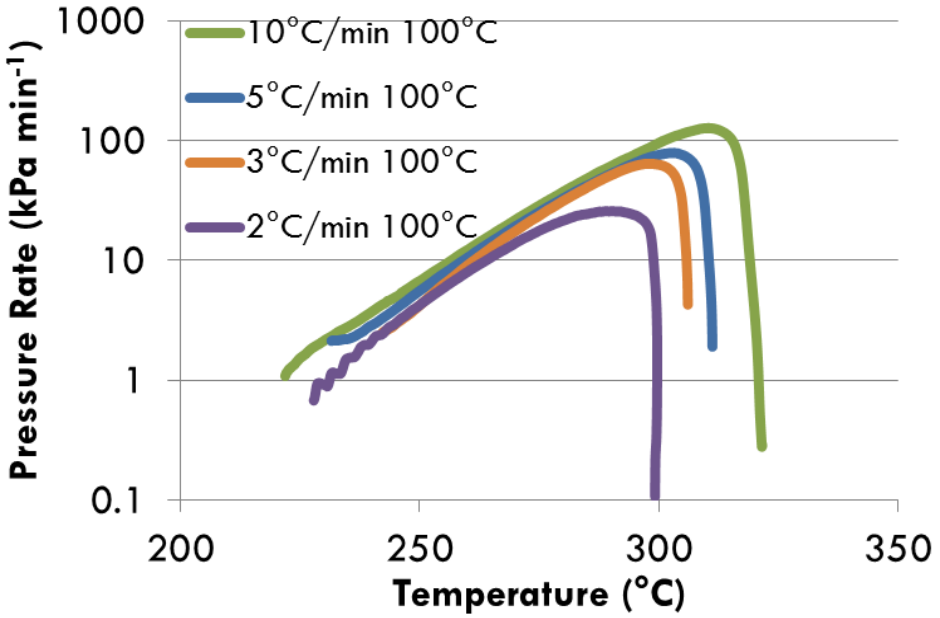

Figure 45. Pressure-rise rate *vs*. temperature profile of AN decomposition under various heating rates

The temperature *vs*. time profile in Figure 46 and the pressure *vs*. time profile in Figure 47 show that with faster heating rate, the time for the runaway reaction was decreasing, *i.e.*, the time of reaction was 106 min for the experiment with 2 °C·min^{-1}, the time of reaction was 69 min for the experiment with 3 °C·min^{-1}, the time of reaction was 61 min for the experiment with 5 °C·min^{-1}, and the time of reaction was 45 min for the experiment with 10 °C·min^{-1}. The two figures also show that the final temperature and final pressure increased with faster heating rate. It can be concluded that the faster the heating rate, the more violently the reaction occurs.

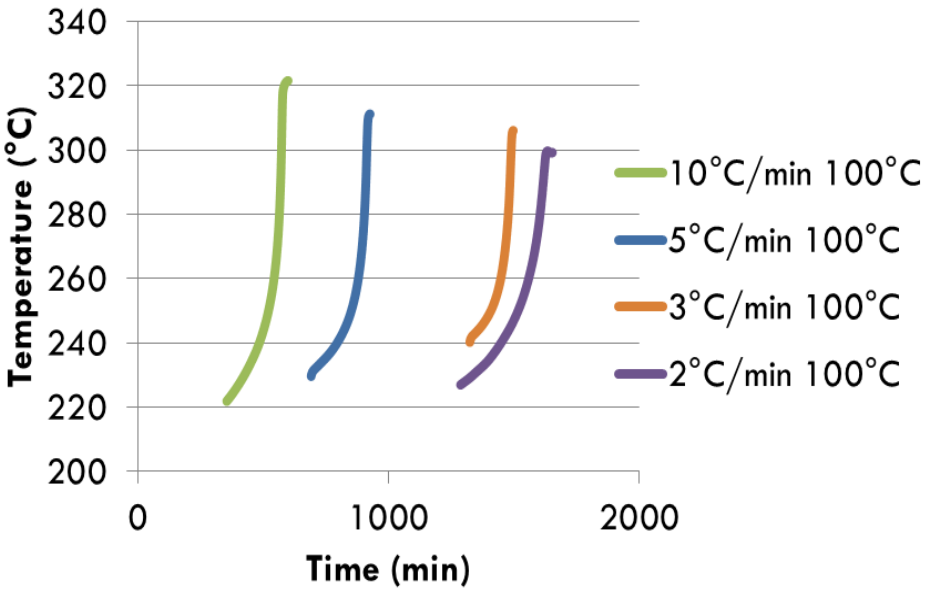

Figure 46. Temperature *vs*. time profile of AN decomposition under various heating rates

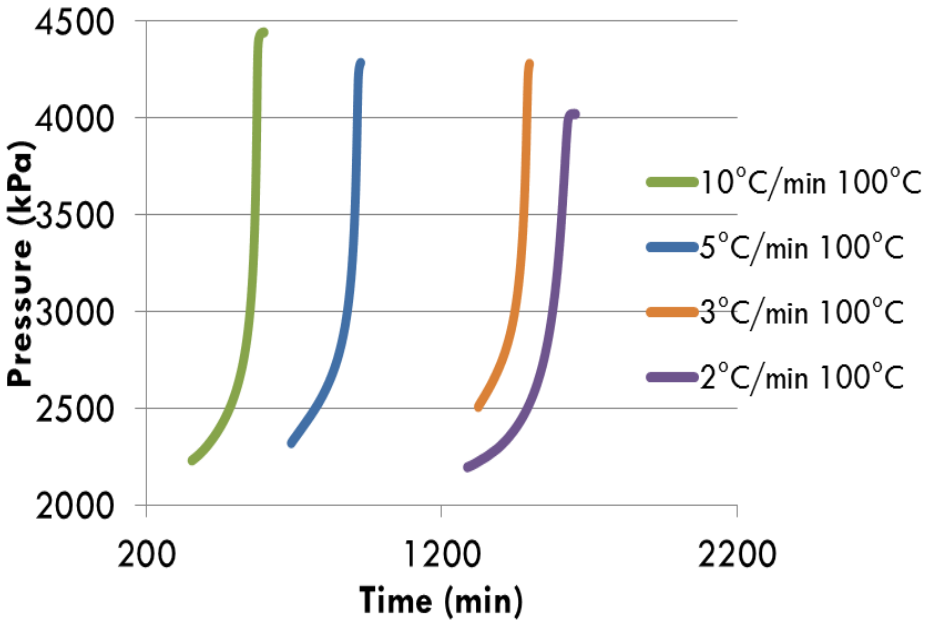

Figure 47. Pressure *vs*. time profile of AN decomposition under various heating rates in the APTAC

As a conclusion, when the heating rate is faster, the self-heating rate and the pressure-rise rate increase faster and the reaction occurs more violently. It is because when AN was suddenly heated up, the heating process was considered continuous, the time of adiabatic condition for wait and search was reduced, increasing the self-accelerating reactions of AN, thus, AN decomposition occurred faster. Therefore, if AN is suddenly heated up, the decomposition is more likely to occur.

5.4 Effect of Starting Temperature of HWS

In the Heat-Wait-Search (HWS) mode of the APTAC, temperature will increase up to a certain temperature point and then HWS will start to occur. When HWS starts at different temperatures, it may affect the AN decomposition.

Now the impact of different starting temperature of HWS is compared here. As can be seen in Table 25 and Table 26, when the heating rate was 5 °C·min^{-1}, different starting temperatures of HWS were tested, including 100 °C and 180 °C; when the heating rate was 3 °C·min^{-1}, different starting temperatures of HWS were tested, including 100 °C and 160 °C. The self-heating rate *vs*. temperature profile, the pressure-rise rate *vs*. temperature profile, and the temperature *vs*. time profile are shown in Figure 48, Figure 49, and Figure 50, respectively. It can be concluded that the employed starting temperature of HWS does not have a significant impact on "onset" temperature and activation energy. However, $(dP/dt)_{max}$, $(dT/dt)_{max}$, ΔH_{rxn}, and T_f all increased with higher starting temperature of HWS, and the time of reaction decreased with higher starting temperature of HWS. At the heating rate of 5 °C·min^{-1}, the time of reaction was 61 min when HWS started at 100 °C, and the time of reaction was 36 min when HWS started at 180 °C. At the heating rate of 3 °C·min^{-1}, the time of reaction was 69 min when HWS started at 100 °C, and the time of reaction was 30 min when HWS started at 160 °C. It is concluded the reaction is more violent when the HWS starts at higher temperatures.

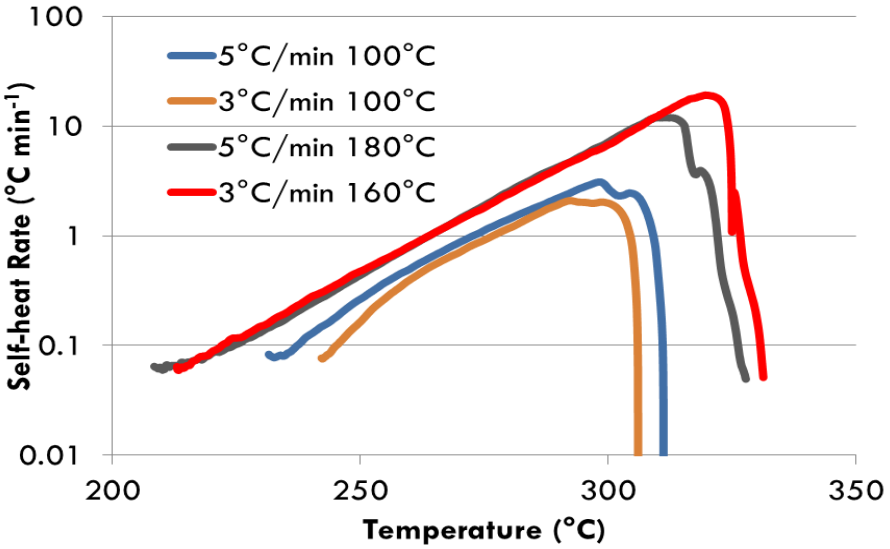

Figure 48. Effect of different starting temperature of HWS: self-heating rate *vs*. temperature

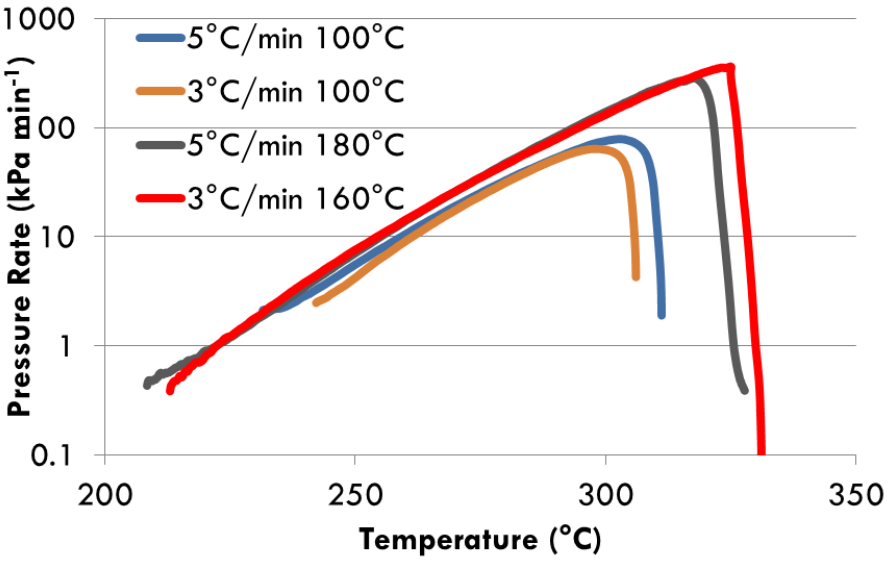

Figure 49. Effect of different starting temperature of HWS: pressure-rise rate *vs*. temperature

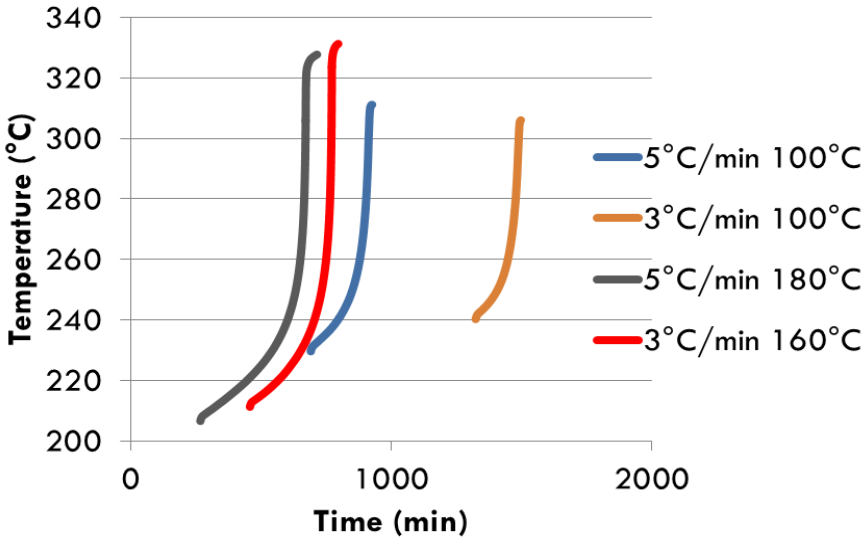

Figure 50. Effect of different starting temperature of HWS: temperature *vs*. time

To further study how the starting temperature of HWS affects AN decomposition, a few more experiments were conducted. 1 g of AN was well mixed with 5 g of sand, and placed into the test cell. The initial heating rate was 10 °C·min^{-1} from ambient temperature. The temperature increment was 10 °C.

HWS started at various temperatures, such as 100 °C, 160 °C, 170 °C, 180 °C, 185 °C, and 190 °C. As reported in Section 1.5, the melting point of AN is 170 °C, and exothermic reaction starts slowly once AN melts. At such temperature, if AN is heated up at a certain rate, the slow decomposition may not be recorded by the equipment since heat is being supplied to the sample; however, if the APTAC is in the Wait-Search mode, the heat might be detected by the equipment. Therefore, it is important to study how the starting temperature of HWS affects the decomposition of AN. The experimental results are reported in Figure 51 and Table 27.

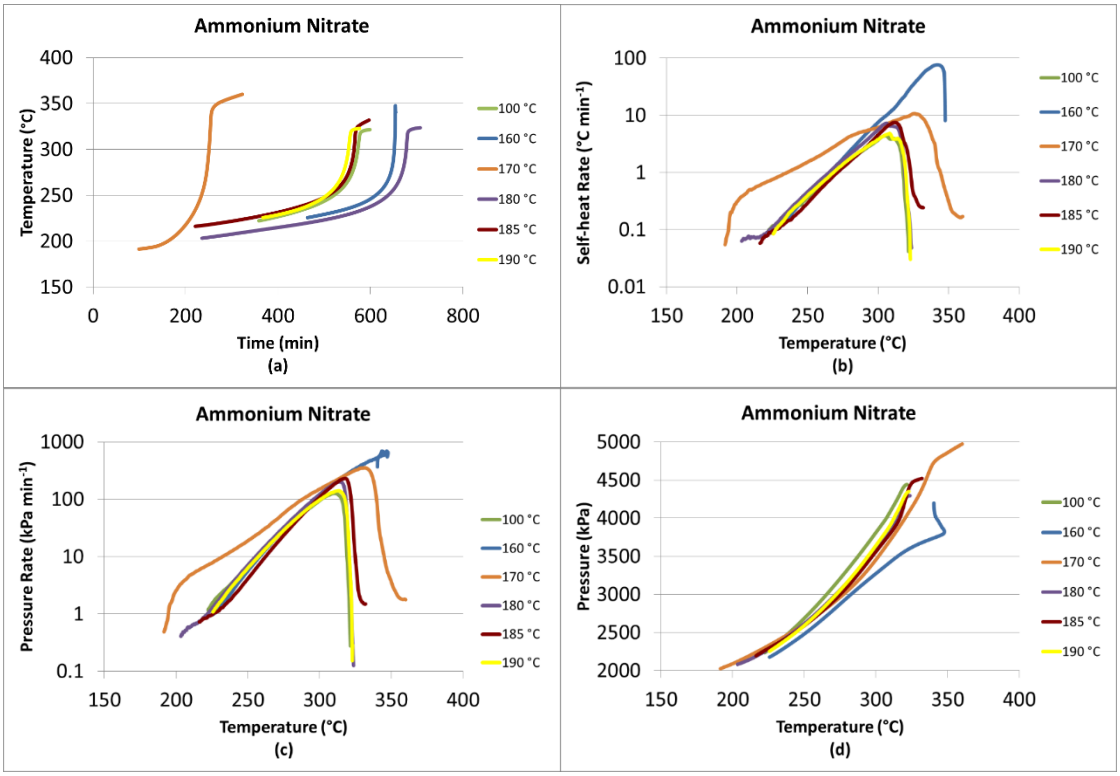

Figure 51. AN decomposition with various starting temperatures of HWS in the APTAC (a) Temperature *vs*. time profile (b) Self-heating rate *vs*. temperature profile (c) Pressure-rise rate *vs*. temperature profile (d) Pressure *vs*. temperature profile

When the HWS started at 170 °C and 180 °C, the "onset" temperature occurred at a lower temperature; and when HWS started at other temperatures including 100 °C, 160 °C, 185 °C, and 190 °C, the "onset" temperature occurred at approximately 220 °C. When the HWS started at 160 °C and 170 °C, the maximum self-heating rates were higher than those of other starting temperatures, and occurred at higher temperatures compared with other experiments. Plus, the final temperatures were higher, the maximum pressure-rise rate was higher. Therefore, it can be concluded that when HWS starts at around AN melting temperature, *i.e.*, 160 °C, 170 °C, and 180 °C, the

decomposition of AN is different from other experiments, and in general, AN decomposes more violently.

Table 27. Experimental results of AN decomposition with various starting temperature of HWS in the APTAC

Starting temperature of HWS (°C)	100	160	170	180	185	190
T_o (°C)	220	226	191	203	216	226
$(dT/dt)_{max}$ (°C·min^{-1})	4	77	11	7	7	5
T_{max} (°C)	306	342	325	306	312	308
T_f (°C)	322	340	360	324	332	323
P_o (kPa)	2223	2177	2026	2082	2195	2254
$(dP/dt)_{max}$ (kPa·min^{-1})	127	693	353	202	231	141
P_{max} (kPa)	4102	3962	4367	3948	4054	4048
P_f (kPa)	4450	4199	4974	4296	4522	4351
P_c (kPa)	1687	1592	1623	1637	1647	1663
$t_{runaway}$ (min)	252	190	224	472	376	209

(Note: each test contains 1 g of AN + 5 g of sand; P_c was obtained at 20 °C)

5.5 Effect of Thermal History – AN Pre-treatment

In order to study the effect of thermal history, to be specific, how changes in temperatures affect the characteristics of AN, an AN sample was pre-treated by heating up the sample and then let it cool down. First, 3.5 g of pure solid AN was weighed and loaded into the test cell and then pre-heated in the RSST. In order to pre-treat the sample, a different heating rate program was employed. For temperatures from ambient

temperature up to 50 °C, the heating rate was 2 °C·min^{-1}; for temperatures from 50 °C to 80 °C, the rate was 1 °C·min^{-1}; and for temperatures from 80 °C up to 100 °C, the rate was 0.25 °C·min^{-1}. It took approximately 125 minutes in total to heat up the sample to 100 °C. When 100 °C was reached, the sample was cooled down by ambient conditions to room temperature. This completed the pre-treatment process. The RSST was vented and the sample was then heated in order to decompose following the procedure described in Section 3.4.2.

The temperature *vs*. time profile and self-heating rate *vs*. temperature profile of the two replicate pre-treatment experiments are shown in Figure 52*(a)* and *(b)*, respectively. The experimental data of pure AN test is also given as a reference in both the figures.

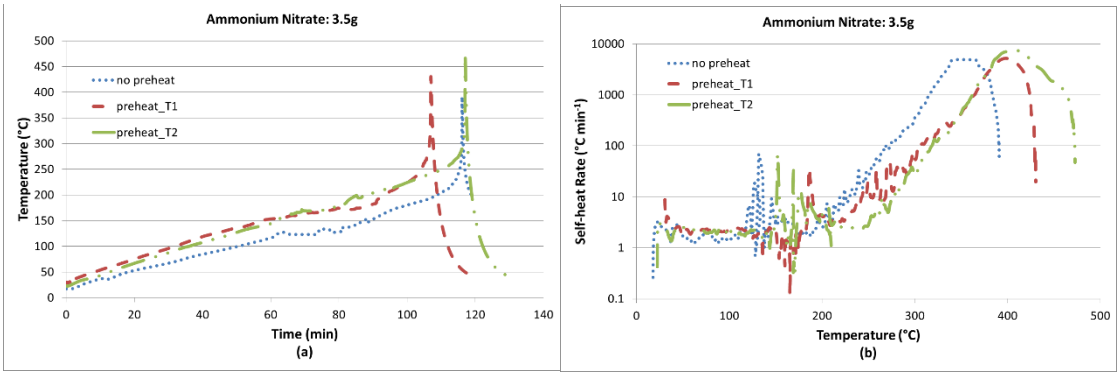

Figure 52. The thermal decomposition of pre-treated AN (a) Temperature profile (b) Self-heating rate

As can be seen from Figure 52*(a)*, the temperature profiles of the two replicate experiments for AN with pre-treatment were identical before the temperatures reached

200 °C. After that, the time to reach "onset" was different for the two replicate experiments. That was most likely caused by the inherent problem of the RSST in testing solid samples as described before. The "onset" temperatures obtained in the two experiments were relatively close. The overall trends and critical parameters were also almost the same. Unlike pure AN, the temperature and the pressure of the pre-treated AN did not start to increase dramatically immediately after 200 °C. This can be seen more clearly from the logarithmic plot of the self-heating rate profile in Figure 52*(b)*.

From the results, the pre-treatment of heating AN mitigates the risks of AN decomposition by inducing the reactions to occur at higher temperatures than AN without the treatment. The "onset" temperature of the pre-treated AN was 247 (±6) °C, with the maximum self-heating rate of 113 (±18) $°C \cdot s^{-1}$, which occurred at 404 (±6) °C.

By comparing the results obtained for pre-treated AN against AN without pre-treatment, it was found that the "onset" temperature increased by 47 °C, and the temperature at maximum self-heating rate increased by 57 °C. The results indicate that the pre-treatment helps to mitigate the runaway behavior of AN. This could also be caused by the removal of water from the samples. It took approximately 12 hours between each thermal pre-treatment and decomposition, therefore the samples with thermal pre-treatment contain much less water than AN without the pre-treatment process. The reasons behind this need further research.

5.6 Effect of Sample Size

The amount of sample can affect how AN decomposes. In order to study how sample size affects the experimental results, AN with various sample sizes have been tested. Three sample masses, 0.2 g AN + 9.8 g sand (test 1), 1 g AN + 9 g sand (test 2), and 1 g AN + 5 g sand (test 3), were well mixed and placed into the test cell. In the APTAC, the initial pad pressure (nitrogen) applied was 120 psia (827 kPa), the initial heating rate was 10 °C·min^{-1} from ambient temperature to 100 °C, then HWS was turned on. The temperature increment was 10 °C. The experimental results of the three tests are summarized in Figure 53 and Table 28.

Comparing test 1 and test 2, both tests were with 10 g of solid in total, and the mass amount of AN in test 2 was five times that of test 1. The time for test 1 was very short since the mass of AN was small, the "onset" temperature was higher than test 2, and the pressure generated was much less than test 2. Comparing test 2 and test 3, where both tests had 1 g of AN, the "onset" temperatures were the same, the maximum self-heating rate of test 3 was higher than that of test 2, as well as the final temperature, "onset" pressure, the maximum pressure-rise rate, and the time to complete the reaction. Therefore, the decomposition of AN was mitigated by the presence of inert material.

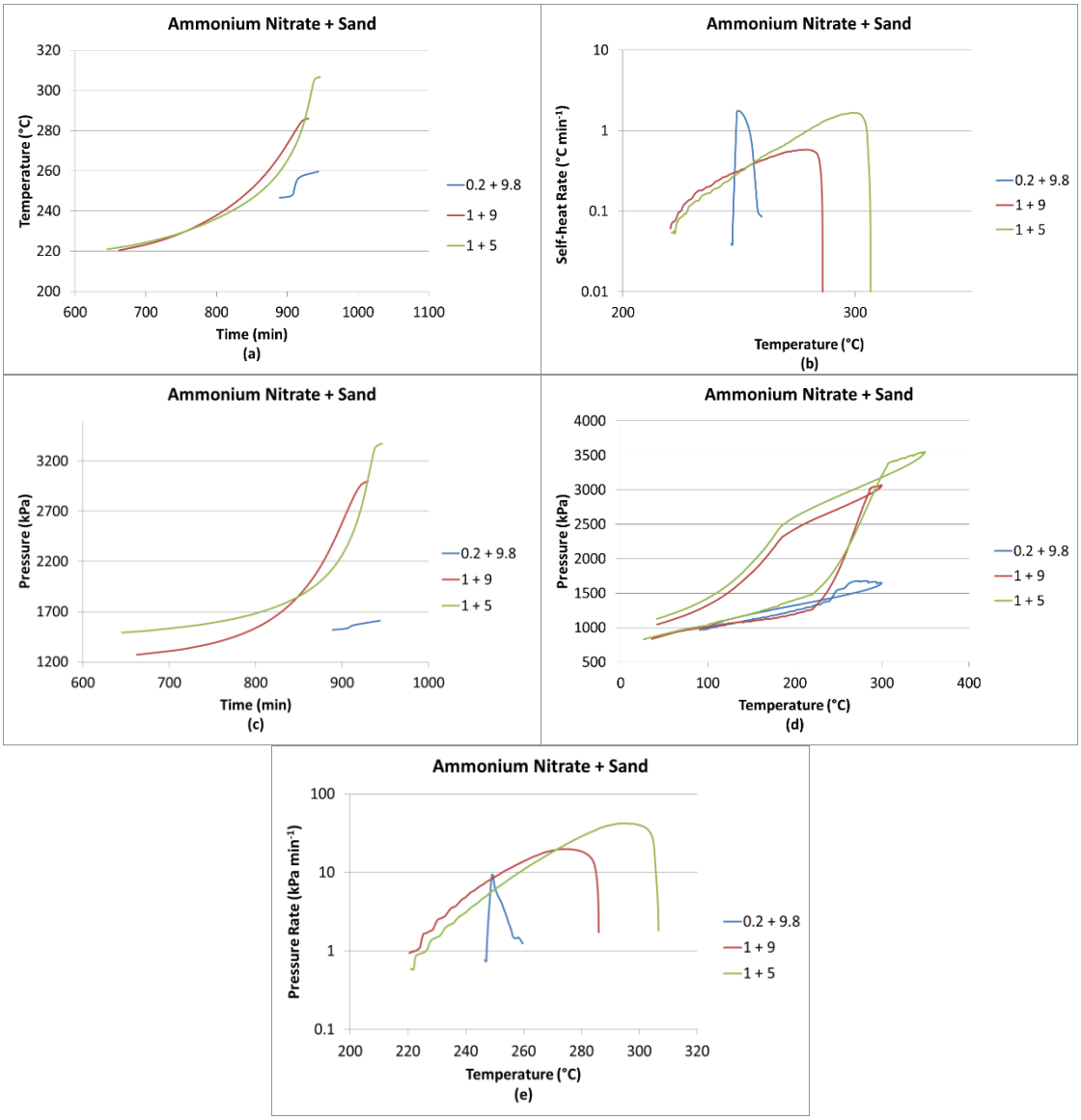

Figure 53. AN decomposition with various sample sizes (a) Temperature *vs*. time profile (b) Self-heating rate *vs*. temperature profile (c) Pressure *vs*. time profile (d) Pressure *vs*. temperature profile (e) Pressure-rise rate *vs*. temperature profile

Table 28. Experimental results of AN decomposition with various sample sizes in the APTAC

Test No.	1	2	3
Sample size, AN (g) + sand (g)	0.2 + 9.8	1 + 9	1 + 5
T_o (°C)	245	220	221
$(dT/dt)_{max}$ (°C·min^{-1})	1.75	0.58	1.67
T_{max} (°C)	250	279	298
T_f (°C)	260	286	307
P_o (kPa)	1519	1271	1492
$(dP/dt)_{max}$ (kPa·min^{-1})	9.33	19.8	42
P_{max} (kPa)	1548	2652	3081
P_f (kPa)	1610	2999	3373
P_c (kPa)	803	1047	1128
$t_{runaway}$ (min)	55	268	301

(Note: P_c was obtained at 20 °C)

5.7 Isothermal Testing

Isothermal mode of the APTAC was used to test AN decomposition. The isothermal temperatures tested include 210 °C and 230 °C. As mentioned earlier, the "onset" temperature of AN in the APTAC is 220 °C. 1 g of AN was well mixed with 5 g of sand, and placed into the test cell. In the APTAC, the initial pad pressure (nitrogen) applied was 200 psia (1379 kPa), the initial heating rate was 10 °C·min^{-1} from ambient temperature to the isothermal temperature (210 °C and 230 °C), then isothermal mode was turned on. The exotherm limit was 0.05 °C·min^{-1}. The experimental results are reported in Figure 54. It can be seen from the figures that no major decomposition was detected once the temperature was constant. However, the temperature increased for a few degrees before it was stable. It might be the decomposition of AN. Interestingly, the pressure was increasing slowly while the temperature was kept constant. It is assumed that in the isothermal mode, the heat released by AN decomposition was supplying heat to maintain the sample at constant temperature; or the reaction was finished before the temperature reached the constant value. More work is needed to study the AN decomposition under isothermal mode.

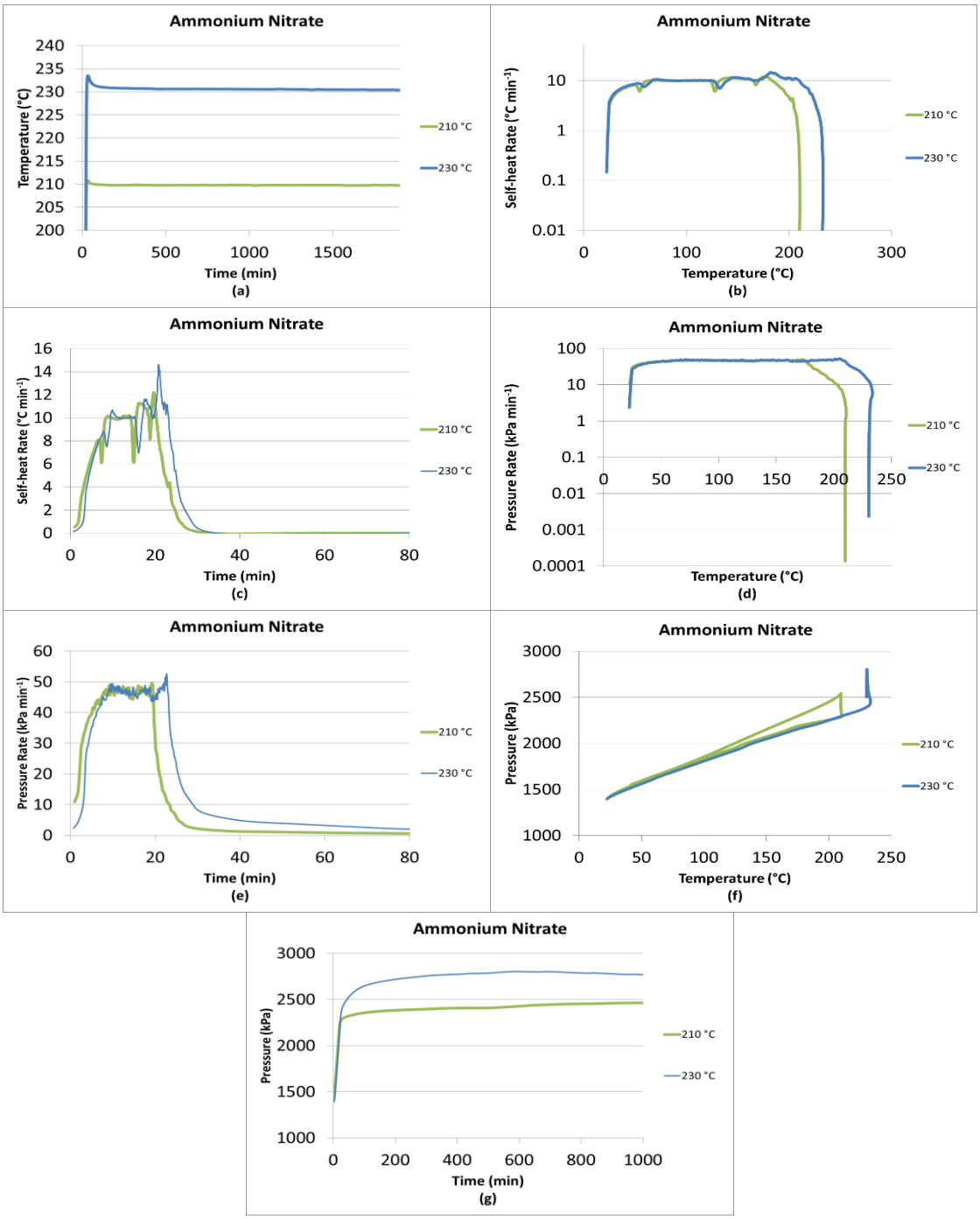

Figure 54. AN decomposition in isothermal mode (a) Temperature *vs*. time (b) Self-heating rate *vs*. temperature (c) Self-heating rate *vs*. time (d) Pressure-rise rate *vs*. temperature (e) Pressure-rise rate *vs*. time (f) Pressure *vs*. temperature (g) Pressure *vs*. time

5.8 Conclusions

In this work, the RSST and the APTAC was used to study the runaway behavior of AN under various conditions, such as in the presence of additives with different concentrations, including water, sodium bicarbonate, potassium carbonate, ammonium sulfate, barium nitrate, sodium nitrate, and ferric sulfate (or iron(III) sulfate, FS, $Fe_2(SO_4)_3$). The amount of water used in this test will help mitigate the explosion potential of AN, increasing "onset" temperature and delaying the time to reach "onset" temperature. If AN could be stored with (or near to) inhibitors, or there is enough water, an AN explosion could be mitigated to a certain extent. Some chemicals act as inhibitors, such as sodium sulfate, ammonium sulfate, barium nitrate, sodium nitrate, sodium hydrogen carbonate, and potassium carbonate, while others act as promoters, such as potassium chloride and ferric sulfate. The presence of inhibitors in solid AN mixtures delayed the "onset" of AN decomposition, because both the "onset" temperatures and temperatures at maximum self-heating rate increased dramatically. The more inhibitor in the mixture, the better the inhibiting effect. However, promoters have the opposite effects. The results show the same trends as the ones reported in literature with other experimental equipment.

The effect of confinement was tested by observing AN decomposition under various overhead initial pressures in the RSST and the APTAC, varying from atmospheric pressure to 200 psia (1.4 MPa). The results were corrected based on the thermal inertia factor. With increasing initial pressure, the "onset" temperature and

activation energy decreased slightly, and the maximum pressure-rise rate increased dramatically; P_o, P_{max}, P_f, and P_c were all higher, and there was more gas generated as $P_{initial}$ increased. As a conclusion, pressure accumulation is hazardous to AN and it is important to keep a low-pressure environment for AN storage and transportation.

AN decomposition is also affected by heating rate, which was studied using the RSST by heating up AN under two heating rates of 0.25 °C·min^{-1} and 2 °C·min^{-1}; and using the APTAC by heating up AN under heating rates of 2 °C·min^{-1}, 3 °C·min^{-1}, 5 °C·min^{-1}, and 10·°C min^{-1}. As a conclusion, when the heating rate is faster, the self-heating rate and the pressure-rise rate increase faster, the activation energy is decreased, and the reaction occurs more violently.

For the effect of temperatures, it can be concluded that when HWS starts at around AN melting temperature, *i.e.*, 160 °C, 170 °C, and 180 °C, the decomposition of AN is different from other experiments, and in general, AN decomposes more violently. For example, the maximum self-heating rate was higher than that of other starting temperatures, and occurred at higher temperatures than other experiments. Plus, the final temperature was higher, the maximum pressure-rise rate was higher. When the starting temperatures are under 160 °C, the reaction is more violent when the HWS starts at higher temperatures.

Thus, when the heating rate is faster or the HWS starts at higher temperatures, the self-heating rate and the pressure-rise rate are faster and the reaction occurs more violently. Therefore, if AN is suddenly heated up, the decomposition is more likely to occur.

The pre-heated AN increased the “onset” temperatures and temperatures at maximum self-heating rate of AN. Using the pre-treatment method presented in this work, the “onset” temperature of AN thermal decomposition was increased by approximately 50 °C compared with that of pure AN.

The experiments of different sample sizes show that the decomposition of AN would be mitigated with inert material. And of course, with smaller amount of sample size, the decomposition is less violent.

The isothermal experiments of AN decomposition could be further studied to identify the induction period and associated hazards of AN in storage.

6. THE COMPLEXITIES OF USING WATER TO FIGHT AMMONIUM NITRATE RELATED FIRES

AN has caused many fires and explosions throughout history, and this chapter discusses extinguishing AN-related fires with water and its possible complications. In terms of fire protection, water suppression systems have been widely used in chemical process facilities as an active protection layer, and they have been successful in tackling most of the fires. However, where in most cases of fire, water acts just as a cooling and hence combustion extinguishing agent, in the case of AN within limits it may favor the conditions for explosion. The main objective of this work is to discuss the role of water as a chemical, interfering physically and chemically with AN-related fire scenarios possibly leading to explosion.

In the aftermath of the West Fertilizer Explosion, the White House issued an Executive Order [116] that required a review of all existing regulations. Despite considerable research (including calorimeter measurements, explosion tests, and molecular simulation) performed on understanding the detonability of AN, incidents like West, Texas, are still occurring, and this calls for gaining even deeper understanding of the underlying causes of its unpredictable behavior at times.

There are a lot of issues to be addressed on how to improve AN safety, as well as how to tackle AN fires in an effective manner. Despite extensive research efforts the precise mechanism of how heated AN can transit from a fast decomposition into a violent detonation is still unknown. Contamination can play a crucial role but this may

be limited to the initial stages of decomposition. Efforts have been made to improve safety of AN-based fertilizers by making non-detonable formulations. This can be achieved by diluting with inert materials with the disadvantage of lowering the fertilizing capacity. By manufacturing very hard non-porous prills even pure AN cannot be initiated to detonate by strong shock waves, at least not in quantities on kilogram-scale confined in steel tube. In a fire, though, these prills will lose their structure. Above 170 °C AN melts while decomposing in gaseous products. In the melt small bubbles are rising. When temperature further rises it starts to foam. Gas bubbles increase the sensitivity to shock and the liquid will be more prone to detonation.

Recently Babrauskas [117] published an excellent overview of the work carried out over the years by different people and organizations to investigate the hazardous properties of AN. He concluded that prevention of incidents means in the first place preventing a fire breaks out in or near an AN store. This requires the use of non-combustible construction materials and the avoidance of combustibles in contact with AN. Certainly for stores containing large amounts of AN the use of sprinkler systems (designed appropriately to deliver the large quantities of water needed to fight AN-related fires) is recommended.

Sprinkler systems are suggested by several agencies to protect AN storage areas, such as the Occupational Safety and Health Administration (OSHA) [65] and the National Fire Protection Association (NFPA) [118]. Sprinkler systems are undoubtedly highly effective to keep combustion caused fires under control. However, it is still unclear whether the capability of sprinkler systems is enough to tackle AN fires and stop

decomposition. This chapter will discuss in Section 6.1 sprinkler systems, in Section 6.2 AN hazards and explosion phenomenology, and in Section 6.3 the complexities of fighting AN storage area fires.

6.1 Sprinkler Systems

As an active fire protection device, fire sprinkler systems have been successfully used to prevent fatalities and property losses. A fire sprinkler system is composed of a water supply system and a water distribution piping system. The water supply system provides pressure and flow rate to the water distribution piping system, which is connected to a fire sprinkler. In the past, fire sprinklers were only used in factory facilities, now more cost-effective sprinkler systems are used at small buildings, such as personal homes [119]. Automatic sprinkler systems are widely used, likely more than any other kind of fixed fire protection systems. All over the world, there are more than 40 million sprinklers fitted each year [119]. The fire sprinkler systems have been effectively and efficiently operating during the past 120 years [120].

Sprinklers are commonly-used fire protection systems. Based on history records, the average fire loss in properties with sprinkler systems is approximately one-tenth of the loss in properties without sprinkler systems [121]. Research on fire sprinkler systems has been continuously improving throughout history. Automatic fire sprinklers were invented by Major Harrison in 1864 in the UK, and further developed and installed by Henry S. Parmelee in 1874 in the US, while trying to protect his piano factory [119,

122]. The oldest recorded sprinkler system, designed by William Congreve [122], was reported in 1812 at the Theatre Royal Drury Lane in the UK, whose updated system is still in use today [119]. It was covered by patent number 3606 dated December 30, 1812 [122]. The development of sprinkler systems began as early as 1723, and improvements have been continuous up through today as new technology is developed [122].

Apart from industry uses, sprinkler systems have also been used in residential areas [123]. NFPA 13 has established the standard for the installation of sprinkler systems in residential occupancies up to and including four stories in height, the purpose of which is to "*provide a sprinkler system that aids in detection and control of residential fires and thus provides improved protection against injury, life loss and property damage*" [124].

Sprinkler systems use water as the main extinguishing material. In most cases, the favorable physical properties of water make it an excellent fire suppression material. Its heat capacity is relatively high, at 4.2 $J \cdot g^{-1} \cdot K^{-1}$. When evaporating, with the heat of vaporization being 2442 $J \cdot g^{-1}$, water will absorb large amount of heat from the surroundings, such as flames and fuel. To be specific, water will expand 1,700 times when it evaporates into vapor, diluting the oxygen and fuel vapors in the surrounding environment [125].

Drop sizes will affect the performance of sprinklers. By using improper drop size, water could likely be wasted. However, the firefighting efficiency and effectiveness can be improved by using the optimized drop sizes [121]. Water drops from sprinkler systems have three main functions: reach the burning fuel surfaces by penetrating the

fire plume; cool the hot gases that are radially spreading; and wet the surrounding combustible materials [121].

In general, in order for fixed water suppression systems to work properly, water supply should be adequate and reliable; automatic actuated systems and water spray patterns should be effective; alarms should be able to indicate the operation or malfunction of the system; and maintenance and testing should be performed on time [126].

NFPA 13 (standard for the installation of sprinkler systems) has been adopted by most local building code officials and fire marshals as law. In most places, unique minor modifications have been added to sprinkler systems [126].

6.2 AN Explosion Phenomenology

AN explosions have been occurring throughout history. There are several possible mechanisms for AN fires and explosions: thermal decomposition, self-ignition, deflagration, and detonation.

Thermal decomposition is a heat driven phenomenon. In most cases, the reaction happens throughout the bulk of the substance at the same time. However, temperature is not the same at different places in solid AN material meaning the reaction rates are different within the material pile depending on local temperature and local composition. The reaction rate and heat produced are highest in places where temperature is highest, so the temperature rises locally exponentially. Therefore, temperature gradients exist

within the pile. The heat development is mainly caused by the reaction between the nitrate-ion as an oxidizing agent and the ammonium-ion as a reducing agent [108]. Heat transfer from high temperature areas to low temperature areas and heat loss to the environment will slow the process of decomposition down.

Due to low heat conductivity of granulated AN and the large quantities of stocks, even small heat effects could lead to localized *self-ignition* under certain conditions. The self-heating which occurs immediately after the production of AN could be caused by crystal conversions, inter-ionic reactions (exchange of ion pairs), and by oxidation of organic material (as contamination), which is usually slight and will only occur shortly after the production [108]. The decomposition is accelerated strongly in the presence of chlorides and acid [127], notably nitric acid, which it produces itself on decomposition, implying that once a decomposition sets in it will have a progressive character. From adiabatic storage test, it was proved that a measureable heat generation of *pure* AN only started just above the melting point, 170 °C, and the heat generated was 40 $mW \cdot kg^{-1}$ [108].

Deflagration is also a heat driven event, including heat conduction and heat convection. However, unlike thermal decomposition, in deflagration the reaction is restricted to a reaction zone moving throughout the material. The deflagration of a fertilizer may start as a result of localized heating, *e.g.*, with a flame, a burning lamp or friction, and by self-heating [108]. In a fertilizer fire, a slowly propagating self-sustaining exothermic decomposition occurs, which does not take place in all spots in the substance at the same time, but is limited to a reaction zone, which travels slowly

through the whole mass. Heat transfer takes place from the reaction zone to fresh material. The reaction zone can move in any direction, but will go fastest where hot decomposition gases penetrate. But the rate of the reaction zone propagation through the fertilizers is low. No shock wave is involved in deflagration. The reaction zone itself is always subsonic in the materials. Unlike normal burning of a combustible substance, the reaction occurs independent of oxygen from the air or any other outside energy supply [108]. It is worth mentioning that in deflagration, if AN in the reaction zone is dissolved by water, it may stop the heat transfer, thus stopping the deflagration. Based on some experimental results [108], fertilizer may not deflagrate in small mass, but will deflagrate in great masses, because in small-scale tests the heat from the reaction zone will be lost to the surrounding instead of igniting fresh material.

For a deflagration (of a fertilizer fire) that takes place in a confined space, pressure will build-up, leading to two possible outcomes. In the first scenario, considering the reaction happening in a closed vessel, heated gas will result in pressure increase, which in turn will increase heat transfer from the reaction zone to fresh material and increase the burning rate. This will cause the pressure to run up progressively steeply, and the vessel may explode. In the second scenario, if the reaction happens at the bottom of the vessel, in addition to the possibility of the first scenario, hot gas may travel upwards through unburned materials, pre-heating the chemicals that has not yet reacted, and increasing the overall reaction rate even more. The water formed in the reaction will condense on the cold fertilizer that has not yet reacted, thus forming a slurry zone that grows continually in volume.

In *detonation*, the reaction also happens in a reaction zone, but here it usually propagates in one direction, in AN with a velocity of 1.5 to 2.5 $km \cdot s^{-1}$. Detonation is introduced by a shock wave generated by other explosions, high velocity projectile impact or fast accelerating (confined) deflagration of the material. In comparison to powerful high explosives and despite its large energy content, AN reacts relatively slowly compared to the propagation velocity of the shock wave front. Unlike thermal decomposition and deflagration, detonation is driven by energy transfer due to compression. To be specific, the compression energy generated by the shock wave increases temperature almost instantaneously, and initiates and accelerates the explosion. Detonation is explained by the Chapman-Jouguet (CJ) plane theory [128].

Shock waves are associated with detonation. In most cases, shock waves generated in material by an energy burst are non-reactive. However, when the material starts to exothermally decompose because of the shock, the wave is then called reactive. A detonation is a reactive shock in which sufficient energy is released to maintain a steady-state. The super-sonic wave propagation velocity is constant throughout the material and is barely influenced by temperature, initial pressure, or boundary conditions. Figure 55 shows the one-dimensional schematic diagram of a shock wave through a detonation zone. In the shock front, the material is suddenly compressed (either irreversible or non-isentropic). Then the reaction occurs and will run to completion in the reaction zone. Zone 0 is in front of the shock front; zone 1 is the main reaction zone, as a consequence of the compression behind the shock front as well as the high temperature of the substance, which decomposes very rapidly into gaseous reaction

products of high pressure and temperature, where the energy released in the reaction zone is partly used to maintain the shock wave [108]; a detonation wave reaches a steady state with wave velocity, where the CJ plane exists. The higher the energy reaching the shock front from the CJ plane, the higher will be the detonation velocity and pressure. For substances, non-ideal detonations are those which do not release all their energy before or at the CJ plane. AN is a known example of such non-ideal detonation, because the propagation rate of the shock wave as well as the velocity of the reaction zone (detonation rate) in fertilizers is relatively much lower than the detonation rate of high explosives [108]. Hence, detonability and detonation rate are both dependent on the reaction rate and the amount of energy released able to support the shock front.

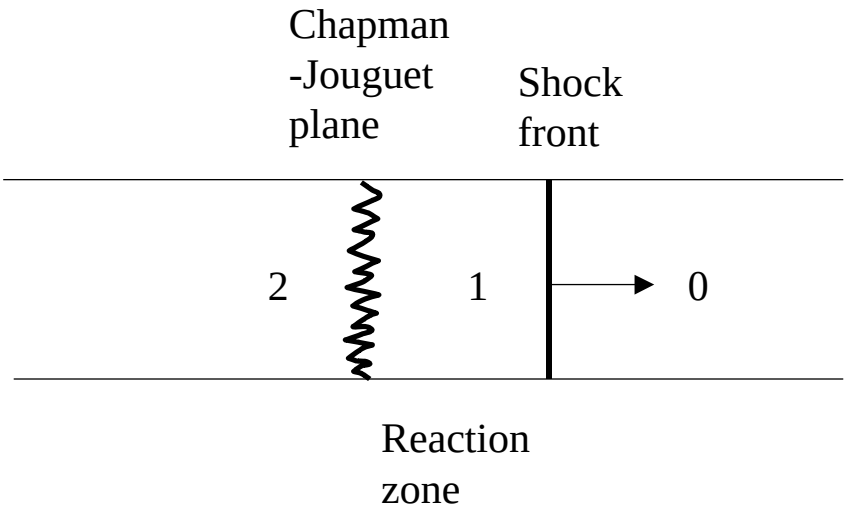

Figure 55. One-dimensional flow model of detonation wave

When AN-based fertilizers detonate, the reaction takes place between the nitrate-ion as an oxidizing agent and the ammonium-ion as a reducing agent. Because the detonation of AN yields mainly H_2O and N_2 and only minor quantities of oxides of nitrogen, pure AN on detonation has a certain surplus in oxygen (positive oxygen balance), as explained in Section 1.5. This surplus in oxygen can be used to oxidize other components, such as ammonium salts and oil [108]. AN-based explosive formulations with fuel oil, ANFO, make use of this increase in energy release. There are generally two types of tests to determine the detonability of fertilizers: denting test and tube test. The latter with a diameter of 2 to 4 inch should be sufficiently long (*e.g.*, 1 meter) so that a steady-state can be observed after a strong shock initiation attempt by a high-explosive booster. The effect in quantitative terms of the confinement by a steel walled tube versus that of an unconfined large diameter pile of AN is still unknown. There is much evidence that fertilizer grade AN failing to detonate in a tube still may do so in a large pile of tens of tons.

AN detonation depends on temperature, confinement, and physical state of the substance [108] (density, porosity, hardness, and size of the grains), which affect the propagation velocity. AN is insensitive to point initiation but sensitive to a relatively weak shock hitting over a considerable large area. This follows from the relatively low reaction velocity and the limited amount of decomposition energy contributing to the shock wave energy. A strong spherically divergent wave will fade, as a rapidly increasing front area has to be supported. Crystal defects, porosity in solid AN, probably gas bubbles in molten AN, and additional fuel sensitize it for shock initiation. As

Babrauskas [117] summarizes there is evidence from various sources that temperature increase enhances the sensitivity of AN to shock, first above 140 °C in solid AN and then further in molten AN. A graph presenting the results of King [129], reproduced here in Figure 56, is most convincing. Elsewhere has been observed that the melt can even become so sensitive that a compression wave from a falling object into the melt can set it off.

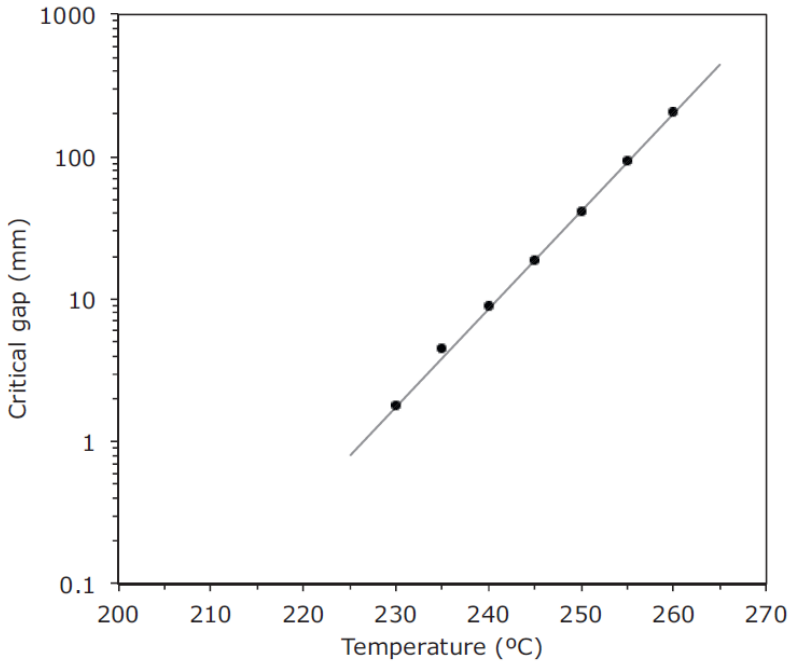

Figure 56. Results of a card gap test to measure the sensitivity of initiating detonation in molten AN as a function of temperature. The test consists of creating with Plexiglass (PMMA) wafers a gap between a booster charge and the sample. The wider the gap the more sensitive the sample. The figure is reproduced from [117]; the work has been performed by King [129]

As mentioned regarding initiation of detonation of AN and mixtures in a fire no clear mechanism or mechanisms are available. Somewhere, though, a compression wave has to be generated. Once a compression wave is created by a local, possibly weak compression or explosion, while running, the wave will result in a shock wave by a gas-dynamic steepening up process. In high explosives the usual mechanism of deflagration to detonation transition is due to hot gas igniting grains it passes, increasing pressure, accelerating energy release generating compression waves, followed by shock formation and detonation. For AN this mechanism may contribute but in a fire a pool of molten AN will exist, not easily permeable for gas. But in a hot reacting mass the wave may continually be amplified by energy released.

Alternatively, it needs to be pointed out that the energy transferred by shock wave from one medium to another depends on density ratio of the media, or rather on the ratio of the products of density and sound velocity (acoustic impedances). When a shock wave travels in air, once it reaches a solid wall or a liquid surface, it will reflect back in air. Little of the shock wave energy will be transferred to the condensed material. Now, hot molten AN is foaming. Hence, although speculative it can be imagined that also an initial local gas explosion (N_2O and NH_3) in the produced gases generates a compression wave working itself up through the decomposing exploding foam to gradually higher density material and finally to detonation which can be transferred to solid AN. As all of this is even more likely at elevated pressure, we shall see in the following how fire water by steam formation can worsen the situation.

Confinement reinforces the conditions for detonation. One can see that when comparing a tube test failure result with the detonation of a self-confining pile as mentioned before. Self-confinement of decomposition at the bottom of a pool of molten AN has been suspected as a possible initiation mechanism. The effect is of course related to easier pressure build-up and lesser energy loss. Evidence that self-confinement is important in "onset" of AN detonation when in a fire, follows already from the fact that it did not succeed to reproduce in tests obtaining a detonation in a fire: quantities applied may be too small or self-confinement conditions, *e.g.*, a pool in a ground recess, not present.

6.3 The Complexities of Fighting AN Storage Area Fires

To extinguish a fire, methods used are shutting off oxygen supply by, *e.g.*, massive use of carbon dioxide or a sand cover, stopping the oxidation reactions in the flame by radical inhibiting agents, such as halogenated hydrocarbons, or cooling with sufficient quantities of water. Because of availability and cost the latter is used by far most of the time. For the following, distinction shall be made between preventing a fire in an AN storage area by non-combustible construction materials or stopping a starting fire externally of the AN proper by a sprinkler system, and the extinguishing of a fire that has already reached the AN itself.

Water is the right chemical to use in terms of regular AN-related fires because AN is an oxidizer, and smoothing agents will have no effect, such as steam, foam, dry

chemicals, sand, or inert gases [130]. However, special care should be taken when attacking an AN fire. According to Lees' Book [79], the use of water sprinklers, fog nozzles, and foam or dry powder extinguishers are ineffective to attack once an AN fire is going. This section will discuss the effect of water on AN fires.

6.3.1 Regulations on the Use of Sprinklers in Connection with AN Storage

The use of sprinkler systems has been regulated and recommended by federal agencies and other agencies, such as OSHA and NFPA.

One of the lessons learned and recommendations from previous incidents [131] indicates: "*AN should be stored in fireproof sprinklered buildings on skids or pallets on concrete floors with at least one foot clearance from walls.*"

OSHA "Explosives and Blasting Agents" (29 C.F.R. §1910.109) has the following requirements for sprinkler systems in AN storage [84]: *"1910.109(i)(3)(ii)(c): The height of piles shall not exceed 20 feet. The width of piles shall not exceed 20 feet and the length 50 feet except that where the building is of noncombustible construction or is protected by automatic sprinklers the length of piles shall not be limited"*; according to 1910.109(i)(7)(i), *"Not more than 2,500 tons (2270 tonnes) of bagged ammonium nitrate shall be stored in a building or structure not equipped with an automatic sprinkler system. Sprinkler systems shall be of the approved type and installed in accordance with 1910.159"* [84].

NFPA 490 [132] and the more recent NFPA 400 [118] provide the recommendation to keep the AN mass cool and to extinguish the fire promptly by applying quickly large volumes of water, and if the fire reaches uncontrollable proportions, the area should be evacuated. NFPA 400 "Hazardous Material Code" [118] addresses the importance of sprinkler systems in AN storage: "*An automatic fire sprinkler system shall be provided… Not more than 2500 tons (2268 metric tons) of bagged ammonium nitrate shall be stored in a building or structure not equipped with an automatic sprinkler system. When approved by the Authority Having Jurisdiction (AHJ), a quantity of bagged ammonium nitrate greater than 2500 tons (2268 metric tons) equipped with an automatic sprinkler system… Sprinkler protection shall be permitted to be required by the AHJ for the storage of less than 2500 tons of ammonium nitrate where the location of the building or the presence of other stored materials can present a special hazard… Sprinkler systems shall be of the approved type and designed and installed in accordance with NFPA 13, Standard for the Installation of Sprinkler Systems… Piles shall comply with the following dimensions: (1) The height of piles shall not exceed 20 ft (6.1 m); (2) The width of piles shall not exceed 20 ft (6.1 m); (3) The length of piles shall not exceed 50 ft (15.2 m), unless otherwise permitted by 11.3.2.2.3(4); (4) Where the building is of noncombustible construction, or is protected by automatic sprinklers, the length of piles shall not be limited*" [118].

The Emergency Response Guidebook (ERG) [133] considers AN as an oxidizer and referenced in the guide 140, and suggests to tackle large fire areas with water from distance and recommends considering initial evacuation of 800 m in the case of AN fire.

NFPA 472 [134] and OSHA 1910.120 HAZWOPER [135] are standards for firefighter training in hazardous material incidents. These standards address hazardous materials in a broad way and are mainly intended to provide the firefighters initial emergency actions, like identifying the material and keeping the public away from the event (defensive action) or mitigating the material by eliminating the leak/source/fire (offensive action). The standards also include a higher level of responder knowledge called specialist that would require additional training on more specific containers or chemicals. But the additional training will depend on the funding and the availability of the firefighters [136].

6.3.2 Tackling a Real AN Fire with Water

If a fire in a storage area reaches the stored AN, an AN fire scenario develops. It means melting and decomposing AN with heat release, gas production and nitric acid formation will accelerate decomposition. If there is not a sufficient amount of water to mitigate the fire, cool down the mass drastically and dissolve and dilute AN, water will evaporate leaving possibly sensitive crystals while steam will increase the pressure locally. All hazardous properties intensify with pressure. So, it will be required to really quickly cool and dilute a liquid pool of molten AN to bring it outside hazardous condition. Such operation will be hampered by still solid AN, which by its hygroscopicity absorbs water strongly.

A procedure is needed to calculate the amount of water needed to put out fires involving AN. A threshold should be identified to know how much water might increase the AN hazards, and how much water would be enough to tackle the fire without increasing its explosion potentials. This is of critical importance to guide the firefighters responding to fires involving AN. In AN incidents involving fires, which often lead to explosions, if water is used to mitigate the fire, care should be taken to use ample quantities of water to tackle the fire [137]. In terms of AN fire and explosion, small amounts of water help mitigate deflagration, but not thermal decomposition or detonation.

In the case of the West fertilizer plant explosion, the fire was beyond the extinguishment stage, with limited resources and inadequate water supply [138]. If water is far from enough, the following factors are to be considered: First, the AN would not be heated uniformly, and some parts could be heated up faster than the rest. Second, the water applied may not be able to be absorbed by the particular part it has been meant for due to the relative position of the heated part and water spray. Third, water loss by leaks in the firefighting process should be considered. Leakage water may reach AN. Last but not least, if water on hot AN boils off, a large amount of steam will be produced, increasing pressure, which as already mentioned is quite dangerous to AN. The amount of water necessary to cool down the AN, considering the quantity (270 tons) reported in the Tier II report [139], would have been huge. Theoretically, the amount of water required to control the fire would be larger than the total daily water demand of the entire city of West, Texas. A typical continuous water supply is between 2,000 and

10,000 gpm (gallon per minute) for 4 hours [126]. The annual water demand for West, TX in 2010 was 459 acre-foot which corresponds to an average of the daily water consumption of 409,768 gallons of water [140]. In addition, this capacity was reduced as two wells supplying water were out of service that day, leaving the available water from a pump station of 167,000 gallons and an above-ground water tower of 150,000 gallons [138]. To prevent AN fires and explosions, AN should be maintained at low temperatures (at least below the "onset" temperature, 200 °C). At 200 °C, the decomposition reaction would still take place, but very slowly. Considering an AN mass of 270 tons [139], a heat capacity of 1.7 $kJ \cdot kg^{-1} \cdot K^{-1}$ [141]; and the heat capacity of water is 4.2 $kJ \cdot kg^{-1} \cdot K^{-1}$ [141]. To give a conservative rough estimation, if AN is to be cooled down (by water) from 200 °C to 20 °C, while water is heated up (by AN) by 20 °C, by comparing the heat capacity of both materials, the amount of water required would be approximately 260,000 gallons, which is close to the daily water supply in West on that day. Even with an adequate water supply, it is uncertain whether firefighters had enough time to extinguish the fire before the AN exploded, because the explosion occurred 21 minutes after the fire was reported. Therefore, although large amounts of water will mitigate AN fires, the use of insufficient amounts of water may increase the risk and this needs more attention and research.

There are other factors that make it difficult to tackle AN fire with water. In a fertilizer fire scenario, the hot gaseous reaction products are danger factors by igniting and causing fire of wooden constructions. It can also be hard to fight a fertilizer fire, because in many cases, the reaction zone is deep within the mass and cannot be reached

due to the strong gas evolution. Plus, it could be difficult to locate the fire core due to the generation of smoke [108].

6.3.3 Water Contamination with AN

AN is very hygroscopic by nature [142], and it readily absorbs water vapor from the atmosphere and forms aggregates with high mechanical resistance. In some cases, water vapor causes partial dissolution of powder which can lead to caking [90], self-compression, and self-confinement. According to Health and Safety Executive (HSE) [137], AN should be kept away from water contamination to prevent caking, which can increase the AN detonation potentials. For this reason, AN loading under raining and snowing conditions is not recommended. The humidity level that can aggravate AN detonation has not been identified in literature and needs to be further studied. The deliquescence relative humidity (DRH) of AN at 298 K has been discussed in literature [143], reported to be between 61.5% and 62%. The efflorescence relative humidity (ERH) values for AN/water particles has been reported to be 25-32% RH [143]. A thermodynamic extrapolation method to predict the temperature and relative humidity variation of the AN dissociation constant has been developed [144].

If water vapor is formed in fire scenarios, due to the high solubility of AN in the hot condensed water, a slurry may be formed with a portion of the AN that has not yet reacted. This may create some problems including caking as described in the previous paragraph. Another example of the slurry is that in a sea-going vessel loaded with AN in

bulk, it may reduce the stability of the vessel, thus, the vessel may capsize under unfavorable conditions [108].

6.3.4 The Use of Water in AN Fires under Confinement

The effect of water is even worse for AN storage in a confined space, such as a warehouse storage. Confinement plays an important role in an AN explosion, and was believed to help trigger the explosion in the Port Neal AN plant incident [81]. Steam at 200 psig (1.5 MPa) was first applied to the AN product line on the suction side of the product pumps of the incident, which remained applied until the time of the explosion, producing confinement and triggered the incident. The reaction then became exothermic and self-sustaining, and large volumes of gases were formed. The effect of the rapidly expanding gas resulted in adiabatic compression of the bubbles in the AN solution which resulted in a more rapidly expanding wave front for deflagration propagation [44]. The European Fertilizer Manufacturers Association's **(**EFMA) guidance document [145] states that AN has high resistance to detonation; however, heating under strong confinement can lead to explosive behavior [82]. According to NFPA 49, if AN is subjected to strong shocks or heat under confinement causing a pressure build-up, it may undergo detonation [83].

In Section 4 and Section 5, the RSST has been used to study the decomposition of AN under various conditions [66]. It is concluded that with increasing initial pressure, the "onset" temperature decreased slightly, and the maximum pressure-rise rate

increased dramatically; “onset” pressure, pressure at maximum pressure-rise rate, final pressure, and the pressure after cooling down were all higher; and there was more gas generated as the initial pressure increased. It has also been pointed out that higher degree of confinement results in greater possibility of deflagration/detonation [44], and the rate of propagation for deflagration of the reaction zone increases with elevated pressure [108]. If the AN is sufficiently sensitized and the threshold temperature for thermal decomposition is reached, the mass of the AN may create sufficient pressure build-up [146]. As a conclusion, pressure accumulation is hazardous to AN and it is important to keep a low-pressure environment for AN storage and transportation. More work needs to be done on determining to what extent confinement will affect AN decomposition, especially when water will be applied. For example, if a certain amount of AN is stored in a warehouse, how much space must be left within the warehouse to make sure the degree of confinement in the warehouse will not result in catastrophic explosions in case extinguishing water is applied in an AN fire.

Water may also flood AN into drains where confinement does exist, thus, the hazards and risks of AN would be increased.

6.3.5 Steam Formation Leading to Pressure Rise

Pure AN will start decomposing endothermically if its temperature exceeds 170 °C, and after that exothermic reactions will take place, as described previously in Section 1.5. During this period, explosive reactions may be triggered. In these temperature

ranges, water will evaporate, generating rapidly a huge amount of steam, which will result in rapid pressure build-up at the bottom of AN piles, especially in a confined space.

For example, according to saturated steam tables a volume of 1 m^3 contains 10 kg steam of about 20 bar at (210+273 =) 483 K. Hence, it means that the volume expansion is 100 times. At a heat of vaporization of 44 $MJ \cdot kmol^{-1}$, a mol. weight of 18 $kg \cdot kmol^{-1}$, and a specific heat at constant volume of 1.46 $kJ \cdot kg^{-1} \cdot K^{-1}$, 10 kg water would need about 26 MJ to reach that condition.

At decomposition 1 kg of AN will produce by its hot products 1 m^3 gas, while the heat generated is 2,620 $kJ \cdot kg^{-1}$ [147]; the mean specific heat of the gases at constant volume will be about 1 $kJ \cdot kg^{-1} \cdot K^{-1}$. It means that when 10 kg AN is decomposed in a volume of 1 m^3 at an initial pressure of 1 bar at ambient temperature, the pressure will reach 10 bar, but due to the temperature increase by 2,620 K, pressure will rise to a maximum (adiabatically) of $10 \cdot (2620+273)/273 \approx 105$ bar. It also means that this amount would just produce the heat of 26 MJ to heat the water to steam of 20 bar, given it will not have to heat its own reaction products to 105 bar. Although in an open containment gases will vent quickly, the calculation gives an estimate of pressures that can exist locally, even though on a temporary basis.

For comparison reasons, it is interesting to see the size of an AN pile which could create the same pressure of 20 bar. At a density of grained AN of 1,500 $kg \cdot m^{-3}$ the height of AN pile will have to reach a height of $2000/(1.5 \times 9.81) = 135$ m.

The calculated pile height is impressive. Therefore, if water is present in an AN storage area and evaporates at the bottom, the pressure of an AN pile will be even higher as venting is obstructed, which favors the conditions of AN explosion.

In general, the use of small amounts of water is prejudicial for an AN fire or explosion. In this case, most of the water will vaporize. Therefore, again, when attacking an AN fire, a large quantity of water to flood the fire should be used. Hence, the presence of insufficient water at elevated temperature increases AN fire and explosion risks, because of the increased pressure generated by water evaporation [79].

6.3.6 The Use of Water in AN Fires with Contamination

The effect of water is also dangerous because of contamination and catalysis. When a storage area is involved in a fire, water may interact with various kinds of materials, react with them or dissolve them. This can promote AN decomposition with the contamination, *e.g.*, chlorides acting as catalyst. Ettouney *et al.* [80] showed that by various metal oxide catalyzing and increasing acidity and temperature, AN in solution with a concentration of 95% can still explode.

Presles *et al.* reported that moistened AN and sodium dichloroisocyanurate (DClCNa) mixture could produce NCl_3, a highly unstable explosive product, leading to the detonation of the mixture in the applied lab-scale [72], so that a pile of AN-DClCNa mixture with its bottom part locally moistened will become very sensitive and dangerous. In their experiment, AN-DClCNa mixture was first poured into a vertical

tube, then a small amount of water was injected in the mixture at 1 cm from the bottom of the tube with a needle through the tube wall or through the bottom plate closing the tube. It was observed that as soon as water is injected, exothermic chemical reactions start, as was evidenced both by camera records and thermocouple measurements.

6.4 Conclusions and Recommendations

The development of sprinkler systems has been improving throughout history to meet the needs for fire protection of various types of industries as well as residential areas. Sprinklers have been proven to be successful in a large number of situations. The sprinklers in a storage area help to keep the fire risk down due to combustible construction materials (which in direct contact should not be there). However, the effectiveness of sprinkler systems on certain kind of chemicals, such as AN, has not been clearly studied and proven. Sprinkler will certainly be useful outside the AN bins properly, but not for fighting a fire of AN itself. If AN is not heavily contaminated, the risk of self-ignition is very remote. To start an AN fire, material in contact with it or located close to it must be on fire, or some kind of heat source within the AN pile to bring the material to its melting point or higher. This will act as a trigger, or at lower temperature a combination of a heat source and a contamination will induce ignition.

The theory of AN explosion phenomenology has been discussed and ways how a local decomposition can work itself up to a detonation proposed. Insufficient amount of water may lead to AN contamination, resulting in caking or slurry; when water

evaporates, pressure will increase, as well as the degree of (self-)confinement; what's more, water may act as catalyst by carrying contaminations catalyzing AN decomposition, promoting the degree of risks. More research efforts are needed in studying the conditions that would trigger AN fires and explosions, especially the behavior of water and humidity on AN when in a confined space.

Attention should be paid in tackling AN-related fires with insufficient amounts of water. Sprinkler systems in AN stores should be carefully designed. AN may be cooled but not wetted. "Fire", *i.e.*, fast decomposition of a mass of AN in, *e.g.*, a bin or a pool can only be extinguished safely by drenching it with large amounts of water, which seems not easily achievable in practice. Where exactly the thresholds are would be a matter of further research. So, we are left with the dilemma: water is the only agent to fight a fire in an AN store, but too small amounts may exacerbate the conditions for a usually catastrophic explosion instead of attenuation, and we do not have a grasp on what is considered as small.

7. CONCLUSIONS AND FUTURE WORK

This section summarizes the main findings of the work presented in this dissertation (Section 7.1) and it outlines the opportunities to continue this work (Section 7.2).

7.1 Conclusions

This dissertation involved calorimetry and analytical work for the investigation of ammonium nitrate (AN) decomposition, a commonly used fertilizer, which paved the way toward inherently safer storage conditions for AN. From a safety perspective, AN is not considered a flammable or combustible material at ambient temperatures; however, it is a strong oxidizing agent that can detonate under certain conditions. AN is associated with several types of hazards including fire and explosion, which have occurred time and again in the past century.

This research advanced the understanding of the root causes associated with AN explosions, and identified ways to make the AN storage inherently safer. This work focused on the condition-dependent AN decomposition, including the effect of additives, confinement, heating rate, thermal history, heating temperature, and sample size. Pseudo-adiabatic calorimetry (RSST) and adiabatic calorimetry (APTAC) were used to study the characteristics of AN decomposition. Thermodynamic and kinetic parameters were evaluated; models were proposed to predict the adiabatic temperature rise of AN

mixtures with two additives; decomposition pathways were analyzed; safer conditions for AN storage were identified; and AN hazards and explosion phenomenology were reported. In addition, this research discussed the role of water as a chemical, interfering physically and chemically with AN-related fire scenarios possibly leading to explosion.

The topics covered in this work involved:

1) The evaluation of the thermal stability of pure AN using adiabatic calorimetry, to determine its runaway behavior and parameters associated with its decomposition, which provided a better understanding of the hazards of AN.

2) The identification of inhibitors and promoters for the study of additives through various experiments, including the study of single additive and the mixture of two additives.

3) The calculation of the thermodynamic and kinetic parameters of the AN decompositions both individually and with additives, and the identification of the key parameters, such as the “onset” temperature and maximum self-heating rate. Further, this work proposed mathematical models to predict the results of certain additives.

4) The analysis of the mechanisms of decomposition associated with AN for both pure AN and AN mixture with additives. Thus, the decompositions were explained from a fundamental point of view.

5) The study of the condition-dependent thermal decomposition of AN, including the effect of additives, initial pressure, heating rate, temperature, thermal history, sample size, and isothermal testing. Further, the safe conditions for AN storage and transportation was determined.

6) The correction of the experimental results based on thermal inertia factor and analyzed the corrected values. Therefore the errors introduced by the test cells of the calorimetry were eliminated and more accurate results were obtained.

7) The explanation of the AN explosion phenomenology and the discussion of the complexities of fighting AN storage area fires. It contributed to the better understanding of how AN fires propagate to deflagration or detonation, and raised the issue of tackling AN fires with inadequate amount of water.

The main conclusions of this dissertation are summarized here.

Thermal stability analyses showed that AN in pure solid form is stable up to approximately 200 °C in the RSST and 220 °C in the APTAC. The decomposition behavior of AN is similar to the results reported in literature using DSC. The presence of additives influences the "onset" temperature, the rate of decomposition, and the maximum temperature and pressure developed during AN decomposition.

The RSST and the APTAC were first used to study the effects of two additives, sodium sulfate and potassium chloride, and the mixture of sodium sulfate and potassium chloride, with different concentrations of the additives. Sodium sulfate is a good inhibitor for AN in that the addition of sodium sulfate can hugely mitigate AN decomposition, while potassium chloride is a promoter for AN because it intensifies the runaway reaction. To be specific, in the RSST, when AN is mixed with Na_2SO_4, it helps mitigate AN decomposition by increasing the "onset" temperature and temperature at maximum self-heating rate, decreasing the heat of reaction, and increasing the activation energy. For example, the "onset" temperature is 268 (±1) °C when AN is mixed with

12.5 wt.% of sodium sulfate, which is higher than that of pure AN, 200 (±10) °C. However, when AN is mixed with KCl, it acts as a promoter as it decreases the "onset" temperature and temperature at maximum self-heating rate, increases the maximum rate of temperature rise as well as the maximum rate of pressure-rise, and increases the heat of reaction, thus, making AN decomposition start earlier and generate heat faster. For example, the "onset" temperature is 152 (±9) °C when AN is mixed with 12.5 wt.% of potassium chloride.

When sodium sulfate and potassium chloride are mixed together with AN, the "onset" temperature is increased, inhibiting the decomposition; however, the maximum self-heating rate and pressure-rise rate are also increased, and the severity of decomposition increases. The mitigating effect of SO_4^{2-} on AN is likely to counteract the promoting effect of Cl^-. Different researchers proposed decomposition mechanisms to explain the behavior of the mixture when the two additives are added to AN. Models were proposed to predict the adiabatic temperate rise and the difference between the temperature at maximum self-heating rate and the "onset" temperature, for sodium sulfate and potassium chloride as additive both together and separately, which agree well with experimental data. It is evident that to avoid AN explosion potentials, AN should be separately stored from promoters, even when inhibitors are also present.

Later on, the RSST and the APTAC was used to study the runaway behavior of AN under various conditions, such as in the presence of other additives with different concentrations, including water, sodium bicarbonate, potassium carbonate, ammonium sulfate, barium nitrate, sodium nitrate, and ferric sulfate (or iron(III) sulfate, FS,

$Fe_2(SO_4)_3$). Inhibitors and promoters were identified. In the case of inhibitors, the "onset" temperature and temperature at maximum self-heating rate increase; whereas in the presence of promoters, these temperatures will decrease. Typically, the maximum temperature and pressure rise rate for promoted reactions are larger than that for inhibited reactions. The temperature difference, between maximum rate of temperature-rise and pressure-rise, for promoted reactions are larger than that for inhibited reactions. The more inhibitor in the mixture, the more the inhibiting effect. However, promoters have the opposite effects. The results show the same trends as the ones reported in literature. If AN could be stored with (or near to) inhibitors, or there is enough water, an AN explosion could be mitigated to a certain extent.

The effect of confinement was tested by observing AN decomposition under various overhead initial pressures in the RSST and the APTAC, varying from ambient pressure to 200 psia (1.4 MPa). The results were corrected based on the thermal inertia factor. With increasing initial pressure, the "onset" temperature and activation energy decreased slightly, and the maximum pressure-rise rate increased dramatically; P_o, P_{max}, P_f, and P_c were all higher, and there was more gas generated as $P_{initial}$ increased. As a conclusion, pressure accumulation is hazardous to AN and it is important to keep a low-pressure environment for AN storage and transportation.

AN decomposition is also affected by heating rate, and the effect of heating rate was studied using the RSST and the APTAC by heating up AN under different heating rates. As a conclusion, when the heating rate is faster or the HWS starts at slightly higher temperatures, the self-heating rate and the pressure-rise rate increase faster, the

activation energy is decreased, and the reaction occurs more violently. Therefore, if AN is suddenly heated up, the decomposition is more likely to occur.

For the effect of temperatures, it can be concluded that when HWS starts at around AN melting temperature, *i.e.*, 160 °C, 170 °C, and 180 °C, the decomposition of AN is more hazardous to AN. For example, the maximum self-heating rate was higher than that of other starting temperatures, and occurred at higher temperatures than other experiments. When the starting temperatures are under 160 °C, the reaction is more violent when the HWS starts at higher temperatures, the self-heating rate and the pressure-rise rate increase faster and the reaction occurs more violently.

The pre-heated AN increased the "onset" temperatures and temperatures at maximum self-heating rate of AN. Using the pre-treatment method presented in this work, the "onset" temperature of AN thermal decomposition was increased by approximately 50 °C compared with that of pure AN.

The experiments of different sample sizes show that the decomposition of AN would be mitigated with inert material. And of course, with smaller amount of sample size, the decomposition is less violent. Therefore, the size of AN piles should be limited.

In case of AN fires, the effectiveness of sprinkler systems has not been clearly studied and proven in literature. Sprinklers will certainly be useful outside the AN bins properly, but not for fighting a fire of AN itself. While it is clear that water remains the choice for tackling AN-related fires, it must be understood that a significantly sufficient quantity of water should be used to fight these fires. In fact, there is evidence to believe that insufficient quantities of water may exacerbate the fires and consequences. If AN is

not heavily contaminated, the risk of self-ignition is very remote. To start an AN fire, material in contact with it or located close to it must be on fire, or some kind of heat source within the AN pile to bring the material to its melting point or higher. This will act as a trigger, or at lower temperatures a combination of a heat source and contamination will induce ignition.

The theory of AN explosion phenomenology has been discussed and ways how a local decomposition can work itself up to a detonation proposed. Insufficient amount of water may lead to AN contamination, resulting in caking or slurry; when water evaporates, pressure will increase, as well as the degree of (self-)confinement; what's more, water may act as catalyst by carrying contaminations catalyzing AN decomposition. More research efforts are needed in studying the conditions that would trigger AN fires and explosions, especially the behavior of water and humidity on AN when in a confined space. Attention should be paid to tackling AN-related fires with insufficient amounts of water. Sprinkler systems in AN stores should be carefully designed. Where exactly the thresholds are would be a matter of further research.

Overall, this dissertation provides sufficient information to select inhibitors that make AN safer as a fertilizer, and it also represents a step forward toward safer conditions for AN transportation and storage. This work demonstrates the complexity and the multiple studies required for making AN safer as a fertilizer. It serves as a foundation to further the understanding of AN. In addition, the data, techniques, approaches utilized in this dissertation illustrate a methodology for the study of the reactive chemicals of interest.

7.2 Future Work

This section summarizes the opportunities to continue the study of AN thermal stability. It also provides recommendations for future work, based on the challenges faced during this study.

7.2.1 Recommendations on Experimental Conditions

Before moving to the future work, the major recommendations of this work are presented here.

In the APTAC, the sample size should be ideally large for accurate measurement; however, due to the properties of AN, large sample sizes were not applicable in that it may damage the equipment. Therefore, AN was mixed with sand to reduce its explosivity. But the mixture could result in other concerns, like the results were not for pure AN and the repeatability of solid mixtures. So when testing AN using the APTAC in the future, other solvents could be adopted to increase the sample size and solve the problem caused by sand. But the dilemma is that AN is usually used in its solid forms as fertilizers, solvent may not represent the situation of solid sample. Alternatively, other calorimetry such the RSST and the DSC could be a better choice.

In each of the experiments, the characteristics of the sample before the experiments and residues after the experiments could be observed using equipment such as X-ray powder diffraction (XRD).

The isothermal experiments of AN decomposition in this work reported in Section 5.7 could be further studied to understand its behavior observed in this dissertation, thus, to identify the induction period and associated hazards of AN in storage.

The effect of water on AN should also be further studied in order to identify the hazards and risks of fighting AN-related fires with insufficient quantities of water.

In terms of the systematic study of the safe storage conditions for AN as fertilizers, process design could be employed. First, the risks associated with AN-related fires and explosions could be analyzed; then, the identified conditions should be studied in details to provide better storage areas for AN.

7.2.2 Molecular Simulation

Molecular simulation using Gaussian software could be conducted to understand AN and its interaction with additives, as well as at different conditions, from a more fundamental point of view. Gaussian software could be used to analyze the behavior of one or a few molecules. This software has been used to study AN [148, 149], using density-functional theory. As its name implies, ammonium nitrate (AN) can be viewed as an ionic solid made up of ammonium cations (NH_4^+) and nitrate anions (NO_3^-), as shown in Figure 57. To be more efficient, the study of AN could be related to other similar chemicals (*e.g.*, hydroxylamine [150, 151], with both experimental data and simulation data available). At first, a small quantity needs to be studied and then

correlations can be proposed to extrapolate its properties to larger quantities. The effect of temperature, concentration, and effect of impurities could also be studied from the fundamental level.

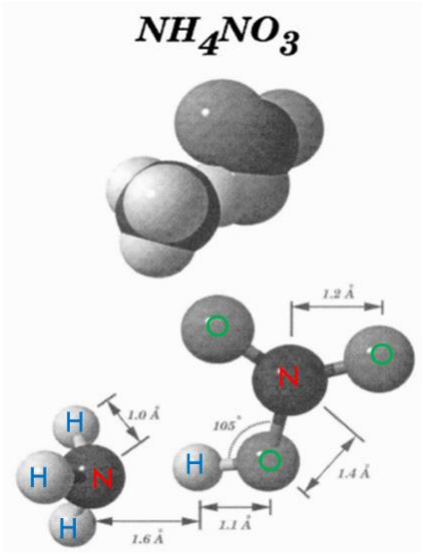

Figure 57. Optimized structure of AN molecule. The figure is reproduced from [149]

7.2.3 Effect of Additives

More additives apart from what were studied in this dissertation could be studied following the same approach to gain a more thorough understanding of AN in the presence of additives. It is important to understand their mechanism and further explore their properties for mitigation of explosion potentials of AN. Different concentrations of AN mixture with additives could be studied in calorimeters, such as the DSC, RSST, and

APTAC. The pH value of the mixtures should also be studied. The data should be compared with the results from other calorimetry reported in literature.

For example, the RSST could be used to study 3.5 g of AN mixed with 0.1 g and 0.5 g of additive. The results of the additives can be used to construct a matrix as in Table 29, where some of the additives were already studied in this dissertation (marked in Table 29) and the rest (blank cells) could be tested in the future. The experimental results, such as the "onset" temperature, could be filled in the matrix, and then the mechanisms of AN decomposition with different anions/cations could be systematically analyzed. Some of the additives that could be studied are potassium sulfate, calcium sulfate, potassium dihydrogen phosphate, sodium carbonate, ammonium carbonate, urea, and iron sulfate.

Table 29. The matrix to study the additives for AN

Anions / Cations	NO_3^-	SO_4^{2-}	Cl^-	HCO_3^-	CO_3^{2-}
NH_4^+		inhibitor			
Na^+	inhibitor	inhibitor		inhibitor	
K^+			promoter		inhibitor
Ba^{2+}	inhibitor				
Fe^{3+}		promoter			
Ca^{2+}					

The effects of organic chemicals, acid, and chloride should be further studied to understand how and why they make AN decomposition more severe.

While testing the effect of additives, it is important to measure the particle size of both AN and the additives. Because particles with different sizes could result in various characteristics in the decomposition of AN.

In addition, the AN mixtures with the additives should be applied to plants and test their agricultural benefits as fertilizers.

7.2.4 Effect of Humidity and Surrounding Gas Atmosphere

The study of the effect of humidity will help improve the understanding of fighting AN fires with water. To study the effect of humidity, test samples could be placed in a humid environment for a certain time period. The pre-treatment time may vary between a few hours and a few days. The relative humidity should be varied from 0% to 100%. The results obtained from these experiments could help make recommendations on suitable storage conditions for AN.

The effect of gas atmosphere is another important topic to study. In storage areas, the gas atmosphere might influence AN behavior. Different gases can be used as initial overhead pad gas. For the reasons explained in Section 1.6, O_2, NH_3, N_2, Ar, He, and CO_2 rich atmosphere could be tested. During the experiment, gases should be purged through the reaction mixture in the RSST or the APTAC and then pressurized.

7.2.5 Design of Experiments

Factorial design could be adopted to identify the key factors that affect AN decomposition. Then the selected dominant factors that affect AN decomposition could be further investigated.

Several factors would contribute to the thermal decomposition of AN, including the type of additives, the concentration of additives, confinement caused by pressures, humidity level, heating rate, and gas atmosphere. It is important to use Design of Experiments [152] methods to systematically study those factors. Fractional factorial designs [152] could be employed. Fractional factorial design means that the experimental runs are a subset of the full factorial design [152]. The subset is chosen to test the most important parameters of the system, which uses only a fraction of the effort of a full factorial design. After identifying the important parameters, recommendations and suggestions on safely handling and storing AN could be proposed. Inherently safer design could be proposed to help mitigate AN explosion potentials.

7.2.6 Scale-up Design

In runaway reactions, the hazard does not always vary linearly with the amount of reactant. Therefore, it is important to determine if the reaction follows a trend upon scale-up. To determine the effect of an amount of sample on the thermal decomposition of AN, in the first stage, molecular simulation could be used to study a small quantity of

AN, usually the behavior of several molecules. Then different kinds of calorimeters, such as APTAC and RSST, should be used to study a few grams of AN. Tests for samples with larger amounts could be conducted based on cube tests, hot plate tests, or large-scale detonation tests. After that, a scale-up methodology could be proposed to predict larger-scale AN decomposition behaviors.

Summarizing the data from molecular modeling, calorimetry, and various sample size tests, a scale-up procedure could be proposed to establish a systematic method of predicting the behavior of AN in large-scale from small-scale data analysis of modeling. It not only brings improvements in the safety and the efficiency of AN study, but also results in a reduction of time and resources.

REFERENCES

1. Texas, *Texas City, Texas, Disaster, April 16, 17, 1947*. 1947, Fire Prevention and Engineering Bureau of Texas, Dallas, Texas; The National Board of Fire Underwriters, New York, New York.: http://www.local1259iaff.org/report.htm.

2. Marlair, G. and Kordek, M.-A., *Safety and security issues relating to low capacity storage of AN-based fertilizers.* Journal of Hazardous Materials, 2005. **123**(1–3): p. 13-28.

3. HSE, *Storing and handling ammonnium nitrate*. 1996: http://www.hse.gov.uk/pubns/indg230.pdf.

4. EPA, *Explosion hazard from ammonium nitrate*. 1997, Chemical Emergency Preparedness and Prevention Office: http://www.epa.gov/osweroe1/docs/chem/ammonitr.pdf.

5. Patnaik, P., *Handbook of inorganic chemicals*. 2002: McGraw-Hill.

6. Zygmunt, B. and Buczkowski, D., *Influence of ammonium nitrate prills' properties on detonation velocity of ANFO.* Propellants, Explosives, Pyrotechnics, 2007. **32**(5): p. 411-414.

7. EPA, *Request For Information: Accidental release prevention requirements: risk management programs under the Clean Air Act, Section 112 (r)(7)*, in *40 CFR Part 68*. 2014, Environmental Protection Agency. 40 CFR Part 68.: Federal Register - The daily journal of the United States Government.

8. FactFish, *Ammonium nitrate, consumption (tonnes) - for all countries*. Fact Fish: http://www.factfish.com/statistic/ammonium%20nitrate%2C%20consumption.

9. Feick, G. and Hainer, R.M., *On the thermal decomposition of ammonium nitrate. Steady-state reaction temperatures and reaction rate.* Journal of the American Chemical Society, 1954. **76**(22): p. 5860-5863.

10. Martorell, S., Soares, C.G., and Barnett, J. *Safety, Reliability and Risk Analysis: Theory, Methods, and Application. Volume 1*. in *European safety and reliability conference. ESREL 2008, and 17th SRA-EUROPE.* September, 22-25, 2008. Valencia, Spain: 2009 Taylor & Francis Group.

11. *Arizona master gardener manual. Ch. 1 Environmental factors that affect plant growth*. Cooperative Extension, College of Agriculture, The University of

Arizona: http://ag.arizona.edu/pubs/garden/mg/botany/water.html#nutrition p. 34 - 38.

12. *Plant analysis handbook - Nutrient content of plant*. Agricultural & Environmental Services Laboratories: http://aesl.ces.uga.edu/publications/plant/Nutrient.asp.

13. Stewart, W.M., Dibb, D.W., Johnston, A.E., and Smyth, T.J., *The contribution of commercial fertilizer nutrients to food production.* Agron. J., 2005. **97**(1): p. 1-6.

14. *Glossary of soil science term*. Soil Science Society of America: https://www.soils.org/publications/soils-glossary

15. Lear, H., *Ammonium Nitrate Outlook 2012*. 2012, Affinity. The Noble Metals N2O abatement and related products newsletter.

16. Isherwood, K.F., *Mineral Fertilizer Use and the Environment*. 2000, International Fertilizer Industry Association (IFA), United Nations Environment Programme.

17. Andreozzi, R., Aquila, T., Caprio, V., and Insola, A., *Adiabatic calorimetry for safety studies in nitration processes.* Thermochimica Acta, 1992. **199**(0): p. 159-164.

18. Koerner, B., *Why do we use explosive fertilizer*. 2005: http://www.slate.com/articles/news_and_politics/explainer/2005/01/why_do_we_use_explosive_fertilizer.html.

19. Sfiligoj, E., *A good alternative to ammonium nitrate*. 2013, CropLife: http://www.croplife.com/article/34114/a-good-alternative-to-ammonium-nitrate.

20. Carlier, L., Baert, J., and Vliegher, A., *Use and efficiency of a liquid nitrogen fertilizer on grassland.* Fertilizer research, 1990. **22**(1): p. 45-48.

21. Oommen, C. and Jain, S.R., *Ammonium nitrate: a promising rocket propellant oxidizer.* Journal of Hazardous Materials, 1999. **67**(3): p. 253-281.

22. Oxley, J.C., Smith, J.L., Rogers, E., and Yu, M., *Ammonium nitrate: thermal stability and explosivity modifiers.* Thermochimica Acta, 2002. **384**(1–2): p. 23-45.

23. *Ammonium Nitrate*. Internaltional Programe on Chemical Safety, INCHEM: http://www.inchem.org/documents/icsc/icsc/eics0216.htm.

24. Sun, J., Sun, Z., Wang, Q., Ding, H., Wang, T., and Jiang, C., *Catalytic effects of inorganic acids on the decomposition of ammonium nitrate.* Journal of Hazardous Materials, 2005. **127**(1–3): p. 204-210.

25. Hadden, R.M. and Rein, G., *Small-scale experiments of self-sustaining decomposition of NPK fertilizer and application to events aboard the Ostedijk in 2007.* Journal of Hazardous Materials, 2011. **186**(1): p. 731-737.

26. *Tianjin explosion: China sets final death toll at 173, ending search for survivors*, in *Theguardian*. 2015, The Guardian: http://www.theguardian.com/world/2015/sep/12/tianjin-explosion-china-sets-final-death-toll-at-173-ending-search-for-survivors.

27. *Investigation report of Tianjing explosion on August 12, 2015*. 2016; Available from: http://www.chinasafety.gov.cn/newpage/newfiles/201600812baogao.pdf.

28. *China experts focus on chemicals in Tianjin explosion*, in *CNBC*. 2015, CNBC: http://www.cnbc.com/2015/08/14/china-experts-focus-on-chemicals-in-tianjin-explosion.html.

29. *China probe says stored chemical caused Tianjin blasts*, in *Ledger-Enquirer*. February 5, 2016: http://www.ledger-enquirer.com/news/business/article58598868.html.

30. Guardian, *Fertilizer explosions listed and US facilities mapped*. 2013, Theguardian.

31. Heather, D. *A review of past ammonium nitrate accidents and lessons learned.* in *Workshop on ammonium nitrate. 30 January to 1 February, 2002*. 2002. European Fertilizer Manufactures Association. European Commision Joint Research Centre. Ispra, Italy.

32. Nygaard, E.C., *Safety of ammonium nitrate.* International Society of Explosives Engineers. , 2006(2006G Volume 2).

33. Wood, M. and Duffield, S., *Ammonium nitrate safety*. 2002, Summary report of the workshop on ammonium nitrate held on 30 January - 1 February 2002, Ispra, Italy.

34. Atfield, C., *Truck explosion injures eight, closes Mitchell Highway*, in *Brisbane Times*. 2014: brisbanetimes.com.au.

35. ABC, *Ammonium nitrate truck explosion*, in *ABC (Australian Broadcasting Corporation) News*. 2014.

36. Petruk, T., *Truck hauling ammonium nitrate caught fire in B.C.*, in *Global News, Kamloops, B.C.* 2014.

37. Purtill, J. and Liston, G., *Road train driver unhooked trailer 'moments' before ammonium nitrate exploded, witnesses say*, in *ABC*. 2014: www.abc.net.au.

38. *Tier Two: Emergency and hazardous chemical inventory*, in *January 1 to December 31, 2012.* April 18, 2013, West Fertilizer Plant: http://msnbcmedia.msn.com/i/msnbc/Sections/NEWS/Adair%20Grain%20Inc%202012%20Tier%202%20Report.pdf.

39. CSB *Investigation report of the West Fertilizer Company Fire and Explosion*. 2016.

40. *Frantic search for survivors after deadly Texas fertilizer plant blast*, in *CBSNews*. 2013, CBS News: http://www.cbsnews.com/8301-201_162-57580185/frantic-search-for-survivors-after-deadly-texas-fertilizer-plant-blast/.

41. Dechy, N., Bourdeaux, T., Ayrault, N., Kordek, M.A., and Le Coze, J.C., *First lessons of the Toulouse ammonium nitrate disaster, 21st September 2001, AZF plant, France.* Journal of Hazardous Materials, 2004. **111**(1–3): p. 131-138.

42. Li, X.-R. and Koseki, H., *Study on reactivity of ammonium nitrate contaminated by sodium dichloroisocyanurate* Sci. Tech. Energetic Materials, 2005. **66**(6): p. 431-435.

43. Barthelemy, F., Hornus, H., Roussot, J., Hufschmitt, J.-P., and Raffoux, J.-F., *Report to the Minister for Regional Development and the Environment on the accident that occurred at the Grande Paroisse company factory in Toulouse on 21st September 2001*. 2001: General Inspectorate for the Environment, Paris.

44. Thomas, M.J., Cummings, A., Gomez, M., Bradford, W.J., Spanholtz, R.B., and Salinas, A., *Chemical accident investigation report: Terra Industries, Inc., Nitrogen Fertilizer Facility, Port Neal, Iowa*. 1996, Environmental Protection Agency (EPA).

45. Ruskin, A., Beard, O.W., and Schaffer, R.L., *Blast hypertension: Elevated arterial pressures in the victims of the texas city disaster.* The American Journal of Medicine, 1948. **4**(2): p. 228-236.

46. *Explosion in a nitrogenous fertiliser plant, 21 September 1921, Oppau, Germany*. 2008, French Ministry of Environment: http://www.aria.developpement-durable.gouv.fr/wp-content/files_mf/FD_14373_oppau_1921_ang.pdf.

47. Department., O.C.P., *Alfred P. Murrah building bombing. After action report.* http://web.archive.org/web/20070703233435/http://www.terrorisminfo.mipt.org/pdf/okcfr_App_C.pdf.

48. Li, X.-R. and Koseki, H., *Study on the contamination of chlorides in ammonium nitrate.* Process Safety and Environmental Protection, 2005. **83**(1): p. 31-37.

49. Gunawan, R. and Zhang, D., *Thermal stability and kinetics of decomposition of ammonium nitrate in the presence of pyrite.* Journal of Hazardous Materials, 2009. **165**(1–3): p. 751-758.

50. Turcotte, R., Lightfoot, P.D., Fouchard, R., and Jones, D.E.G., *Thermal hazard assessment of AN and AN-based explosives.* Journal of Hazardous Materials, 2003. **101**(1): p. 1-27.

51. Fogler, H.S., *Elements of Chemical Reaction Engineering. Fourth Edition*. 2005, Prentice Hall.

52. Topal, U., Ozkan, H., and Sozeri, H., *Synthesis and characterization of nanocrystalline BaFe12O19 obtained at 850C by using ammonium nitrate melt.* Journal of Magnetism and Magnetic Materials, 2004. **284**(0): p. 416-422.

53. Oxiey, J.C., Kaushik, S.M., and Gilson, N.S., *Thermal stability and compatibility of ammonium nitrate explosives on a small and large scale.* Thermochimica Acta, 1992. **212**(0): p. 77-85.

54. MacNeil, J.H., Zhang, H., Berseth, P., and Trogler, W.C., *Catalytic decomposition of ammonium nitrate in superheated aqueous solutions.* Journal of the American Chemical Society, 1997. **119**(41): p. 9738-9744.

55. Rosser, W.A., Inami, S.H., and Wise, H., *The kinetics of decomposition of liquid ammonium nitrate.* The Journal of Physical Chemistry, 1963. **67**(9): p. 1753-1757.

56. Chaturvedi, S. and Dave, P.N., *Review on thermal decomposition of ammonium nitrate.* Journal of Energetic Materials, 2012. **31**(1): p. 1-26.

57. Patil, D.G., Jain, S.R., and Brill, T.B., *Thermal decomposition of energetic materials 56. On the fast thermolysis mechanism of ammonium nitrate and its mixtures with mangnesium and carbon.* Propellants, Explosives, Pyrotechnics, 1992. **17**(3): p. 99-105.

58. Saunders, H.L., *LXXXI.-The decomposition of ammonium nitrate by heat.* Journal of the Chemical Society, Transactions, 1922. **121**(0): p. 698-711.

59. Brower, K.R., Oxley, J.C., and Tewari, M., *Evidence for homolytic decomposition of ammonium nitrate at high temperature.* The Journal of Physical Chemistry, 1989. **93**(10): p. 4029-4033.

60. Bedford, G. and Thomas, J.H., *Reaction between ammonia and nitrogen dioxide.* Journal of the Chemical Society, Faraday Transactions 1: Physical Chemistry in Condensed Phases, 1972. **68**(0): p. 2163-2170.

61. Davis, T.L. and Abrams, A.J.J., *The Dehydration of Ammonium Nitrate.* Journal of the American Chemical Society, 1925. **47**(4): p. 1043-1045.

62. Merrill, C., *Nitrous Oxide Explosive Hazards*. 2008, Air Force Research Laboratory, Edwards AFB, CA.

63. Raynie, D.E., *Warning concerning the use of nitrous oxide in supercritical fluid extractions.* Analytical Chemistry, 1993. **65**(21): p. 3127-3128.

64. Kapteijn, F., Rodriguez-Mirasol, J., and Moulijn, J.A., *Heterogeneous catalytic decomposition of nitrous oxide.* Applied Catalysis B: Environmental, 1996. **9**(1–4): p. 25-64.

65. OSHA, *Explosives and Blasting Agents (29 C.F.R. §1910.109)*. Occupational Safety and Health Administration (OSHA): http://www.osha.gov/pls/oshaweb/owadisp.show_document?p_id=9755&p_table=STANDARDS.

66. Han, Z., Sachdeva, S., Papadaki, M., and Mannan, M.S., *Calorimetry studies of ammonium nitrate – Effect of inhibitors, confinement, and heating rate.* Journal of Loss Prevention in the Process Industries, 2015. **38**: p. 234-242.

67. Han, Z., Sachdeva, S., Papadaki, M.I., and Mannan, M.S., *Ammonium nitrate thermal decomposition with additives.* Journal of Loss Prevention in the Process Industries, 2015. **35**: p. 307-315.

68. Rubtsov, Y.I., Strizhevskii, A.I., and Kazakov, A.I., *Possibilities of lowering the rate of thermal decomposition of AN.* Zhurnal Prikladnoi Khimii, 1989. **62**: p. 2169-2174.

69. Zhu, Z. and Guo, Z., *Discussion on the prior evaluation of the explosion of ammonium nitrate.* China Safety Sci. J. **10**(2000): p. 70–74.

70. Keenan, A.G., Notz, K., and Franco, N.B., *Synergistic catalysis of ammonium nitrate decomposition.* J. Am. Chem. Soc. **4**(1969): p. 3168–3171.

71. Duh, Y.S., Kao, C.S., Lee, C., Hsu, C.C., and Yu, S.W. *Thermal hazards evaluation and emergency relief vent sizing of nitrous oxide production process from ammonium nitrate decomposition*. in *Proceedings of the Second International Conference and Exhibition on Loss Prevention Safety, Health and Environment in the Oil, Chemical and Process Industries*. 1995. Singapore.

72. Presles, H.N., Khasainov, B.A., Vidal, P., Montassier, V., Ermolaev, B.A., and Sulimov, A.A., *Phenomenological description of the spontaneous detonation mechanism in moistened ammonium nitrate – sodium dichloroisocyanurate mixture*, in *15th international detonation symposium*. 2014: San Francisco, CA, July 13-18, 2014.

73. Cook, M.A. and Talbot, E.L., *Explosive sensitivity of ammonium nitrate - hydrocarbon mixtures.* Industrial & Engineering Chemistry, 1951. **43**(5): p. 1098-1102.

74. Levchenko, I.V., Klyakin, G.F., Vyazenova, I.A., and Taranushich, V.A., *Thermal decomposition of ammonium nitrate with three-component additives.* Russian Journal of Applied Chemistry, 2011. **84**(9): p. 1511-1515.

75. Boddington, T., Hongtu, F., Laye, P.G., Nawaz, M., and Nelson, D.C., *Thermal runaway by thermal analysis.* Thermochimica Acta, 1990. **170**(0): p. 81-87.

76. Klyakin, G.F. and Taranushich, V.A., *Phase stabilization of ammonium nitrate with binary additives consisting of potassium nitrate and complexone salts.* Russian Journal of Applied Chemistry, 2008. **81**(5): p. 748-751.

77. Klimova, I., Kaljuvee, T., Türn, L., Bender, V., Trikkel, A., and Kuusik, R., *Interactions of ammonium nitrate with different additives.* Journal of Thermal Analysis and Calorimetry, 2011. **105**(1): p. 13-26.

78. Oxley, J.C., Kaushik, S.M., and Gilson, N.S., *Thermal stability and compatibility of ammonium nitrate explosives on a small and large scale.* Thermochimica Acta, 1992. **212**(0): p. 77-85.

79. Mannan, M.S., *Ch11. Process design*, in *Lees' loss prevention in the process industries (fourth edition)*. 2012, Butterworth-Heinemann: Oxford. p. iv.

80. Ettouney, R.S. and El-Rifai, M.A., *Explosion of ammonium nitrate solutions, two case studies.* Process Safety and Environmental Protection, 2012. **90**(1): p. 1-7.

81. Shockey, D.A., Simons, J.W., and Kobayashi, T., *Cause of the Port Neal ammonium nitrate plant explosion.* Engineering Failure Analysis, 2003. **10**(5): p. 627-637.

82. EFMA, *Guidance for the compilation of safety data sheets for fertilizer materials, ammonium nitrate fertilizers*. 1996, European Fertilizer Manufacturers Association.

83. Spencer, A.B. and Colonna, G.R., *NFPA fire protection guide to hazardous materials, 13th ed.* 2002, NFPA International, Quincy, MA, USA.

84. Lee, P.P. and Back, M.H., *Kinetic studies of the thermal decomposition of nitroguanidine using accelerating rate calorimetry.* Thermochimica Acta, 1988. **127**(0): p. 89-100.

85. Andersen, W.H., Bills, K.W., Dekker, A.O., Mishuck, E., Moe, G., and Schultz, R.D., *The gasification of solid ammonium nitrate.* Jet Propulsion, 1958. **28**: p. 831-832.

86. Andersen, W.H. and Chaiken, R.F., *Application of surface decomposition kinetics to detonation of ammonium nitrate.* ARS Journal, 1959. **29**: p. 49-51.

87. Russell, T.P. and Brill, T.B., *Thermal decomposition of energetic materials 31—Fast thermolysis of ammonium nitrate, ethylenediammonium dinitrate and hydrazinium nitrate and the relationship to the burning rate.* Combustion and Flame, 1989. **76**(3–4): p. 393-401.

88. Andersen, W.H., Bills, K.W., Mishuck, E., Moe, G., and Schultz, R.D., *A model describing combustion of solid composite propellants containing ammonium nitrate.* Combustion and Flame, 1959. **3**(0): p. 301-317.

89. Kulbhushan Joshi, V.R., Ali S. Rangwala, *Effect of weathering of coal and organic dusts on their spontaneous ignition.* Fire Technology, 14 September 2012: p. 1-14.

90. Komunjer, L. and Affolter, C., *Absorption–evaporation kinetics of water vapour on highly hygroscopic powder: Case of ammonium nitrate.* Powder Technology, 2005. **157**(1–3): p. 67-71.

91. Maschio, G., Ferrara, I., Bassani, C., and Nieman, H., *An integrated calorimetric approach for the scale-up of polymerization reactors.* Chemical Engineering Science, 1999. **54**(15–16): p. 3273-3282.

92. Maschio, G., Feliu, J.A., Ligthart, J., Ferrara, I., and Bassani, C., *The Use of Adiabatic Calorimetry for the Process Analysis and Safety Evaluation in Free Radical Polymerization.* Journal of Thermal Analysis and Calorimetry, 1999. **58**(1): p. 201-214.

93. Fauske, *The reactive system screening tool (RSST): An easy, inexpensive approach to the DIERS procedure.* Process Safety Progress, 1998. **17**(3): p. 190-195.

94. Wei, C., Saraf, S.R., Rogers, W.J., and Mannan, M., *Thermal runaway reaction hazards and mechanisms of hydroxylamine with acid/base contaminants.* Thermochimica Acta, 2004. **421**(1–2): p. 1-9.

95. Fauske & Associates, I., *FAI/94-25, Reactive system screening tool system manual, methodology and operations*. July, 1994.

96. Kumpinsky, E., *A Study on Resol-Type Phenol-Formaldehyde Runaway Reactions.* Industrial & Engineering Chemistry Research, 1994. **33**(2): p. 285-291.

97. Grolmes, M.A., Leung, J.C., and Fauske, H.K. *Reactive systems vent sizing evaluations*. in *Proceedings of the International Symposium on Runaway Reactions, CCPS*. March 1989. Cambridge, MA.

98. Saenz-Noval, L.R., *Evaluation of Alternatives for Safer and More Efficient Eeactions: A Study of the N-oxidation of Alkylpyridines*, in *Chemical Engineering Department*. 2011, Texas A&M University: College Station, TX.

99. Townsend, D.I. and Tou, J.C., *Thermal hazard evaluation by an accelerating rate calorimeter.* Thermochimica Acta, 1980. **37**(1): p. 1-30.

100. Kossoy, A. and Akhmetshin, Y., *Identification of kinetic models for the assessment of reaction hazards.* Process Safety Progress, 2007. **26**(3): p. 209-220.

101. Burelbach, J.P. and Theis, A.E., *Thermal Hazards Evaluation Using the ARSST*, in *3rd Internaltional Symposium on Runaway Reactions, Pressure Relief Design, and Effluent Handling*. 2005, Design Institute for Emergency Relief Systems (DIERS) Users Group: Cincinnati, Ohio.

102. Yaws, C.L., *Chemical properties handbook : physical, thermodynamic, environmental, transport, safety, and health related properties for organic and inorganic chemicals*. 1999, New York: McGraw-Hill.

103. Fisher, H.G., Forrest, H.S., Grossel, S.S., Huff, J.E., Muller, A.R., Noronha, J.A., Shaw, D.A., and Tilley, B.J., *Emergency Relief System Design Using DIERS Technology: The Design Institute for Emergency Relief Systems (DIERS) Project Manual*. 1992: Design Institute for Physical Property Data/AIChE.

104. Etchells, J. and Wilday, J., *Workbook for Chemical Reactor Relief System Sizing. HSE*. 1998: Health & Safety Executive.

105. Janzen, H.H. and Bettany, J.R., *Release of available sulfer from fertilizers.* Canadian Journal of Soil Science, 1986. **66**(1): p. 91-103.

106. Fauske, *FAI/94-25, Reactive system screening tool system manual, methodology and operations*. 1994: Fauske & Associates, Inc.

107. Wood, B.J. and Wise, H., *Acid Catalysis in the Thermal Decomposition of Ammonium Nitrate.* The Journal of Chemical Physics, 1955. **23**(4): p. 693-696.

108. Groothuizen, T.M., Lindeijer, E.W., and Pasman, H.J., *Danger aspects of fertilizers containing ammonium nitrate, Stikstof - Dutch Nitrogenous Fertilizer Review, No. 14*. 1970: Centraal Stikstof Verkoopkantoor nv (CSV); Central Nitrogen Sales Organization Ltd.; 360 Thorbeckelaan; The Hague, The Netherlands.

109. Nalewaja, J.D., Manthey, F.A., Szelezniak, E.F., and Anyska, Z., *Sodium Bicarbonate Antagonism of Sethoxydim.* Weed Technology, 1989. **3**(4): p. 654-658.

110. Munns, D.N., *Soil acidity and growth of a legume. I. Interactions of lime with nitrogen and phosphate on growth of Medicago sativa L. and Trifolium subterraneum L.* Australian Journal of Agricultural Research, 1965. **16**(5): p. 733-741.

111. WebAssign, *Density, melting points, and boiling points*. 2014.

112. MSDS, *Safety data sheet of sodium bicarbonate*. 2014, Sigma-Aldrich.

113. Barclay, K.S. and Crewe, J.M., *The thermal decomposition of ammonium nitrate in fused salt solution and in the presence of added salts.* Journal of Applied Chemistry, 1967. **17**(1): p. 21-26.

114. Adamopoulou, T., Papadaki, M.I., Kounalakis, M., Vazquez-Carreto, V., Pineda-Solano, A., Wang, Q., and Mannan, M.S., *Thermal decomposition of hydroxylamine: Isoperibolic calorimetric measurements at different conditions.* Journal of Hazardous Materials, 2013. **254–255**(0): p. 382-389.

115. Theoret, A. and Sandorfy, C., *Infrared spectra and crystalline phase transitions of ammonium nitrate.* Canadian Jounal of Chemistry, 1964. **42**: p. 57-62.

116. Obama, B. *Executive Order -- Improving Chemical Facility Safety and Security*. Executive Order 13650. August 1, 2013; Available from: http://www.whitehouse.gov/the-press-office/2013/08/01/executive-order-improving-chemical-facility-safety-and-security.

117. Babrauskas, V., *Explosions of ammonium nitrate fertilizer in storage or transportation are preventable accidents.* Journal of Hazardous Materials, 2016. **304**: p. 134-149.

118. *NFPA 400. Hazardous Materials Code*. 2013, National Fire Protection Association (NFPA).

119. *Industrial Fire Sprinklers*. Fire Safety Advice Centre: http://www.firesafe.org.uk/industrial-fire-sprinklers/.

120. *Fire Sprinklers*. http://www.h2ofiresprinklers.co.uk/fire_sprinklers.php.

121. Yao, C. and Kalelkar, A.S., *Effect of drop size on sprinkler performance.* Fire Technology, 1970. **6**(4): p. 254-268.

122. *A History of Sprinkler Development*. Incendia Consulting. Fire Safety Consultant Engineers: http://incendiaconsulting.com/History%20of%20Sprinkler%20Development.pdf.

123. Madrzykowski, D. and Fleming, R.P., *Review of Residential Sprinkler Systems: Research and Standards.* NISTIR 6941. December 2002: National Technical Information Service, Technology Administration, U.S. Department of Commerce. http://fire.nist.gov/bfrlpubs/fire02/art137.html.

124. *NFPA 13D. Standard for the Installation of Sprinkler Systems in One- and Two-Family Dwellings and Manufactured Homes, 1999 ed*. National Fire Protection Association, Quincy, MA.

125. Liu, Z. and Kim, A.K., *A Review of Water Mist Fire Suppression Technology: Part II—Application Studies.* Journal of Fire Protection Engineering, 2001. **11**(1): p. 16-42.

126. CCPS, *Guidlines For Fire Protection in Chemical, Petrochemical, and Hydrocarbon Processing Facilities*. 2003: Center for Chemical Process Safety of the American Institute of Chemical Engineers. 3 Park Avenue, New York, NY 10016-5991.

127. Han, Z., Sachdeva, S., Papadaki, M.I., and Mannan, S., *Effects of inhibitor and promoter mixtures on ammonium nitrate fertilizer explosion hazards.* Thermochimica Acta, 2016. **624**: p. 69-75.

128. Goranson, R.W., *A method for determining equations of state and reaction zones in detonation of high explosives, and its application to pentolite, composition-B, baratol, and TNT.* Classified Los Alamos Rept. LA-487, 1945.

129. King, A.W., *Shock Initiation Characteristics of Ammonium Nitrate (Ph.D.Dissertation).* 1979, Queen's Univ., Kingston, ON, Canada.

130. *Fires in Agricultural Chemicals*. National Ag Safety Database: http://nasdonline.org/document/248/d000049/fires-in-agricultural-chemicals.html.

131. *Texas City, Texas, Disaster, April 16, 17, 1947*, in *Fire Prevention and Engineering Bureau of Texas, Dallas, Texas; The National Board of Fire Underwriters, New York, New York.* 1947: http://www.local1259iaff.org/report.htm.

132. NFPA. *National Fire Protection Association: Code for the Storage of Ammonium Nitrate*. NFPA 490. 2002.

133. PHMSA, *Emergency Response Guidebook*. 2012: Department of Transportation, Pipeline and Hazardous Materials Safety Administration, Transport Canada, CIQUIME.

134. NFPA. *National Fire Protection Association: Standard for professional competence of responders to hazardous materials incidents*. 1997.

135. OSHA. *Occupational Safety and Heath Administration: Hazardous waste operations and emergency response*. 29 CFR 1910.120.

136. Moats, J. and Loyd, J. *Questions about fire fighter training. Personnal Communication.* 2014.

137. HSE, *Storing and Handling Ammonium Nitrate*. 1996, Health and Safety Executive, UK: http://www.hse.gov.uk/pubns/indg230.pdf.

138. Abbott Volunteer Fire Department, Bruceville-Eddy Volunteer Fire Department, Dallas Fire Rescue Department, Mertens Volunteer Fire Department , Navarro Mills Volunteer Fire Department, and West Volunteer Fire Department, *Firefighter Fatality Investigation, West Texas April 17, 2013*. 2014.

139. *Tier Two Emergency and Hazardous Chemical Inventory: Adair Grain Inc, West Fertilizer Co.* 2012.

140. Southern Trinity Groundwater Conservation District, *Groundwater Management Plan*. 2010.

141. AIChE, *DIPPR Project 801, Evaluated Standard Thermophysical Property Values*, ed. Design Institute for Physical Properties Sponsored by AIChE. 2012: Design Institute for Physical Property Research, American Institute of Chemical Engineers.

142. Laurent, B. and Kemira, S.A., *Straight ammonium nitrate fertilizer granule-prill stabilization: theoretical possibilities*, in *IFA Technical Conference*. 2002: Chennai, India.

143. Lightstone, J.M., Onasch, T.B., Imre, D., and Oatis, S., *Deliquescence, Efflorescence, and Water Activity in Ammonium Nitrate and Mixed Ammonium Nitrate/Succinic Acid Microparticles.* The Journal of Physical Chemistry A, 2000. **104**(41): p. 9337-9346.

144. Stelson, A.W. and Seinfeld, J.H., *Relative humidity and temperature dependence of the ammonium nitrate dissociation constant.* Atmospheric Environment (1967), 1982. **16**(5): p. 983-992.

145. EFMA, *Guidance for Sea Transport of Ammonium Nitrate Based Fertilizers.* European Fertilizers' Manufacturers Association (EFMA), Belgium, 2004.

146. Sykes, W.G., Johnson, R.H., and Hainer, R.M., *Ammonium nitrate explosion hazards.* Chemical Engineering Progress, 1963. **59**(1): p. 66-71.

147. Lindner, V., *Explosives and Propellants*, in *Kirk Othmer Encyclopedia of Chemical Technology, 4th Ed, Vol 10*. 1993, Wiley New York.

148. Barlič, B., Hadži, D., and Orel, B., *Normal coordinate analysis of the two forms of the hydrogen dinitrate ion.* Spectrochimica Acta Part A: Molecular Spectroscopy, 1981. **37**(12): p. 1047-1048.

149. Doyle, R.J. and Dunlap, B.I., *Rearrangements of ammonium nitrate cluster Ions with high internal energy.* J. Phys. IV France, 1995. **05**(C4): p. C4-417-C4-422.

150. Wei, C., Rogers, W.J., and Mannan, M.S., *Thermal decomposition hazard evaluation of hydroxylamine nitrate.* Journal of Hazardous Materials, 2006. **130**(1–2): p. 163-168.

151. Wei, C., Rogers, W.J., and Mannan, M.S., *Reaction pathways of hydroxylamine decomposition in the presence of acid/base*. 2004, American Institute of Chemical Engineers, Annual Meeting: New York, N.Y.

152. *Engineering statistics handbook*. 2012, NIST. US Commerce Department's Technology Administration: http://www.itl.nist.gov/div898/handbook.